8/1980

LBL-10868 c.2

Lawrence Berkeley Laboratory
UNIVERSITY OF CALIFORNIA

ENERGY & ENVIRONMENT DIVISION

AN EXPERIMENTAL AND THEORETICAL STUDY
OF HEAT TRANSFER WITH COMBUSTION

Hasan A. Heperkan
(Ph.D. thesis)

May 1980

Prepared for the U.S. Department of Energy under Contract W-7405-ENG-48

DISCLAIMER

LBL-10868

AN EXPERIMENTAL AND THEORETICAL STUDY OF HEAT TRANSFER WITH COMBUSTION

By

Hasan A. Heperkan
(Ph.D. thesis)

Lawrence Berkeley Laboratory
University of California
Berkeley, California 94720

Prepared for the U. S. Department of Energy
under Contract W-7405-ENG-48

AN EXPERIMENTAL AND THEORETICAL STUDY OF HEAT TRANSFER WITH COMBUSTION

Contents

AN EXPERIMENTAL AND THEORETICAL STUDY OF HEAT TRANSFER WITH COMBUSTION

Hasan A. Heperkan
Energy and Environment Division, Lawrence Berkeley Laboratory
and Department of Mechanical Engineering
University of California, Berkeley, California 94720

ABSTRACT

For internal combustion engines, a knowledge of the heat transfer to the walls is important for determining the quenching of wall reactions leading to high carbon emissions, the durability of engine components and the loss of energy from the gases in the combustion chamber. This work is concerned with the determination of the heat transfer during combustion.

A number of experiments were performed in a shock tube to determine the heat flux at the wall. A combustible mixture, $2H_2 + O_2 + 27Ar$, was used as the test gas. The gas was ignited by a reflected shock wave. A detonation wave was formed which moved away from the wall while the combustion zone diffused slowly toward the wall. The wall heat flux was determined by utilizing the measurement of the wall temperature variation with respect to time using a thin film platinum resistance thermometer. In addition a determination of the heat flux was also made by solving the conservation equations in the gas boundary layer near the wall.

The results yielded values for the location of the combustion zone as a function of time. The combustion zone diffused slowly toward the end wall and then remained at a constant distance away from the wall. This distance can be considered as a quenching distance for the combustion zone.

A set of experiments was also performed in a constant volume vessel. The wall heat flux was calculated in the presence of a flame propagating towards the wall. A methane-air mixture at an equivalence ratio of 1 was used. The gas was ignited by a spark plug mounted on the wall.

Ralph Frey

ACKNOWLEDGEMENTS

The author wishes to express his sincere gratitude to his advisor, Professor Ralph Greif, for his valuable advice, aid, guidance and patience throughout the course of this work.

Thanks are extended to Professor A. K. Oppenheim, Professor R. Seban, Professor S. Davis, Professor P. Pagni, Dr. L. Cohen, Dr. A. Mertol, Al Shaw, V. Locke, R. Palmer, graduate students J. Naccache, D. Huang for their valuable suggestions, contributions and help to this study and to Ken Hom in assisting the experiments.

The author wishes to thank Mrs. Carmen Hubbard for her expert typing and Mrs. Gloria Pelatowski for her effort in rendering the graphs.

The author would also like to thank the residents of Hesse Hall for their moral support, and finally, his parents for their understanding and encouragement in support of the achievement of this goal.

NOMENCLATURE

Symbols

ρ - density

C_p - specific heat at constant pressure

ρ_g - density of platinum

k - thermal conductivity

t_g - film thickness

T - temperature

t - time variable

α - thermal diffusivity

x - space variable

q - heat flux

ξ - dummy integration variable

c_s - specific heat of the solid

u - velocity

ψ - transformed space variable

θ - non-dimensional temperature

λ - non-dimensional thermal conductivity

η - similarity variable

a - power in thermal conductivity relation

C - constant

ε - dimensionless difference between q_{wg} and q_{ws}

h_s - heat transfer coefficient based on q_{ws}

h_g - heat transfer coefficient based on q_{wg}

Symbols (continued)

U - non dimensional temperature for pre-ignition

Δt - time increment

$\Delta\psi$ - space increment

M - stability factor

h - enthalpy

y - mass fraction

V - diffusion velocity

D - diffusion coefficient

h_i^o - enthalpy of formation

δ - gas boundary layer thickness

p - pressure

γ - ratio of the specific heats

v - non dimensional temperature for the combustion period

τ - transformed time variable

$F(\psi)$ - initial temperature distribution for the combustion period

ψ_B - gas boundary layer thickness in the transformed coordinates

$\Delta\tau$ - transformed time increment

A - coefficient in the evaluation of the Duhamel integral

B - coefficient in the evaluation of the Duhamel integral

T_p - temperature at point P

a_1 - speed of sound in the test section

v_s - speed of the incident shock wave

M_s - Mach number of the incident shock wave

R - ideal gas constant

Symbols (continued)

C_v - specific heat at constant volume

MW - molecular weight

F - initial non dimensional temperature

ϕ - non dimensional temperature

$A(t)$, $B(t)$, $C(t)$ - coefficients in the temperature distributions

$A(\tau)$, $B(\tau)$, $C(\tau)$ - coefficients in the temperature distributions

$f(\tau)$, $g(\tau)$ - non dimensional temperature

$h(\tau)$ - derivative of the transformed temperature

ψ_p - value of ψ_B at ignition

$\overline{C_p}$ - average specific heat

Le - Lewis number

Subscripts

w	-	at the wall
i	-	initial
s	-	solid
g	-	in the gas
∞	-	infinity
j	-	space indice
k	-	time indice
i	-	species indice
I	-	at ignition
δ	-	at the edge of the gas boundary layer
m	-	last space indice
n	-	last time indice
1	-	conditions in the test sections
2	-	conditions behind the incident shock wave
5	-	conditions behind the reflected shock wave
0	-	initial

I. INTRODUCTION

For internal combustion engines, a knowledge of the heat transfer to the walls is important for determining the quenching of wall reactions leading to high hydrocarbon emissions, the durability of engine components and the loss of energy from the gases in the combustion chamber which plays a dominant role in decreasing the efficiency. Most previous study in the presence of combustion have considered only space and time averaged heat fluxes and heat transfer coefficients. The present work provides results for the time variation of these quantities.

In this study a number of experiments were performed in a shock tube to determine the heat flux at the wall. Argon and also a combustible mixture, $2H_2 + O_2 + 27\ Ar$, were used as the test gases. The gas in the end wall region undergoes a rapid increase in temperature due to shock wave heating from both the incident and reflected shock waves. After the reflection of the shock wave off the end wall, the temperature is large enough to self ignite the mixture. The ignition starts in a region close to the wall. A detonation wave is then formed which moves away from the end wall, while the combustion zone diffuses slowly towards the wall.

To determine the wall heat flux, a thin film resistance thermometer was used at the end wall which provided the variation of the temperature with respect to time. Then, from this measurement, the

heat flux was obtained using a conduction analysis in the thermally semi-infinite solid. The gauges were prepared by painting a thin platinum film on a glass-like base, Macor.

The speed of the incident shock wave was also determined from measurements of the time interval between two signals obtained from pressure transducers mounted on the shock tube. The temperature and pressure in front of the shock wave were also measured.

Another determination of the wall heat flux was obtained by solving the conservation equations in the gas boundary layer near the wall. To solve these equations the location of the combustion zone has to be specified. Several trajectories were chosen for the combustion zone and the results for the heat flux were compared with the previous calculation. The results show that the combustion zone diffuses toward the end wall and then stops at a certain distance away from the wall. This distance is similar to a quenching distance.

In addition the temperature distributions in the gas boundary layer, the heat transfer coefficients and the heat flux from the combustion zone at the edge of the gas boundary layer were calculated.

In combustion engines the knowledge of the heat transfer with the presence of a flame propagating toward the wall is also important. For this purpose experiments were performed in a constant volume chamber. A methane-air mixture at an equivalence ratio close to 1 was used as the test gas. The mixture was ignited at the wall by a spark plug. The wall temperature variation with respect to time was recorded

using a thin film resistance thermometer. The variation of pressure with respect to time was also recorded. The heat flux at the wall was then calculated from the temperature measurements.

II. EXPERIMENTAL APPARATUS AND MEASUREMENTS IN THE SHOCK TUBE

Experiments were performed in a shock tube in order to obtain the end wall heat flux from a gas heated by an incident and reflected shock wave. The flux was determined from measurements of the end wall temperature. The temperature and pressure of the gas outside the wall boundary layers were calculated based on the measured values of the speed of the incident shock wave.

2.1. Shock Tube

The experiments were performed in an aluminum shock tube of rectangular cross-section, 1-1/2 in. (3.84 cm) by 1-3/4 in. (4.48 cm). The tube has two optical windows on each side that are 18.00 in. (46.08 cm) long and 1-1/2 in. (3.84 cm) thick. For the runs with combustion a mixture of 27 Ar + $2H_2$ + O_2 was used as the test or driven gas on the low pressure side of the diaphragm. The driver gas, on the high pressure side, was helium.

Two Kistler pressure transducers (S/N 52036) were mounted on the top of the test section. They were used to detect the arrival of the shock wave at their respective locations. Figure 2.1 shows the calibration curve for the pressure transducer. The same curve was obtained for both transducers. The result indicates an output of 1.0 volts per 9.95 psi (6.8×10^4 Pa). The transducers were placed 4.00 in. (10.16 cm) apart. The resulting signals were recorded on a Textronix dual beam oscilloscope (Model 551). The travel time of the incident shock wave

between the pressure transducers was measured by a Hewlett-Packard electronic digital counter which has an accuracy of the order of 0.1 μsec. An additional pressure transducer was also mounted on top of the expansion section of the shock tube at a location in front of the other two transducers. It was used to trigger the electronic equipment.

2.2. Heat Transfer Gauge

To measure the wall temperature, a thin film platinum gauge, Fig. 2.2, was designed. It was fitted in a head, Fig. 2.3, and mounted at the end wall of the shock tube. These gauges are placed flush to the surface so that they do not disturb the flow. Macor, a ceramic material manufactured by Corning Glass Works, was used for the base of the gauge. Macor has glass-like properties and is machinable with conventional metal-working tools and equipment. It does not have to be heat treated or fired after machining.

The gauge is made by painting a thin film of liquid platinum on the surface of the Macor. The gauge is then placed in an oven to cure. This painting and heating is repeated until the electric resistance of the film reaches approximately 110 ohms. These thin film platinum gauges have a time response of the order of a microsecond.

The thickness of the platinum film is much less than the thermal diffusion depth so that the temperature gradient in the film can be neglected. Under this condition the platinum film senses the instantaneous surface temperature of the substrate. A response lag exists relative to a hypothetical film of zero thickness because of the small, but finite, heat capacity of the film. For a finite gauge thickness,

the substrate surface temperature attains 94% of the ideal temperature change in a time $\tau = 100\ \tau_r$ where [1]:

$$\tau_r = (\rho_g^{\ 2}\ C_p^{\ 2}\ t_g^{\ 2})/(\rho_w\ C_{pw}\ k_w)$$

ρ_g : density of platinum

ρ_w : density of substrate

C_{pg} : specific heat of platinum

C_{pw} : specific heat of ceramic

k_w : thermal conductivity of ceramic

t_g : film thickness

A representative value of τ_r is 7.1×10^{-11} sec [3], while typical values of the dimensions of the platinum film are: 5.5×10^{-3} microns × 1.8 cm × 0.3 cm.

The connection through the gauge is made with platinum wire 0.020 inch (0.051 cm) in diameter. Two copper-constantan thermocouples are also attached to the gauge surface for the calibration procedure. The locations of these thermocouples on the substrate are sufficiently far from the platinum film so that they do not disturb the measurement. The thermocouple wires are almost flush with the surface of the Macor facing the end wall region and are passed through two axial holes in the gauge. An O-ring is also used to maintain the vacuum in the test section.

The gauge is a part of a Wheatstone bridge. The increase in temperature changes the resistance of the platinum film which causes an unbalance in the bridge. A proportional voltage difference, then can be obtained at the ends of the bridge which is then amplified and recorded on a storage Textronix 549 oscilloscope. Figure 2.4 shows this circuit in detail.

For calibration purposes, the gauge is placed in an enclosure that is thermally controlled. Gradual changes in the temperature are measured by the thermocouples on the surface of the gauge and are plotted as a function of the corresponding voltage output of the system. Figure 2.5 shows a typical calibration curve. The initial temperature of the test gas mixture is measured by using one of the thermocouples on the surface of the gauge.

A schematic picture of the experimental set-up is presented in Figure 2.6.

2.3. Measurements in the Shock Tube

Measurements were made in a shock-tube to determine the speed of the incident shock wave which enable the temperature and the pressure in the gas behind the reflected shock wave to be calculated.

The passage of the shock wave is determined from the two pressure transducers placed on the top of the shock tube. The resulting two signals are recorded as the shock wave passes infront of the pressure transducers. An electronic counter gives the time between these two signals. The distance between the pressure transducers is known, so

that the speed of the incident shock wave can be calculated. The speed of sound may be calculated from the measured temperature of the gas in front of the shock wave. The resulting value of the Mach number with the initial values of the temperature and the pressure permit the calculation of the temperature and pressure behind the incident and the reflected shock waves [3]. These values correspond to the temperature and pressure of the gas in front of the end wall at the beginning of the pre-ignition period.

In the remaining part of this chapter two runs with combustion are considered. These are designated 214 and 219. The first set of numbers will correspond to the values for run 214 and the second for run 219.

The high pressure side of the diaphragm is filled with helium to 53 psia (274 cm Hg) for run 214 and 54 psia (279.2 cm Hg) for run 219. The low pressure side is first evacuated by a vacuum pump and then filled with the mixture (27 Ar + $2H_2$ + O_2) to 1.84 psia (95.2 mm Hg) and 1.845 psia (95.4 mm Hg). The pressure was measured by a U-tube manometer. The diaphragm is burst by a hydraulic plunger instantaneously using the electronic control panel. The shock wave passing the first pressure transducer triggers the electronic equipment. The signals from the second and third pressure transducers are recorded on an oscilloscope and the time between the two signals are obtained from a digital counter. The recorded times were 132 μsec and 130 μsec. The initial temperature in the gas was 534.5°R (296.9°K) and 535.1°R (297.3°K). This gives incident Mach numbers of 2.35 and 2.39 respectively. The incident

shock wave reflects off the end wall and the gas temperature behind the reflected shock wave is calculated to be 2407.23°R (1337.35°K). A sample calculation is given in Appendix B. The incident shock wave produced a strong ignition assuring a one-dimensional flow structure in the blast wave, generated by the exothermic reactions [4]. The resulting pressure signals are presented in Figures 2.7 and 2.8 where each increment on the horizontal time scale is 10 μsec. The vertical scale corresponds to the pressure and each increment is 0.2 volts. This is multiplied by the pressure constant to give the pressure. The curve on the bottom is the signal from the second and the curve on the top from the third pressure transducer.

The measurements discussed above are used to calculate the end wall heat transfer as presented in Chapter IV. We first present the end wall heat transfer results based only on the conduction analysis in the thin film gauge.

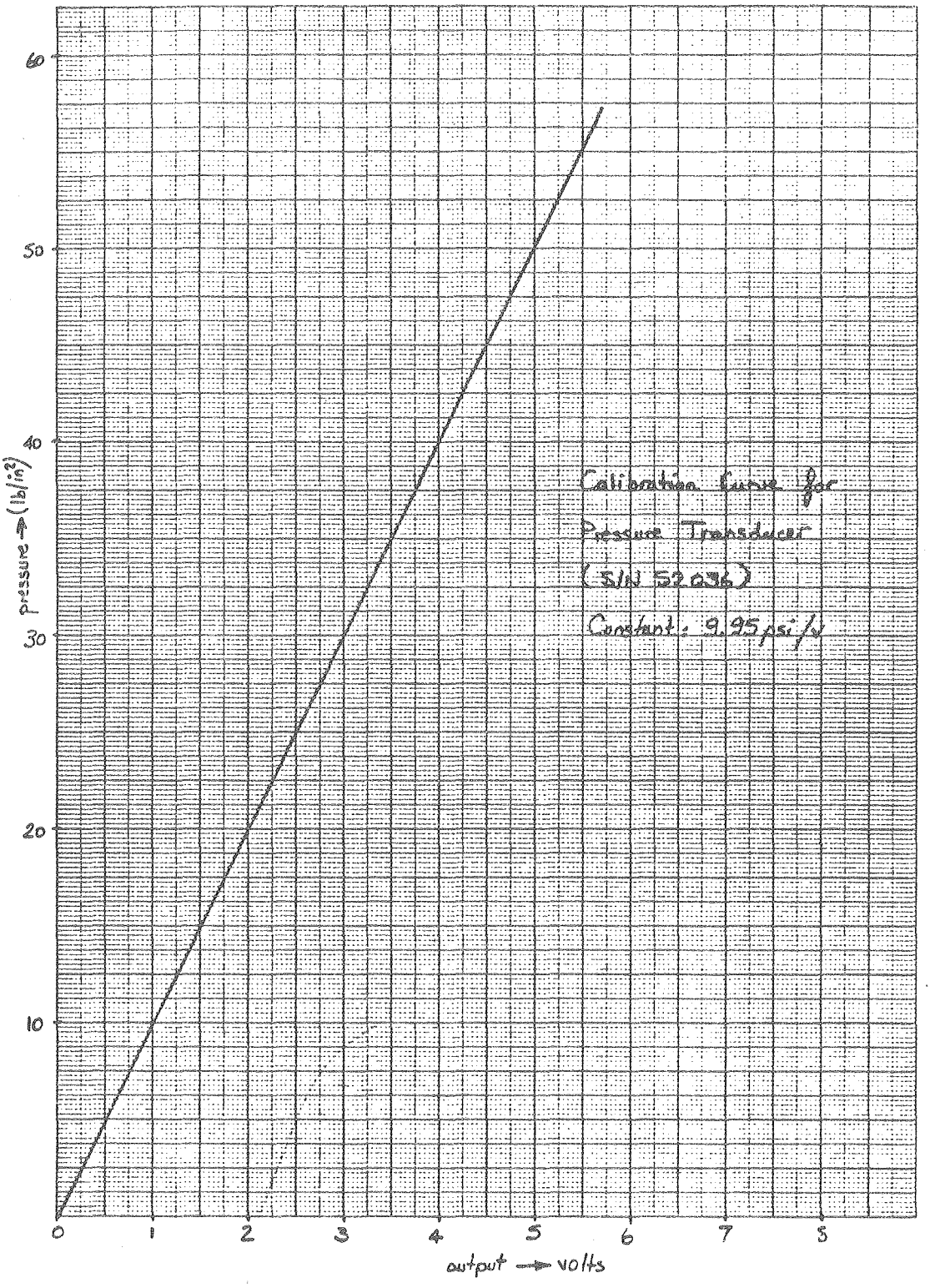

Figure 2.1. Calibration curve for pressure gauge.

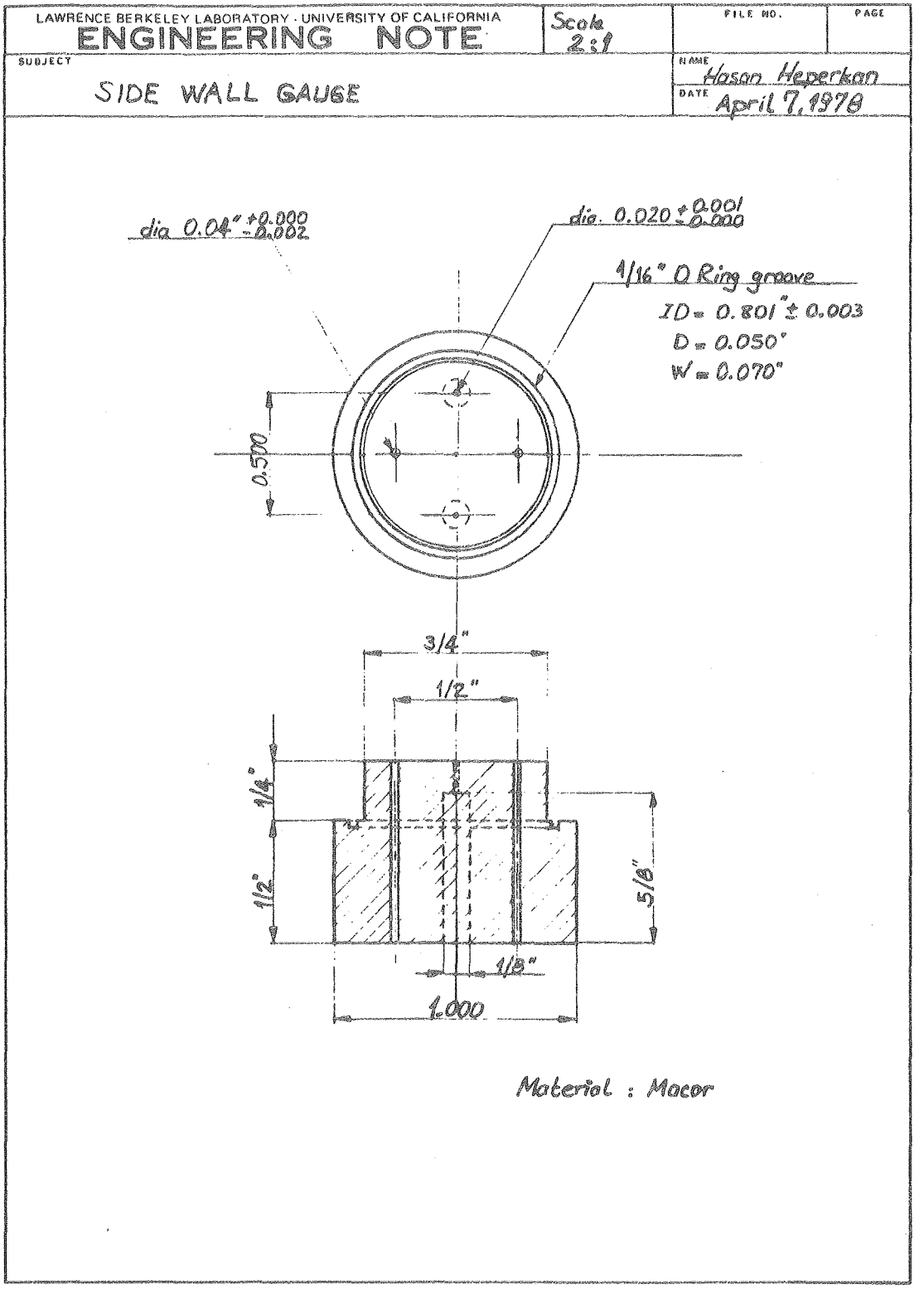

Figure 2.2. Thin film heat transfer gauge.

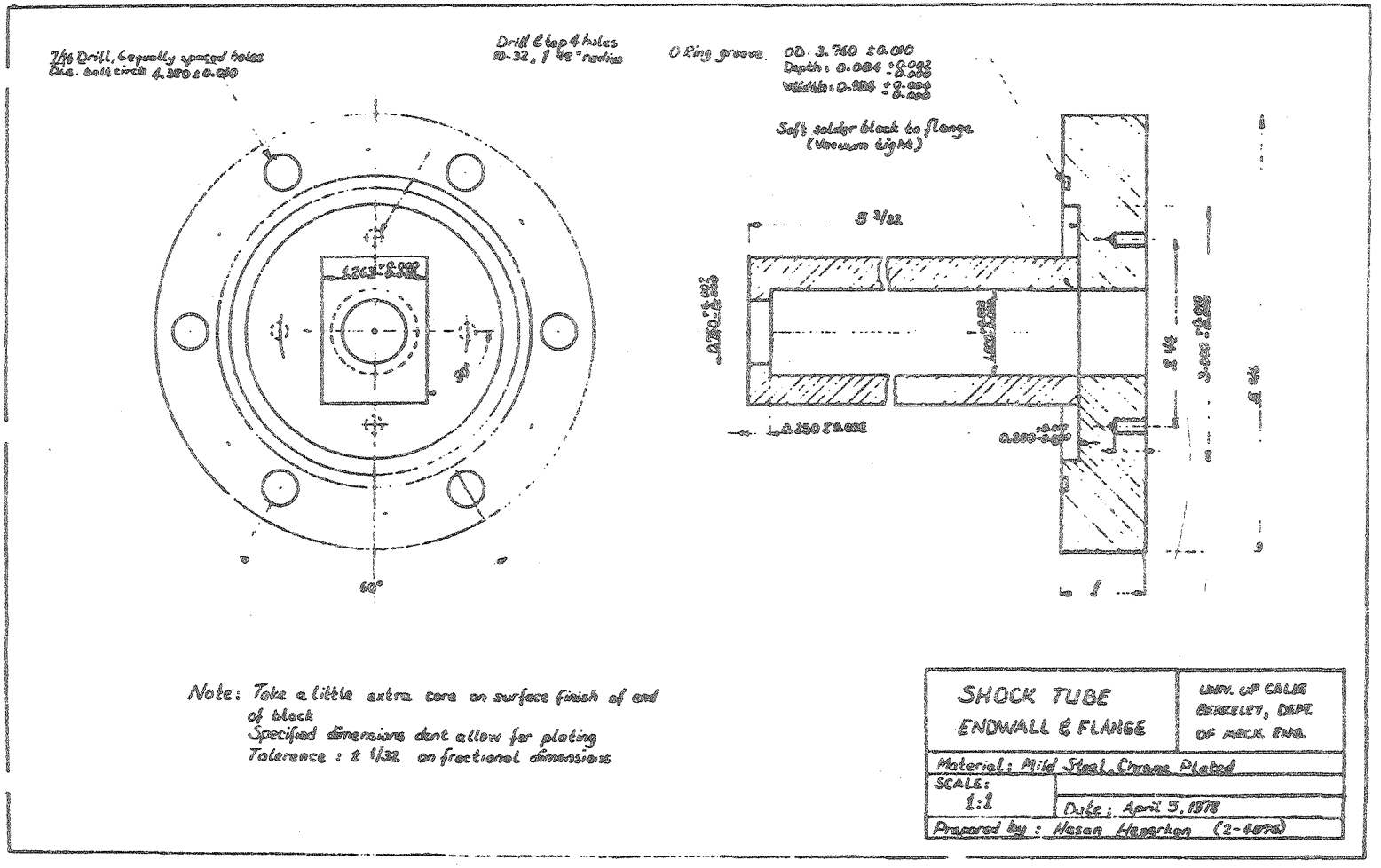

Figure 2.3.a. Shock tube head.

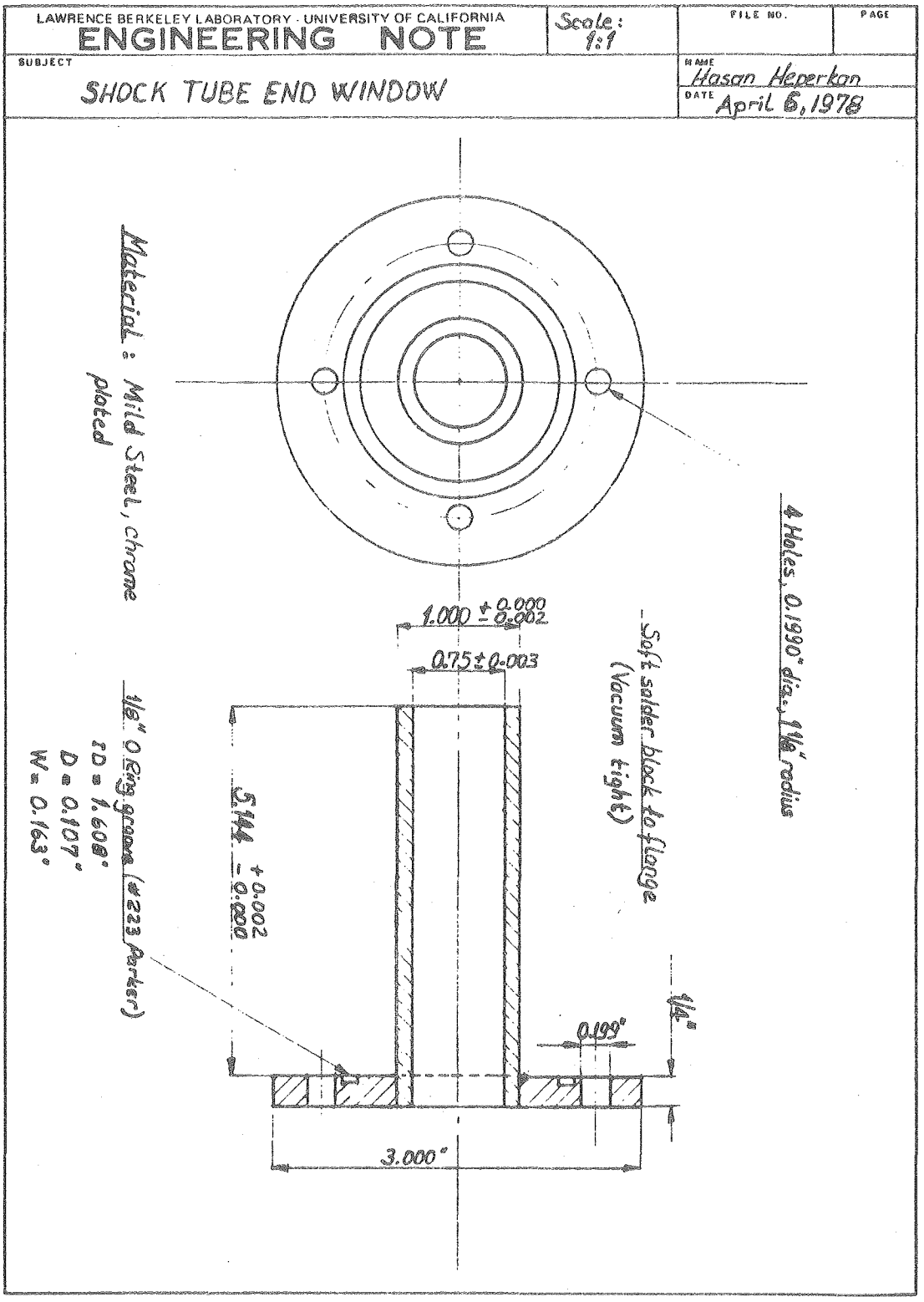

Figure 2.3.b. Shock tube head.

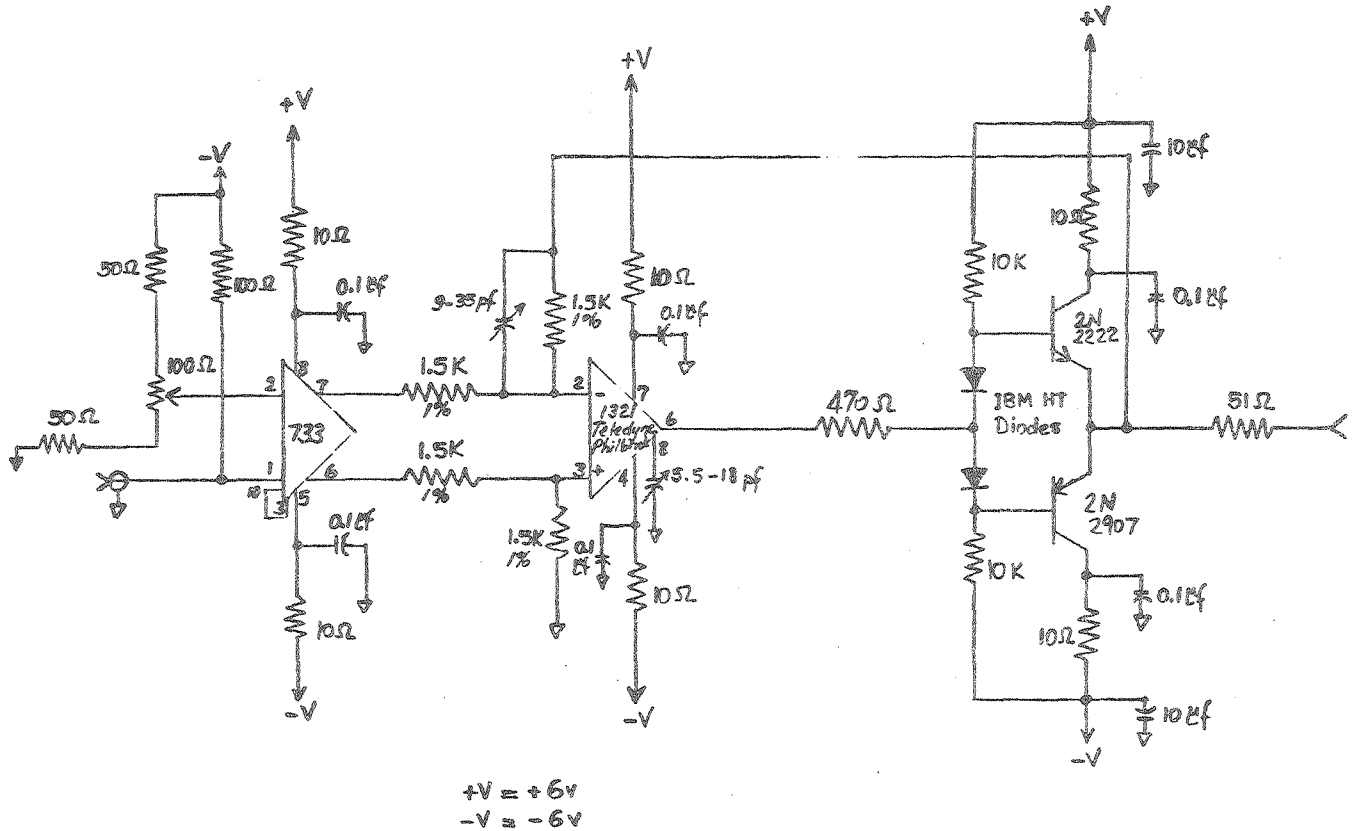

Figure 2.4. Electronic circuit for gauge. 5 MHz DC amplifier for platinum film RTD (11052).

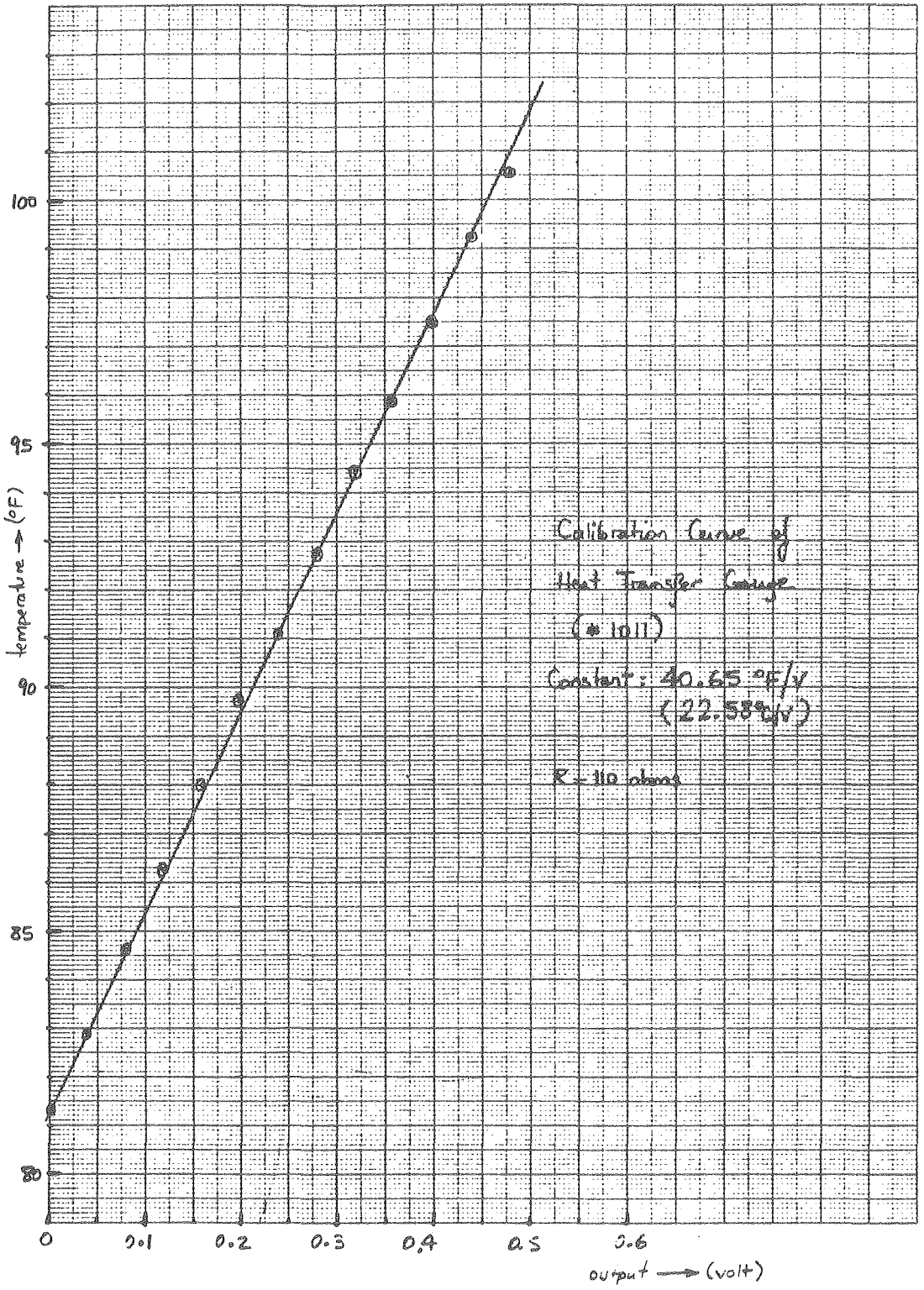

Figure 2.5. Calibration curve for temperature gauge.

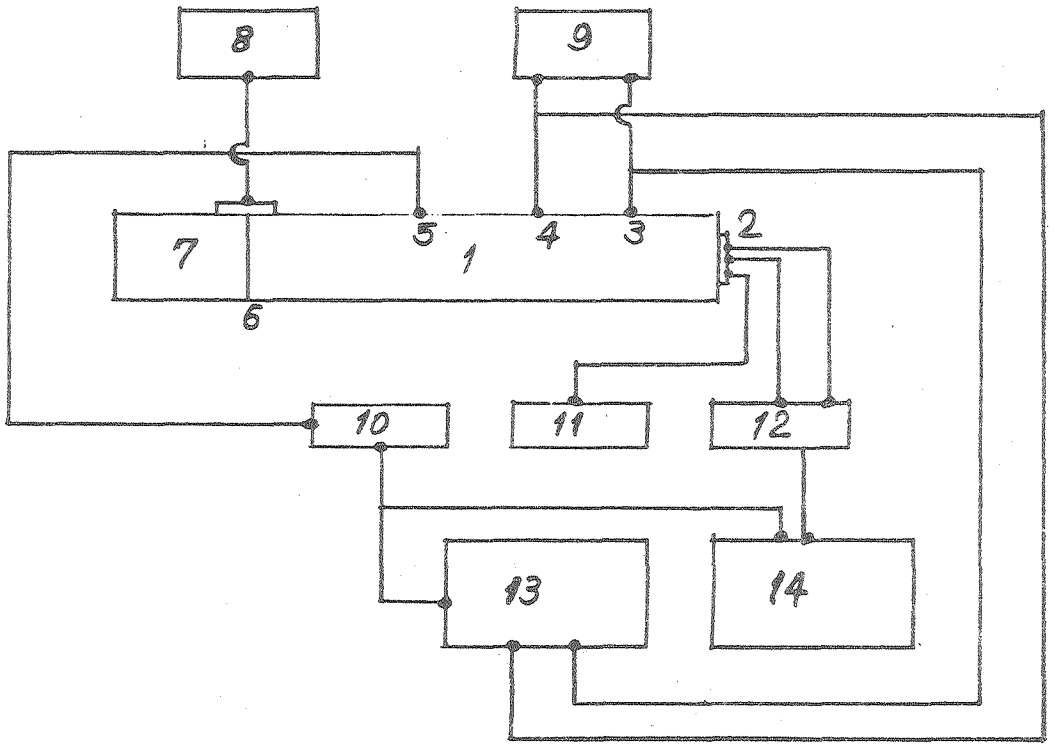

1. Driven Side
2. Heat Transfer Gauge
3. Pressure Transducer
4. Pressure Transducer
5. Trigger
6. Diaphragm
7. Driver Side
8. Control Panel
9. Time Counter
10. Time Delayer
11. Potentiometer
12. Amplifier
13. Oscilloscope
14. Oscilloscope

Figure 2.6. Experimental apparatus.

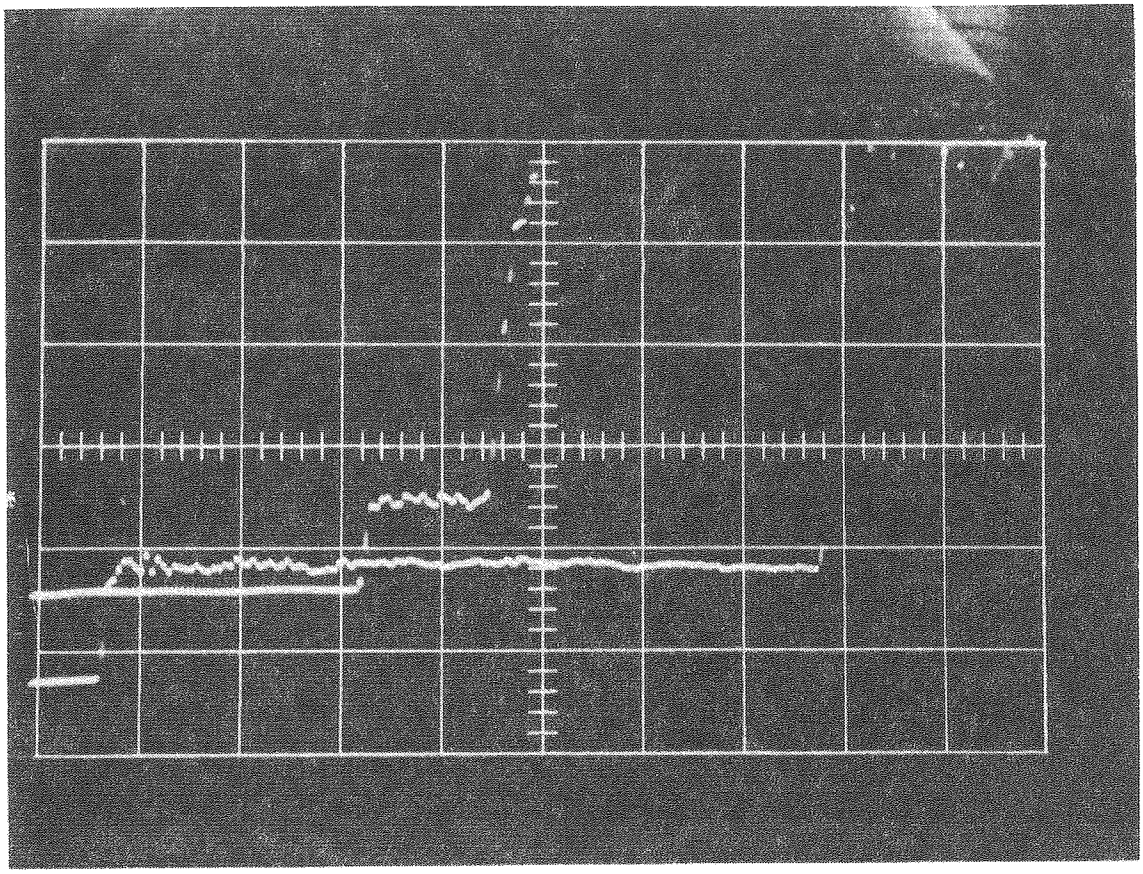

XBB805 6642

Figure 2.7. Pressure measurement, run 214.
Time scale: 10 μsec/cm, Pressure scale: 0.2 v/cm.

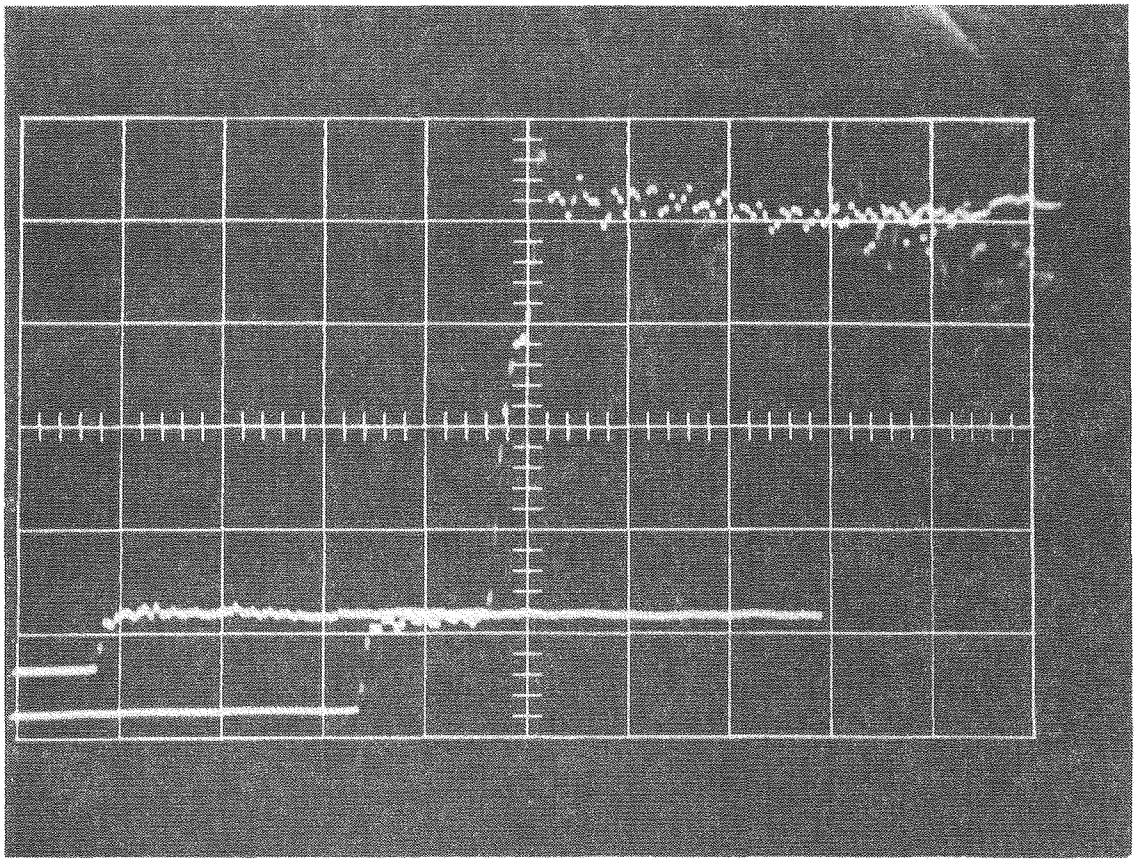

XBB805 6643

Figure 2.8. Pressure measurement, Run 219.
Time scale: 10 μsec, pressure scale: 0.2 v/cm.

III. MEASUREMENTS AND HEAT TRANSFER IN THE SOLID

Experiments were performed in a shock tube to permit the determination of the heat flux at the end wall. This was accomplished by two procedures. The present chapter considers the method which was based on the conduction analysis in the solid (thin film heat transfer gauge as described in Chapter II).

3.1. Measurements

The temporal variation of the temperature at the end wall, T_w, was recorded on an oscilloscope. The signal on this oscilloscope changed from the initial value of 534.5°R (296.9°K) to 542.8°R (301.6°K) for run 214 and from 535.1°R (297.3°K) to 543.1°R (301.7°K) for run 219. The signal remained constant at the new value for about 20 μsec. Then ignition occurred and the signal increased again.

The wall temperature signals for the two runs are shown in Figures 3.1 and 3.2. The horizontal time scale is 4 μsec for each increment; the vertical scale corresponds to temperature and each increment is 0.04 volts. This, multiplied by the calibration constant gives us the temperature.

3.2. Heat Transfer in the Solid

For the small times of interest for the experiment, the wall heat flux can be determined by considering the Macor solid to be a thermally infinite medium since the thermal penetration depth is much smaller than the characteristic dimensions of the gauge. The ceramic

is initially at the room temperature, T_{is}. After the reflection of the shock wave of the end wall, the wall temperature increases to a higher value (Figures 3.1 and 3.2). The one-dimensional conduction equation for a solid is given by:

$$\frac{\partial T}{\partial t} = \alpha_s \frac{\partial^2 T}{\partial x^2} \tag{3.2.1}$$

where α_s is the thermal diffusivity of the solid.

$$\alpha_s = \frac{k_s}{\rho_s c_s} \tag{3.2.2}$$

The initial and boundary conditions are:

$$T(x,0) = T_{is} \tag{3.2.1.a}$$

$$T(0,t) = T_w \tag{3.2.1.b}$$

$$T(\infty,t) = T_{is} \tag{3.2.1.c}$$

For the pre-ignition case both T_{is} and T_w are constant. The solution is given by [5]:

$$\frac{T - T_w}{T_{is} - T_w} = \mathrm{erf}\left(\frac{x}{2\sqrt{\alpha_s t}}\right) \tag{3.2.3}$$

and the heat flux at the end wall by:

$$q_{ws} = -k \frac{\partial T}{\partial x}\bigg|_{x=0} = -k_s \left[\frac{T_{is} - T_w}{\sqrt{\pi \alpha_s t}} e^{-\frac{x^2}{4\alpha_s t}} \right]_{x=0} \tag{3.2.4}$$

or

$$q_{ws} = k_s \frac{T_w - T_{is}}{\sqrt{\pi \alpha_s t}} \tag{3.2.5}$$

For the combustion period, t> 20 μsec, the wall temperature changes continually with time so that:

$$T(0,t) = T_w(t) \tag{3.2.6}$$

The solution in this case can be found using the Duhamel Integral Theorem [4, 5] and the temperature distribution is given by:

$$T(x,t) - T_{is} = (T_w(0) - T_{is})\left(1 - \mathrm{erf}\frac{x}{2\sqrt{\alpha_s t}}\right) + \int_0^t \left(1 - \mathrm{erf}\frac{x}{2\sqrt{\alpha_s (t-\xi)}}\right)\frac{dT_w}{d\xi}\, d\xi \tag{3.2.7}$$

The heat flux at the wall is then given by:

$$q_{ws} = \sqrt{\frac{k_s \rho_s c_s}{\pi}} \int_0^t \frac{1}{\sqrt{(t-\xi)}} \frac{dT_w(\xi)}{d\xi}\, d\xi \tag{3.2.8}$$

or

$$q_{ws} = \sqrt{\frac{k_s \rho_s c_s}{\pi}} \left[\frac{T_w(t) - T_{is}}{\sqrt{t}} + \frac{1}{2} \int_0^t \frac{T_w(t) - T_w(\xi)}{(t-\xi)^{3/2}} d\xi \right] \qquad (3.2.9)$$

The second form (3.2.9) is more convenient to use in numerical calculations since it does not require the calculation of the time derivative of the temperature. Equations (3.2.5) and (3.2.9) yield the results for the wall heat flux that are independent of any assumptions related to the gas. The results depend merely on $T_w(t)$, the wall temperature variation, and the properties of Macor, k_s, ρ_s, c_s. These values are [6]:

$$k_s = 0.968 \text{ Btu/hr ft } ^\circ\text{R } (1.675 \text{ W/m } ^\circ\text{K})$$
$$\rho_s = 146.85 \text{ lb}_m/\text{ft}^3 \ (2352.2S \text{ kg/m}^3)$$
$$c_s = 0.11 \text{ Btu/lb}_m \ ^\circ\text{R } (0.46 \text{ KJ/kg } ^\circ\text{K})$$

The numerical method used to evaluate the integral in Equation (3.2.9) is presented in detail in Appendix A. A sample calculation is given in Appendix B for inert gas runs where the wall temperature is a constant. Note that this is also applicable to the pre-ignition period where the wall temperature is also a constant. The heat fluxes at the end wall calculated from the solid for runs 214 and 219 for the entire time of the experiments are presented in Figures 3.3 and 3.4. In the following chapters comparisons are made of the heat flux, as determined from the solid, with the heat flux as determined from solving the conservation equations in the gas.

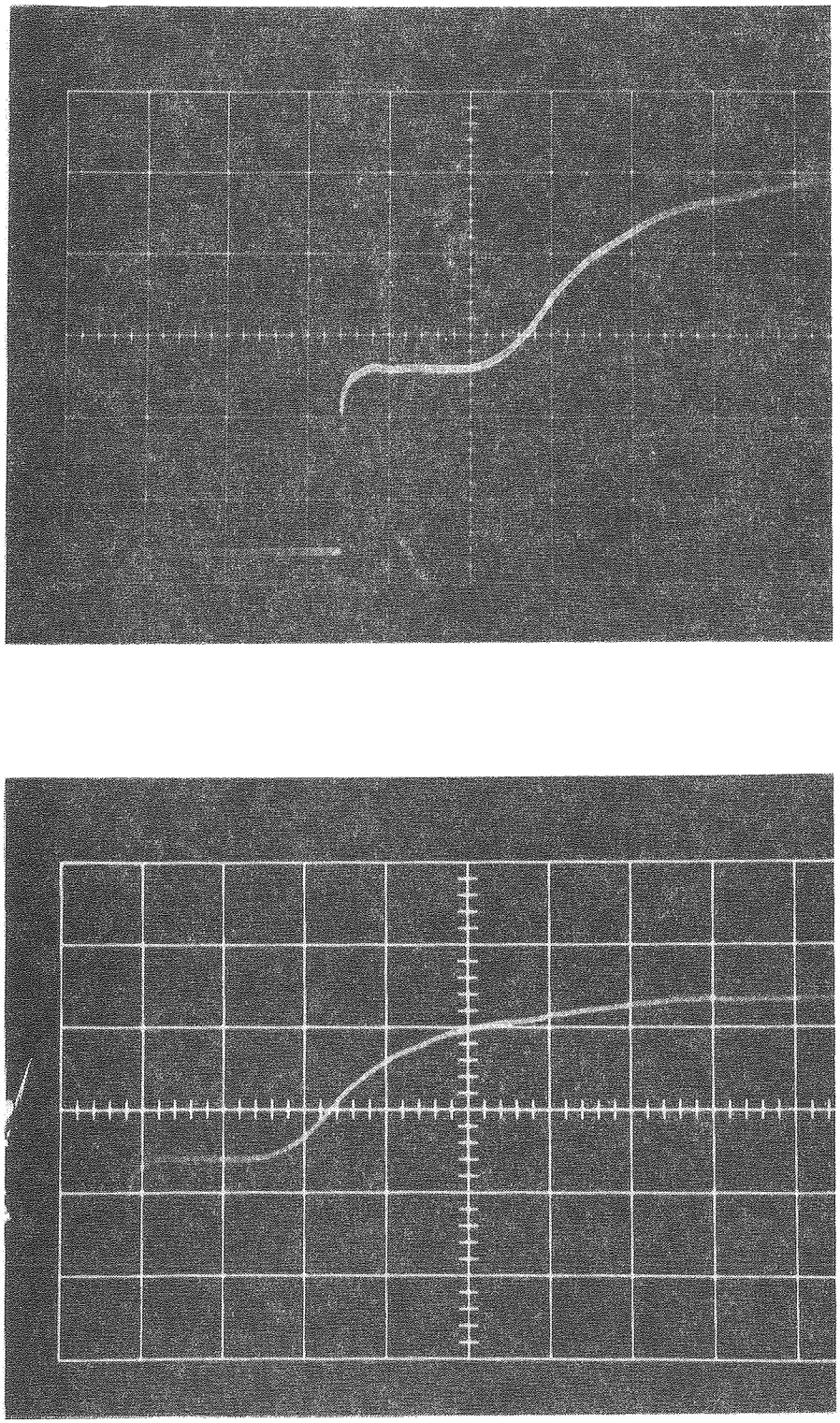

XBB805 6645

Figure 3.1. Surface temperature measurements.

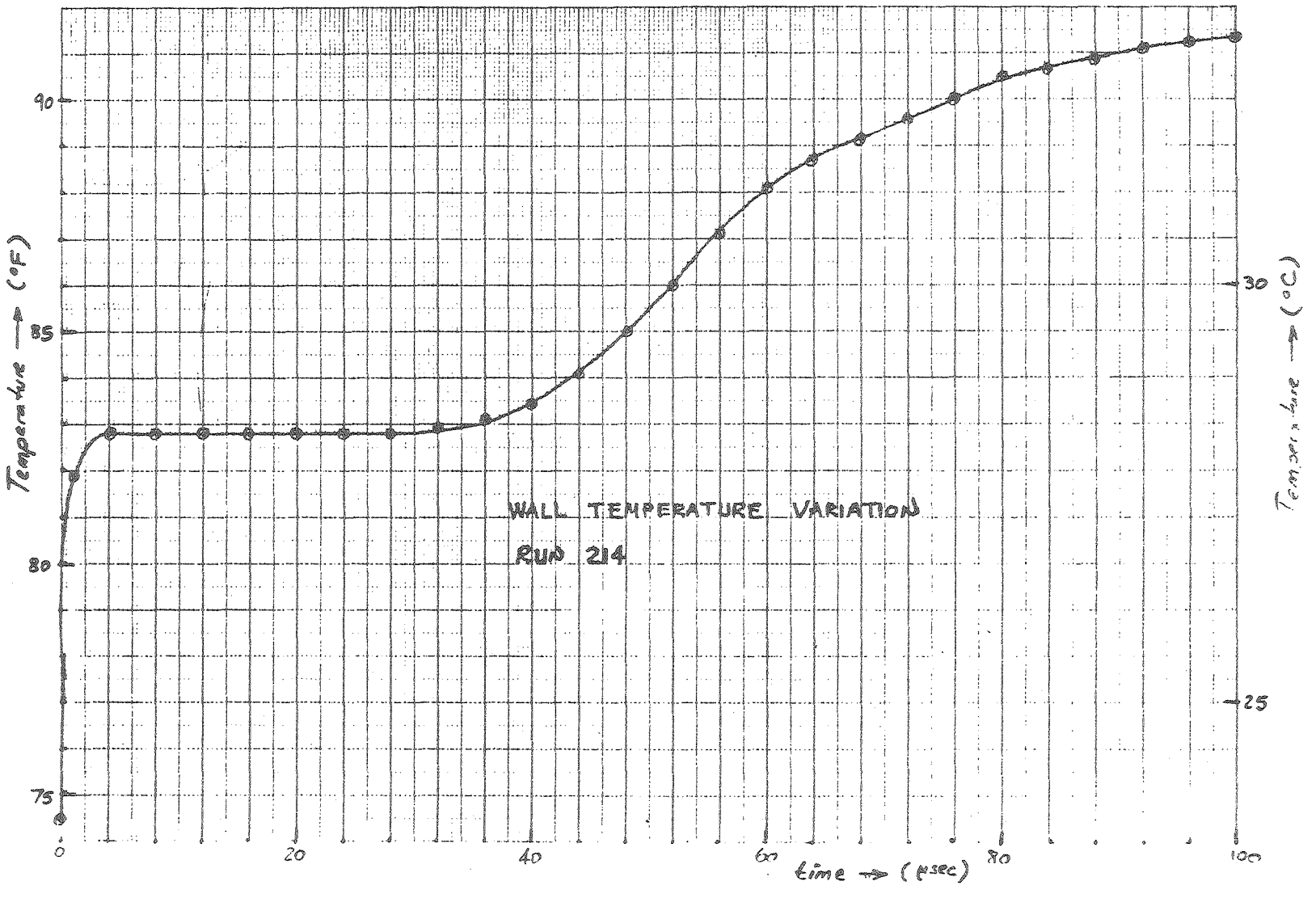

Figure 3.2a. Wall temperature variation.

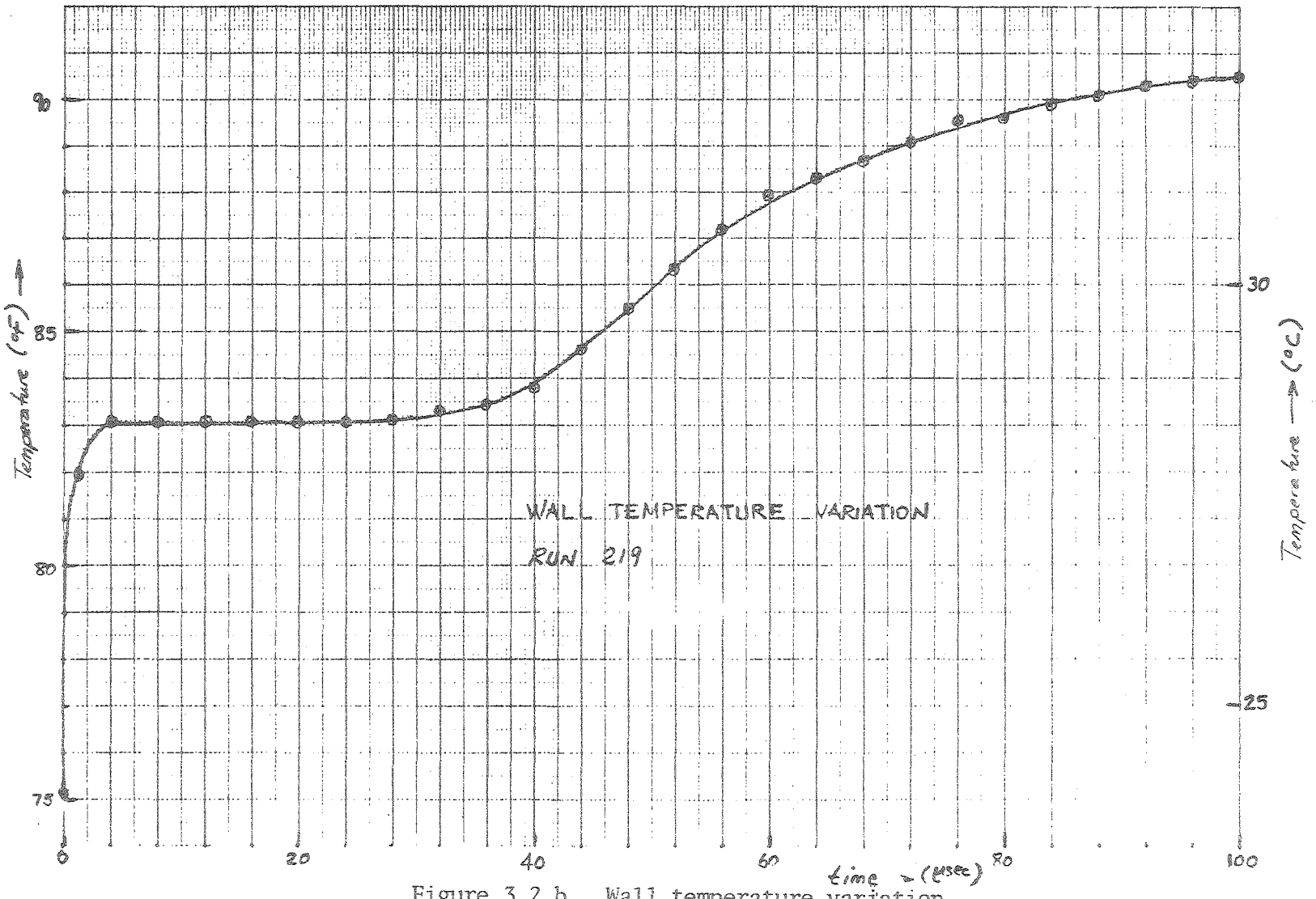

Figure 3.2.b. Wall temperature variation.

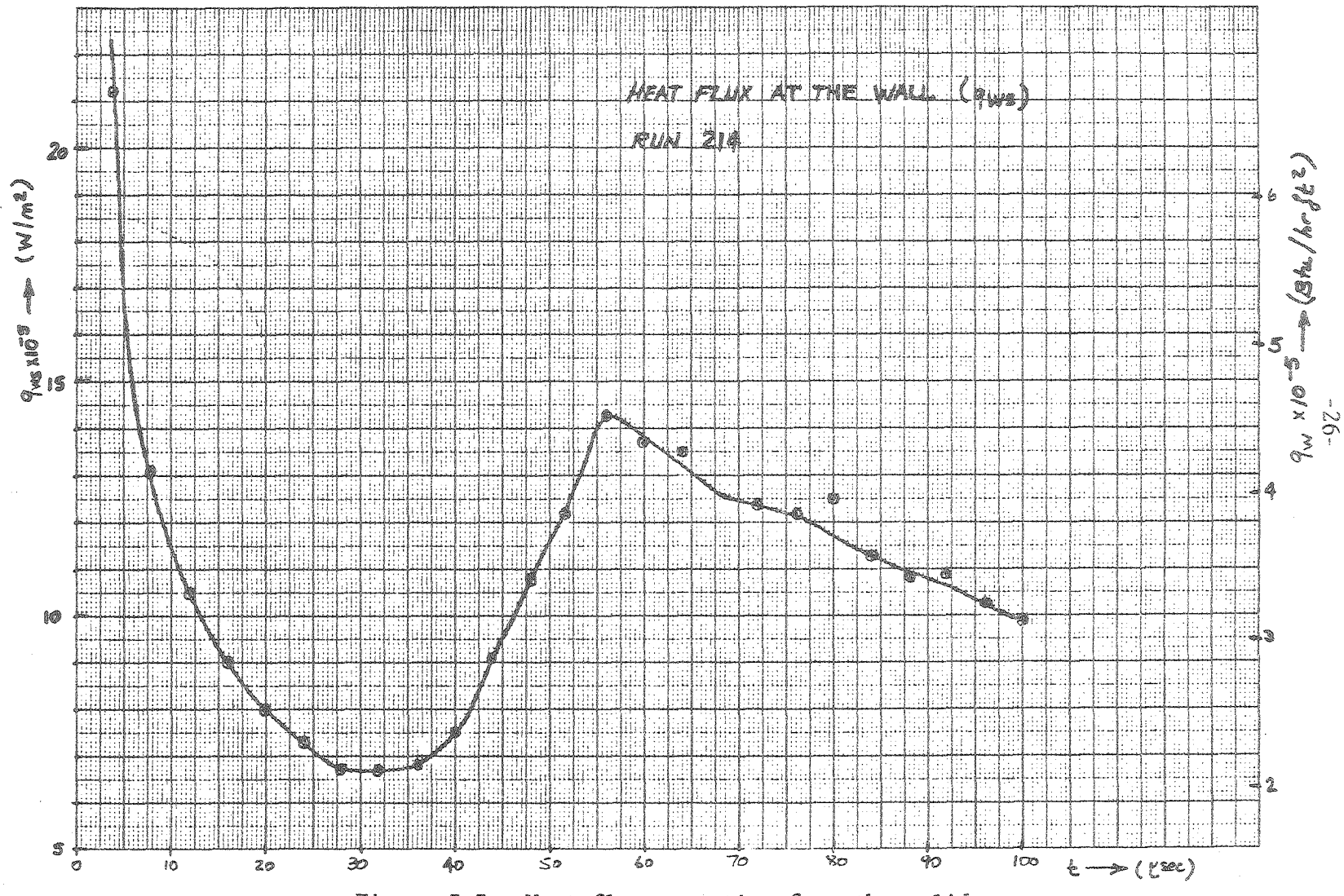

Figure 3.3. Heat flux variation from the solid.

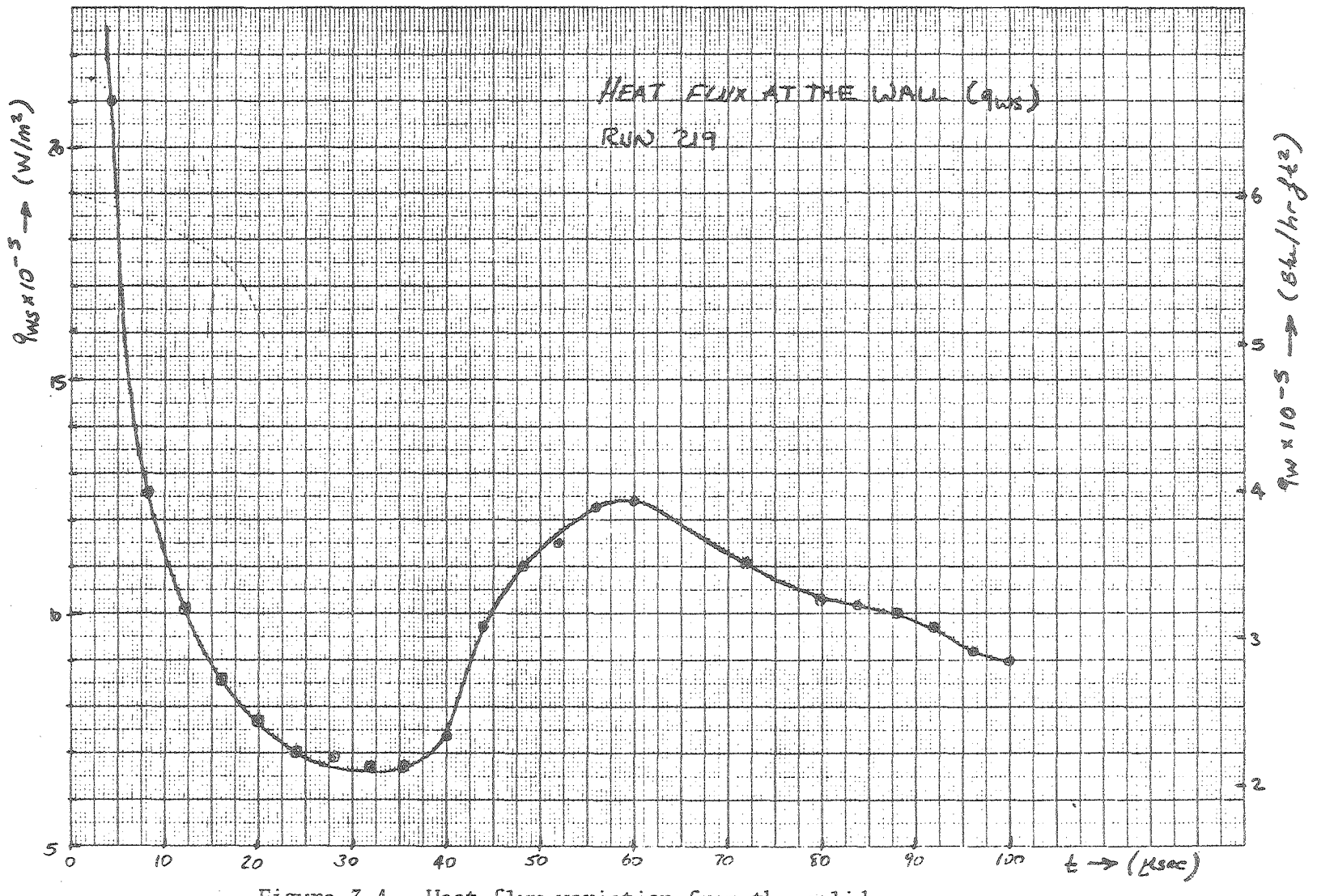

Figure 3.4. Heat flux variation from the solid.

IV. HEAT TRANSFER IN AN INERT GAS

Experiments were performed using an inert gas to provide a simple basis for assessing the accuracy of the experiments and the procedure. For this purpose argon was used as the test gas. Experiments made previously [7] were repeated. The end wall heat transfer was calculated based on the analysis discussed in Chapter III. In addition the end wall heat transfer was calculated from a solution of the conservation equations in the gas.

4.1. Analysis

The gas in the end wall region undergoes a rapid increase in temperature due to shock wave heating from both the incident and reflected shock waves. A thermal boundary layer is formed at the end wall which propagates into the gas. The gas temperature outside the boundary layer remains constant. An analysis based on one-dimensional transport normal to the end wall is therefore appropriate. The unsteady one-dimensional equations of continuity and energy applied to the end wall region are:

$$\frac{\partial \rho}{\partial t} + \frac{\partial}{\partial x}(\rho u) = 0 \tag{4.1.1}$$

$$\rho c_p \left[\frac{\partial T}{\partial t} + u \frac{\partial T}{\partial x} \right] = \frac{\partial}{\partial x}\left[k(T) \frac{\partial T}{\partial x} \right] \tag{4.1.2}$$

The initial and boundary conditions are:

$$T(x, o) = T_{ig} \tag{4.1.2.a}$$

$$T(0, t) = T_w \tag{4.1.2.b}$$

$$T(\infty, t) = T_{ig} \tag{4.1.2.c}$$

The momentum equation yields that the pressure can be taken to be constant normal to the end wall. A stream function ψ is defined according to:

$$\frac{\partial \psi}{\partial x} = \frac{\rho}{\rho_w} \tag{4.1.3}$$

$$\frac{\partial \psi}{\partial t} = -\frac{\rho u}{\rho_w} \tag{4.1.4}$$

where ρ_w is the constant gas density at the wall. The wall temperature remains constant after the shock wave reflects. Making a transformation from x, t to ψ, t coordinates, the derivatives can be expressed as:

$$\left.\frac{\partial}{\partial x}\right|_t = \frac{\rho}{\rho_w} \left.\frac{\partial}{\partial \psi}\right|_t \tag{4.1.5}$$

$$\left.\frac{\partial}{\partial t}\right|_x = -\frac{\rho u}{\rho_w} \left.\frac{\partial}{\partial \psi}\right|_t + \left.\frac{\partial}{\partial t}\right|_\psi \tag{4.1.6}$$

The stream function satisfies the continuity equation. The energy equation in the new coordinates becomes:

$$\frac{\partial T}{\partial t} = \frac{1}{\rho_w C_p} \frac{\partial}{\partial \psi} \left[k \frac{\rho}{\rho_w} \frac{\partial T}{\partial \psi} \right] \tag{4.1.7}$$

Defining a non-dimensional temperature θ, non-dimensional thermal conductivity λ and a thermal diffusivity α_w according to:

$$\theta = \frac{T}{T_w} \tag{4.1.8}$$

$$\lambda = \frac{k}{k_w} \tag{4.1.9}$$

$$\alpha_w = \frac{k_w}{\rho_w C_p} \tag{4.1.10}$$

yields

$$\frac{\partial \theta}{\partial t} = \alpha_w \frac{\partial}{\partial \psi}\left[\lambda \frac{\rho}{\rho_w} \frac{\partial \theta}{\partial \psi}\right] \tag{4.1.11}$$

For argon the specific heat is constant. The pressure remains constant after the reflection of the shock wave off the end wall. In this case for an ideal gas,

$$\frac{\rho}{\rho_w} = \frac{T_w}{T} = \frac{1}{\theta} \tag{4.1.12}$$

Thus the energy equation becomes:

$$\frac{\partial \theta}{\partial t} = \alpha_w \frac{\partial}{\partial \psi}\left[\frac{\lambda}{\theta} \frac{\partial \theta}{\partial \psi}\right] \tag{4.1.13}$$

Since there are no time and length scales in the problem, a similarity solution is sought. A similarity variable η can be defined according to:

$$\eta = \frac{\psi}{\sqrt{2\alpha_w t}} \tag{4.1.14}$$

The partial derivatives can be expressed as:

$$\frac{\partial \eta}{\partial \psi} = \frac{1}{\sqrt{2\alpha_w t}} \tag{4.1.15}$$

$$\frac{\partial \eta}{\partial t} = -\frac{\psi}{2\sqrt{2\alpha_w t^3}} \tag{4.1.16}$$

Substituting into the energy equation yields:

$$\frac{d}{d\eta}\left[\frac{\lambda}{\theta}\frac{d\theta}{d\eta}\right] + \eta\frac{d\theta}{d\eta} = 0 \qquad (4.1.17)$$

The boundary conditions are:

$$\theta(0) = 1 \qquad (4.1.17.a)$$

$$\theta(\infty) = \frac{T_\infty}{T_w} \qquad (4.1.17.b)$$

A power law variation is used for the dependence of the thermal conductivity on the temperature.

$$\frac{k}{k_w} = \lambda = \left[\frac{T}{T_w}\right]^a \qquad (4.1.18)$$

For the special case of a = 1.0, the energy equation reduces to:

$$\frac{d^2\theta}{d\eta^2} + \eta\frac{d\theta}{d\eta} = 0 \qquad (4.1.19)$$

$$\theta(0) = 1 \qquad (4.1.19.a)$$

$$\theta(\infty) = \frac{T_\infty}{T_w} = \theta_\infty \qquad (4.1.19.b)$$

The solution of this ordinary differential equation is:

$$\theta(\eta) = (\theta_\infty - 1)\,\mathrm{erf}(\eta/\sqrt{2}) + 1 \qquad (4.1.20)$$

The heat flux at the wall is given by:

$$q_w = -k\left.\frac{\partial T}{\partial x}\right|_w = -k\left.\frac{\partial T}{\partial \theta}\frac{\partial \theta}{\partial \eta}\frac{\partial \eta}{\partial \psi}\frac{\partial \psi}{\partial x}\right|_w$$

$$= -T_w\sqrt{\frac{k_w \rho_w C_p}{2t}}\left.\frac{\partial \theta}{\partial \eta}\right|_{\eta=0} \qquad (4.1.21)$$

For the special case of a = 1.0 the heat flux simplifies to:

$$q_w = \sqrt{\frac{k_w \rho_w C_p}{\pi t}} \left(1 - T_\infty\right) \tag{4.1.22}$$

For gases where a is not unity the energy equation can be solved numerically [7]. A sample calculation is presented in Appendix B.

4.2. Results and Discussion:

On the basis of the preceding work, two results are obtained for the end wall heat flux, q_{ws}, based on the solid analysis (Chapter 3) and q_{wg}, based on the gas analysis (Chapter 4). The wall temperature variations for an inert gas, argon, are shown in Figure 4.1 and plotted in Figures 4.2 and 4.3 for runs 104 and 108. The temperature at the end wall increases rapidly to a higher value when the shock wave reflects off the wall and stays constant at this value. From this information the heat flux at the wall can be calculated as described in Chapter 3 and q_{ws}, for a step change in the surface temperature is given by:

$$q_{ws} = k_s \frac{T_w - T_{is}}{\sqrt{\pi \alpha_s t}} \tag{4.2.1}$$

The heat flux can also be calculated from the solution of the conservation equations in the gas, q_{wg}, as described in this chapter and is given by:

$$q_{wg} = T_w \sqrt{\frac{k_w \rho_w C_p}{2t}} \left[- \frac{\partial \theta}{\partial \eta} \right]_{\eta = 0} \tag{4.2.2}$$

The derivative at $\eta = 0$ is obtained from a numerical solution of Equation (4.1.17) [7]. The free stream temperature of the gas, outside the end wall boundary layer is calculated from the shock relations [3]. A sample calculation is given in Appendix B. The two heat fluxes have the same functional form, a constant divided by the square root of time.

$$q_w \left(W/m^2\right) = \frac{C}{\sqrt{t\,(sec)}} \tag{4.2.3}$$

The constant is determined by the variables of the specific run. Property values for the solid were given in Chapter 2. For run 104 this constant was 32.3 in q_{wg} and 29.8 in q_{ws}. SI units are used such that if the time is substituted in seconds, the heat flux will be W/m^2. For run 108 the constant was calculated as 29.4 in q_{wg} and 28.8 in q_{ws}. These results are presented in Figures 4.4 and 4.5.

The dimensionless difference between q_{wg} and q_{ws} is given by:

$$\varepsilon = \frac{q_{wg} - q_{ws}}{q_{ws}} \tag{4.2.4}$$

$$\varepsilon = 1 - \sqrt{\frac{\pi k_w \rho_w C_p}{2 k_s \rho_s C_s}} \left[\frac{\partial \theta}{\partial \eta}\right]_{\eta=0} \frac{T_w}{T_w - T_{is}} \tag{4.2.5}$$

This difference is independent of time and depends only on the property values and the wall temperature. The difference was 8.2% for run 104 and 2.6% for run 108. Thus the results from the solid side analysis and the results from the gas side analysis are in good agreement.

A heat transfer coefficient can also be defined based on the heat flux at the wall in the solid, h_s, and in the gas, h_g. They are given by:

$$h = \frac{(-q_w)}{T_\infty - T_w} \tag{4.2.6}$$

such that

$$h_s = \sqrt{\frac{k_s \rho_s C_s}{\pi t}} \quad \frac{T_w - T_{is}}{T_\infty - T_w} \tag{4.2.7}$$

$$h_g = \sqrt{\frac{k_w \rho_w C_p}{2t}} \quad \frac{T_w}{T_\infty - T_w} \quad \left.\frac{\partial \theta}{\partial \eta}\right|_{\eta=0} \tag{4.2.8}$$

T_∞ is the free stream temperature of the gas which is the temperature behind the reflected shock wave. The two heat transfer coefficients are shown in Figures 4.6 and 4.7.

In the next chapter (Chapter 5) the analysis is extended to gas mixtures and in Chapter 6 to reacting gases. For a gas mixture the same analysis can be applied but the appropriate property values should be used.

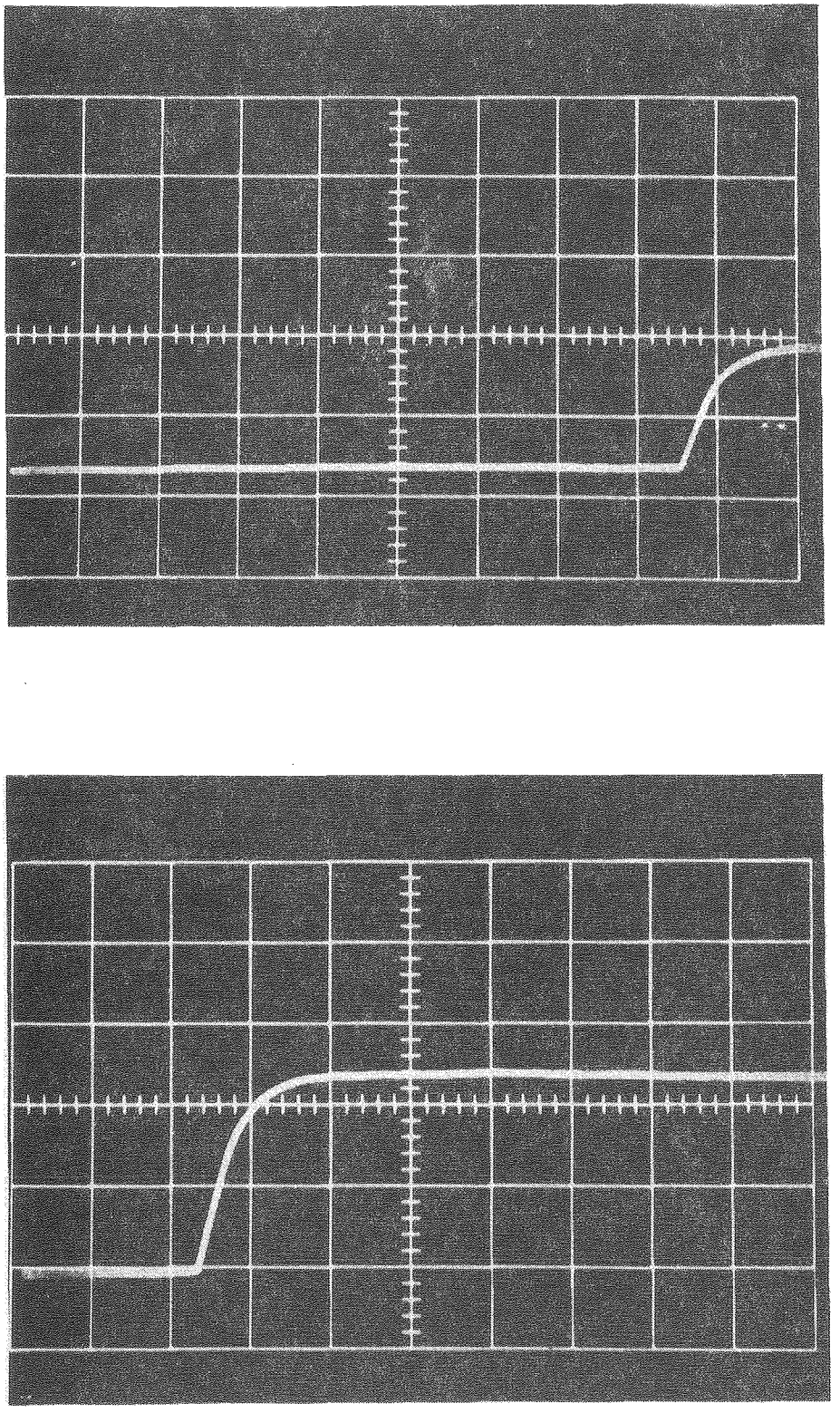

XBB805 6647

Figure 4.1. Surface temperature measurement, inert gas, argon.
Run 104 and Run 108
Time scale: 20 μsec/cm.
Temperature scale: 0.1 v/cm (104)
0.05 v/cm (108)

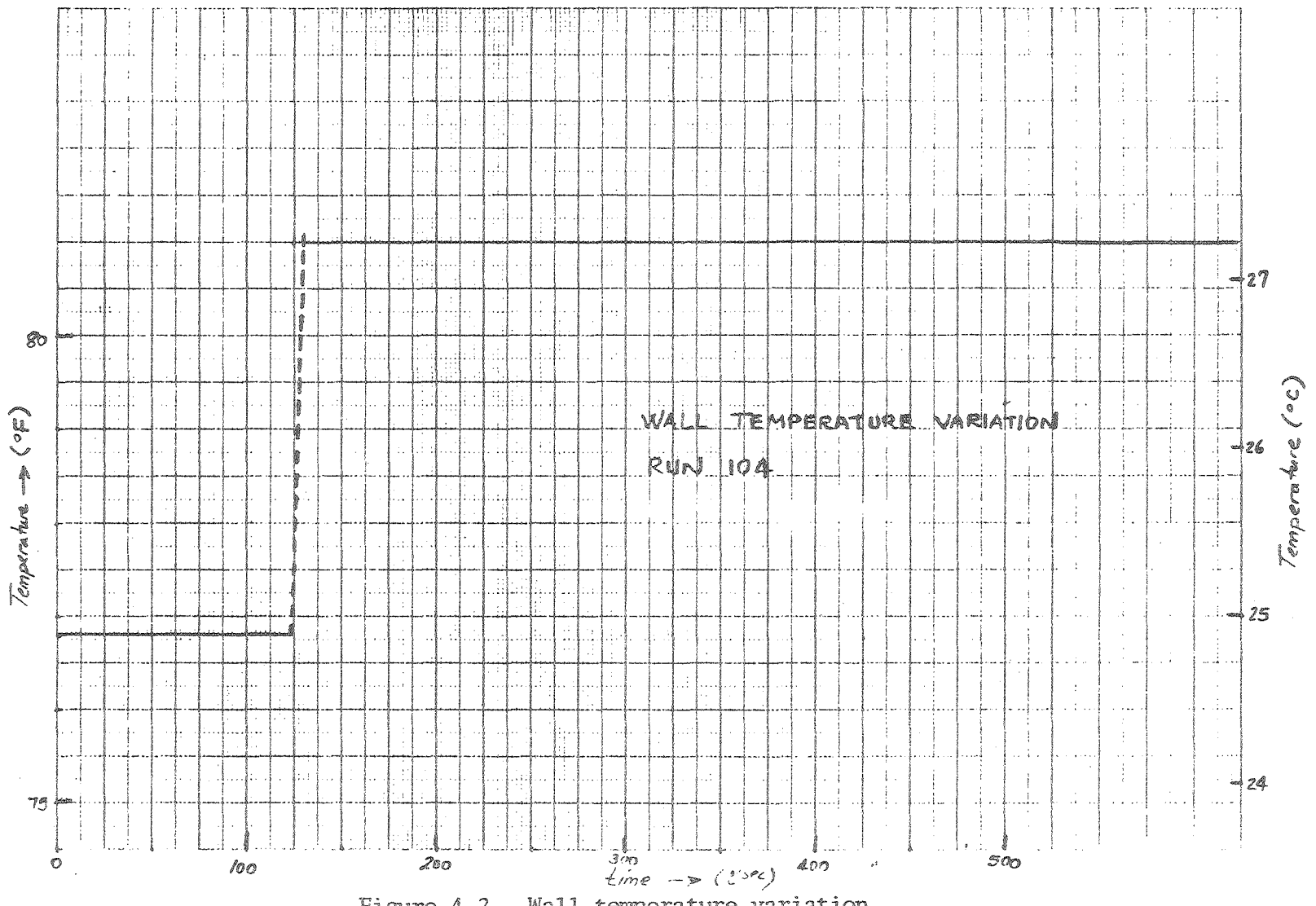

Figure 4.2. Wall temperature variation.

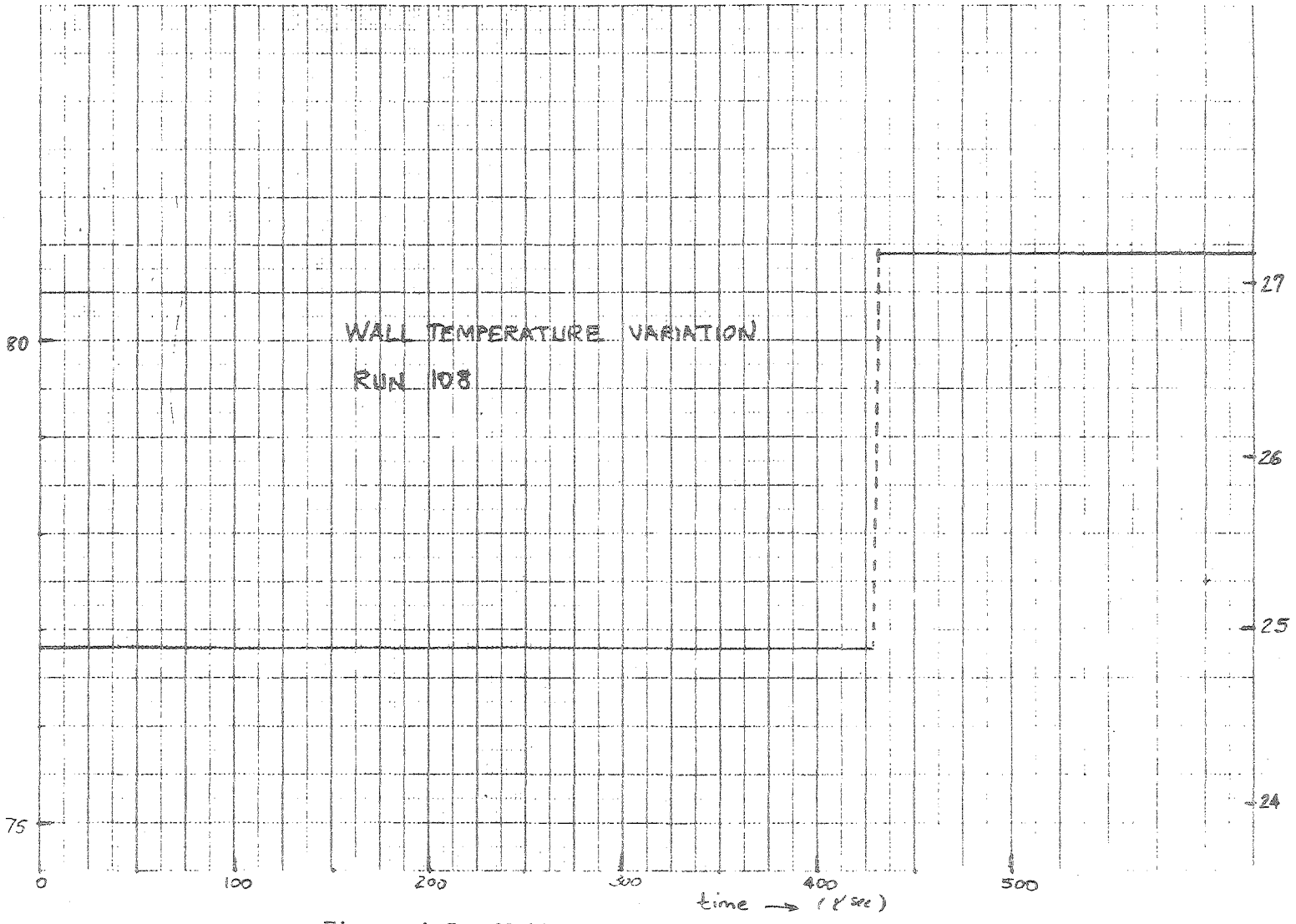

Figure 4.3. Wall temperature variation.

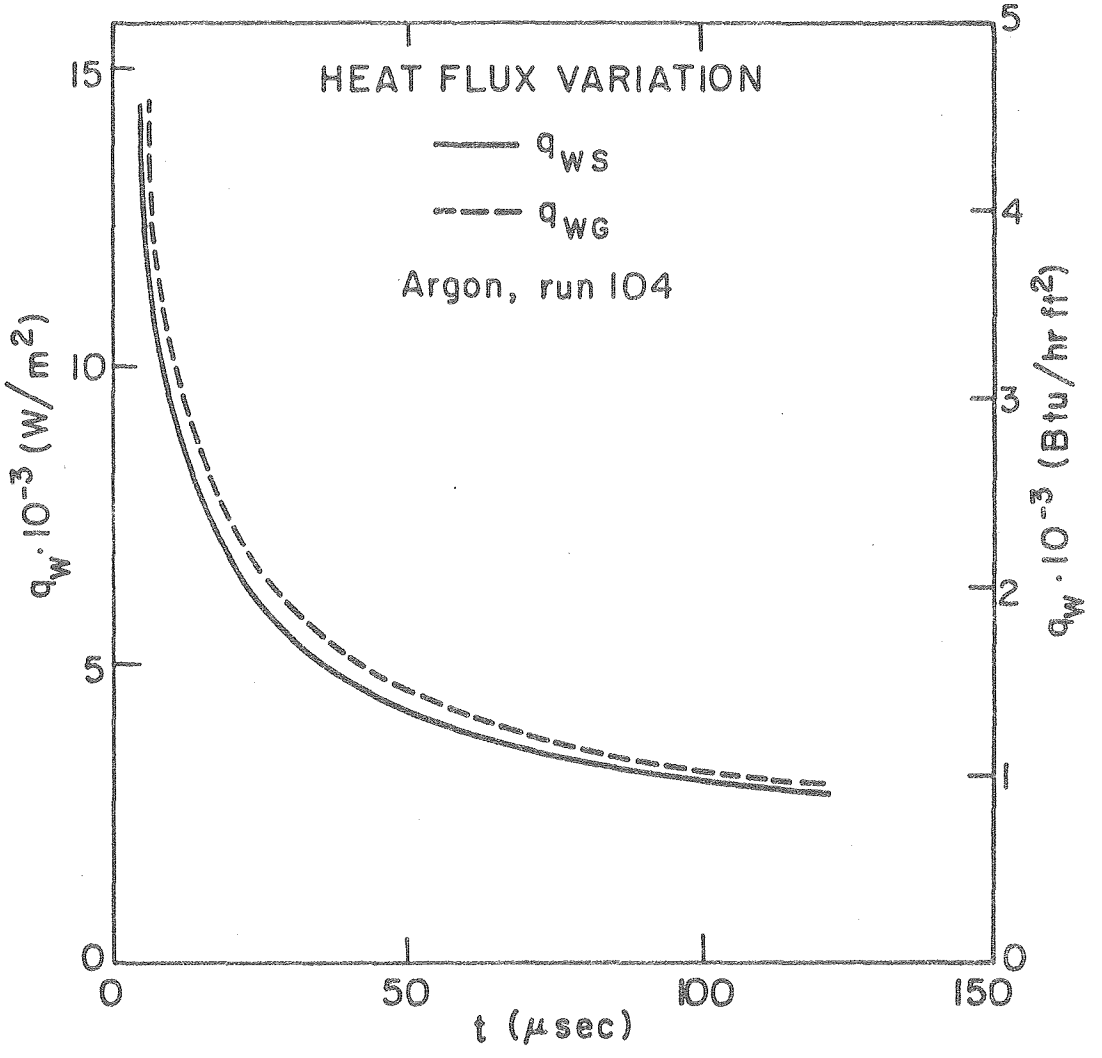

Figure 4.4. Heat flux variation.

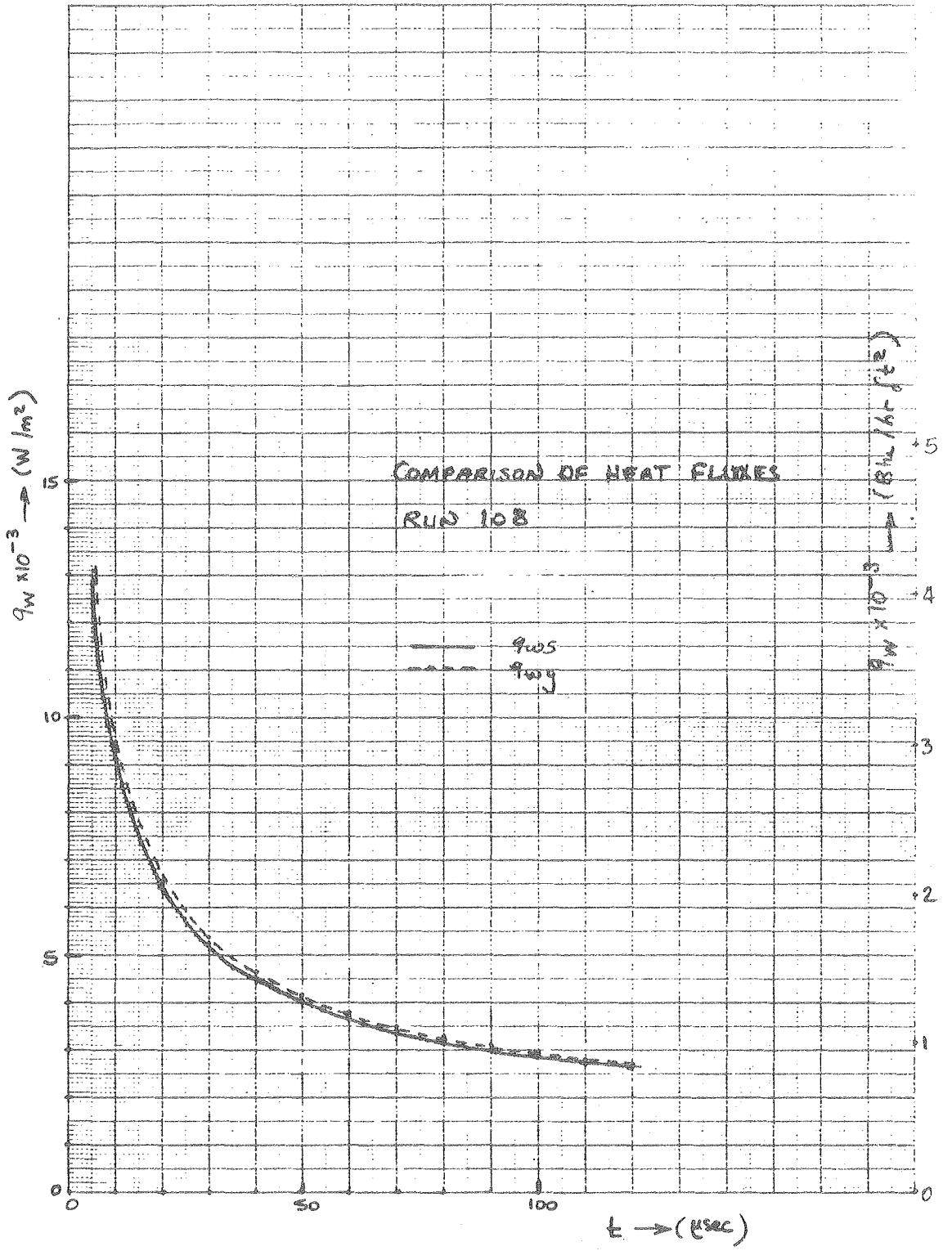

Figure 4.5. Heat flux variation.

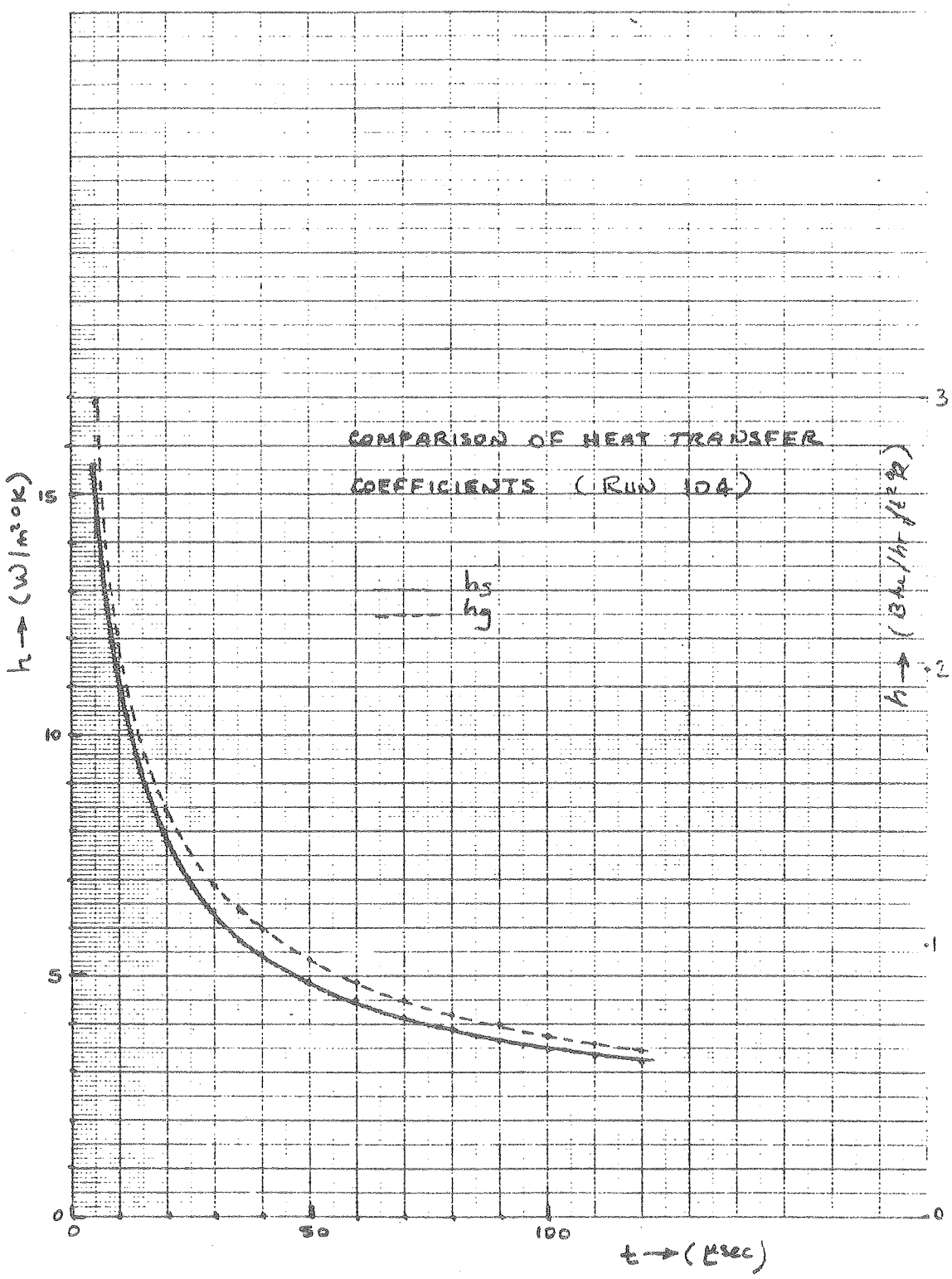

Figure 4.6. Heat transfer coefficient.

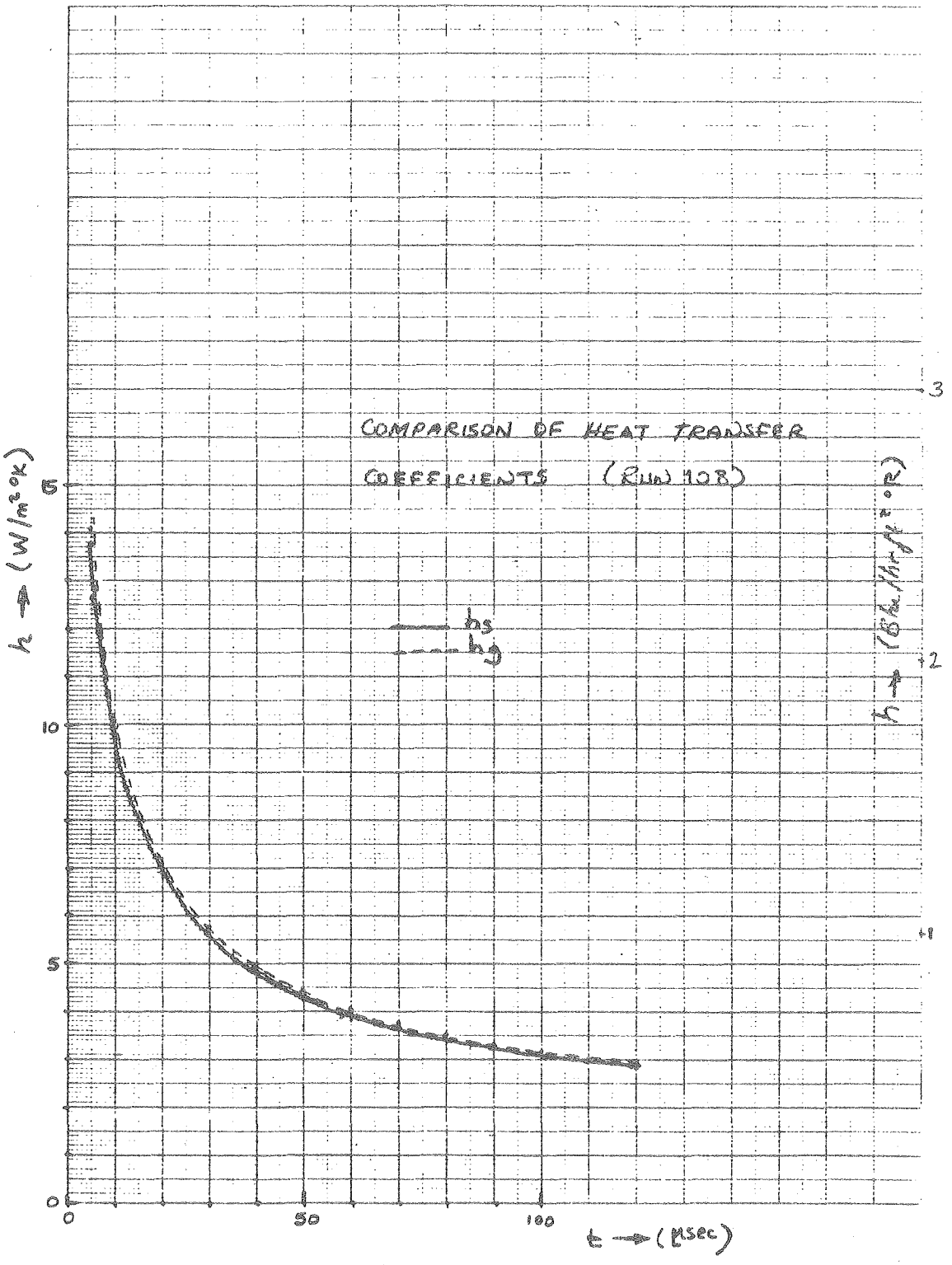

Figure 4.7. Heat transfer coefficient.

V. HEAT TRANSFER IN THE GAS: PRE-IGNITION PERIOD

A mixture composed of hydrogen and oxygen diluted in argon ($2\ H_2 + O_2 + 27\ Ar$) is considered. During the pre-ignition period the mixture is a non-reacting gas and since the species present are uniformly distributed there are no diffusion effects. The gas in the end wall region undergoes a rapid increase in temperature due to shock wave heating from both the incident and the reflected shock waves. An analysis is made based on one-dimensional transport normal to the end wall. The results are compared in terms of the heat flux.

5.1. Analysis

The unsteady one-dimensional equations of continuity and energy as applied to the end wall region are:

$$\frac{\partial \rho}{\partial t} + \frac{\partial}{\partial x}(\rho u) = 0 \tag{5.1.1}$$

$$\rho C_p \left[\frac{\partial T}{\partial t} + u \frac{\partial T}{\partial x}\right] = \frac{\partial}{\partial x}\left[k \frac{\partial T}{\partial x}\right] \tag{5.1.2}$$

The initial and boundary conditions are:

$$T(x,o) = T_{ig} \tag{5.1.2.a}$$

$$T(o,t) = T_w \tag{5.1.2.b}$$

$$T(\infty,t) = T_{ig} \tag{5.1.2.c}$$

The momentum equation yields that the pressure may be taken to be constant. A stream function ψ is defined according to:

$$\frac{\partial \psi}{\partial x} = \frac{\rho}{\rho_{ig}} \tag{5.1.3}$$

$$\frac{\partial \psi}{\partial t} = -\frac{\rho u}{\rho_{ig}} \tag{5.1.4}$$

where ρ_{ig} is the initial constant density of the gas, ρ_5. Making a transformation from x, t to ψ, t coordinates the partial derivatives can be expressed as:

$$\left.\frac{\partial}{\partial x}\right|_t = \frac{\rho}{\rho_{ig}} \left.\frac{\partial}{\partial \psi}\right|_t \tag{5.1.5}$$

$$\left.\frac{\partial}{\partial t}\right|_x = -\frac{\rho u}{\rho_{ig}} \left.\frac{\partial}{\partial \psi}\right|_t + \left.\frac{\partial}{\partial t}\right|_\psi \tag{5.1.6}$$

The stream function satisfies the continuity equation and the energy equation is then given by:

$$\frac{\partial T}{\partial t} = \frac{1}{c_p \rho_{ig}} \frac{\partial}{\partial \psi}\left[k \frac{\rho}{\rho_{ig}} \frac{\partial T}{\partial \psi}\right] \tag{5.1.7}$$

A number of assumptions have been made to solve Equation (5.1.2). The specific heat of the gas is taken to be constant equal to the mass averaged value for the mixture. The gas is treated ideal. The thermal conductivity of the gas is assumed to have a power law dependence with temperature according to:

$$\frac{k}{k_{ig}} = \left[\frac{T}{T_{ig}}\right]^a \tag{5.1.8}$$

For an ideal gas, at constant pressure we have

$$\frac{\rho}{\rho_{ig}} = \frac{T_{ig}}{T} \tag{5.1.9}$$

Using Equations (5.1.8) and (5.1.9) the energy equation becomes

$$\frac{\partial T}{\partial t} = \alpha_{ig} \; T_{ig}^{(1-a)} \frac{\partial}{\partial \psi}\left[T^{(a-1)} \frac{\partial T}{\partial \psi}\right] \tag{5.1.10}$$

where,

$$\alpha_{ig} = \frac{k_{ig}}{\rho_{ig} C_p} \tag{5.1.11}$$

Defining a new non-dimensional temperature U, according to:

$$U = \left[\frac{T}{T_{ig}}\right]^a \tag{5.1.12}$$

yields

$$\frac{\partial U}{\partial t} = \alpha_{ig} U^{\frac{a-1}{a}} \frac{\partial^2 U}{\partial \psi^2} \tag{5.1.13}$$

The boundary and initial conditions are given by:

$$U(0,t) = \left[\frac{T_w}{T_{ig}}\right]^a \tag{5.1.13.a}$$

$$U(\infty,t) = 1 \tag{5.1.13.b}$$

$$U(\psi,0) = 1 \tag{5.1.13.c}$$

Since the change in the wall temperature is small, U(o, t) is taken to be constant to simplify the calculations. The heat flux at the wall is given by:

$$q_w = -k\frac{\partial T}{\partial x}\bigg|_w = -k_w\frac{\partial T}{\partial U}\frac{\partial U}{\partial \psi}\frac{\partial \psi}{\partial x}\bigg|_w$$

$$= -\frac{k_w}{a}\frac{T_{ig}^{(a+1)}}{T_w^{a}}\frac{\partial U}{\partial \psi}\bigg|_{\psi=0} \qquad (5.1.14)$$

A penetration depth can also be evaluated using Equation (5.1.4) as explained in Appendix H.

5.2. Numerical Method

An explicit finite difference method has been used to solve Equation (5.1.13). The difference equation is given by:

$$\frac{U_{j,k+1}-U_{j,k}}{\Delta t} = \alpha_{ig}\, U_{j,k}^{\frac{a-1}{a}}\left[\frac{U_{j+1,k}-2U_{j,k}+U_{j-1,k}}{(\Delta\psi)^2}\right] \qquad (5.2.1)$$

which can be rearranged as follows:

$$U_{j,k+1} = \frac{\alpha_{ig}\Delta t}{(\Delta\psi)^2}\, U_{j,k}^{\frac{a-1}{a}}\left(U_{j+1,k}+U_{j-1,k}\right)+\left(1-2\frac{\alpha_{ig}\Delta t}{(\Delta\psi)^2}U_{j,k}^{\frac{a-1}{a}}\right)U_{j,k} \qquad (5.2.2)$$

Defining the stability factor M as

$$M = \frac{\alpha_{ig}\Delta t}{(\Delta\psi)^2} \qquad (5.2.3)$$

yields

$$U_{j,k+1} = \left(1-2M\,U_{j,k}^{\frac{a-1}{a}}\right)U_{j,k}+U_{j,k}^{\frac{a-1}{a}}M\left(U_{j+1,k}+U_{j-1,k}\right) \qquad (5.2.4)$$

subject to the following initial and boundary conditions:

$$U(j=1, k=1,\ldots,n) = \left[\frac{T_w}{T_{ig}}\right]^a \tag{5.2.4.a}$$

$$U(j=m, k=1,\ldots,n) = 1 \tag{5.2.4.b}$$

$$U(j=1,\ldots,m, k=1) = 1 \tag{5.2.4.c}$$

The location j = m is taken as the point at which the temperature has the value .99 T_{ig}.

The stability criteria for Equation (5.24) is

$$1 - 2M\, U_{j,k}^{\frac{a-1}{a}} \geqslant 0 \tag{5.2.5}$$

or

$$M \leqslant \frac{U_{j,k}^{\frac{1-a}{a}}}{2} \tag{5.2.6}$$

$U_{j,k}$ assumes its smallest value at the wall, which is:

$$(U_{j,k})_{min} = \left[\frac{T_w}{T_{ig}}\right]^a \tag{5.2.7}$$

Therefore the stability condition is

$$M \leqslant \frac{1}{2}\left[\frac{T_w}{T_{ig}}\right]^{(1-a)} \tag{5.2.8}$$

The heat flux at the wall requires the derivative to be evaluated at $\psi = 0$. The different expressions have been used for the evaluation of this derivative [8].

$$\left.\frac{\partial U}{\partial \psi}\right|_{\psi=0} = \frac{U_{2,k} - U_{1,k}}{\Delta \psi} \tag{5.2.9}$$

$$\left.\frac{\partial U}{\partial \psi}\right|_{\psi=0} = \frac{-U_{3,k} + 4U_{2,k} - 3U_{1,k}}{2\Delta \psi} \tag{5.2.10}$$

$$\left.\frac{\partial U}{\partial \psi}\right|_{\psi=0} = \frac{2U_{4,k} - 9U_{3,k} + 18U_{2,k} - 11U_{1,k}}{6\Delta \psi} \tag{5.2.11}$$

This formulation has been used until ignition takes place. When ignition begins the combustion period analysis, presented in the next chapter, is used. For the special case of a = 1, the transformed energy Equation (5.1.13) becomes the diffusion equation and has the well known error function solution [5]. This case is presented in Appendix E.

5.3. Results and Discussion

In this chapter we are only considering the pre-ignition period which corresponds to the first 20 μsec after the shock wave has reflected off the end wall. During this time ignition has not yet occurred and there is no reaction. The work presented in Chapter 4 is applicable to this time period with the property values for the mixture being used. The evaluation of these values are presented in Appendix C.

The complete temporal variations of the temperature of the end wall for runs 214 and 219 were shown in Figure 3.1 and were plotted in Figures 3.2a and 3.2b. The heat flux from the solid analysis, q_{ws}, was also presented in Chapter 3. Now we can compare this result with the heat flux, q_{wg}, obtained from solving the conservation equations in the gas. Equation (5.1.14) gives this heat flux, q_{wg}. The two heat fluxes

are compared in Figure 5.1 for run 214 and in Figure 5.2 for run 219. The results are in good agreement with errors of 4% and 6% at $\tau = 20$ μsec. Also shown on these figures are the heat fluxes obtained with the approximation $a = 1.0$ which permits an exact solution as presented in Appendix E. The mixture contains 90% Ar by volume and the thermal conductivity dependence on temperature for argon is to the 0.7 power [10, 11]. Hence the heat flux curve corresponding to $a = 0.7$ should be closer to the experimental heat flux curve, q_{ws}.

A heat transfer coefficient, h, can be defined similar to Chapter 4 based on the heat flux, q_w.

$$h = \frac{(-q_w)}{T_\infty - T_w} \tag{5.4.1}$$

These results are presented in Figure 5.3 for run 214 and in Figure 5.4 for run 219. The free stream gas temperature, T_∞, and the wall temperature, T_w, do not depend on time for this period. Therefore the variation of the heat transfer coefficient curves and the heat flux curves are similar.

The importance of the work presented in this chapter is that it yields the temperature distribution in the gas boundary layer next to the end wall and a "penetration depth" at the time of ignition ($t = 20$ μsec). This information is essential for the analysis of the combustion period. At 20 μsec this is the initial temperature distribution for the combustion period. Also the penetration depth at 20 μsec is used as the initial location of the combustion zone. This will be discussed in the next chapter.

In Figures 5.5 and 5.6 three temperature profiles are given for t = 5 μsec, 10 μsec, and 20 μsec. As noted above the last one is the initial temperature distribution for the combustion period. The temperatures are obtained from the numerical solution of Equation (5.1.13).

The penetration depth is defined as the distance from the end wall where the temperature of the gas reaches 0.99 T_∞. The variation of the untransformed penetration depth, δ_B, with time is shown in Figure 5.7 for run 214 and in Figure 5.8 for run 219. In order to obtain this penetration depth a transformation back from the ψ coordinate is necessary. This transformation is presented in detail in Appendix H. Since the pressure in the gas is constant for this period the transformation can be expressed in terms of the temperature only.

In the next chapter the temperatuure distribution and the penetration depth at ignition will be used to evaluate the heat transfer in the gas during the combustion period.

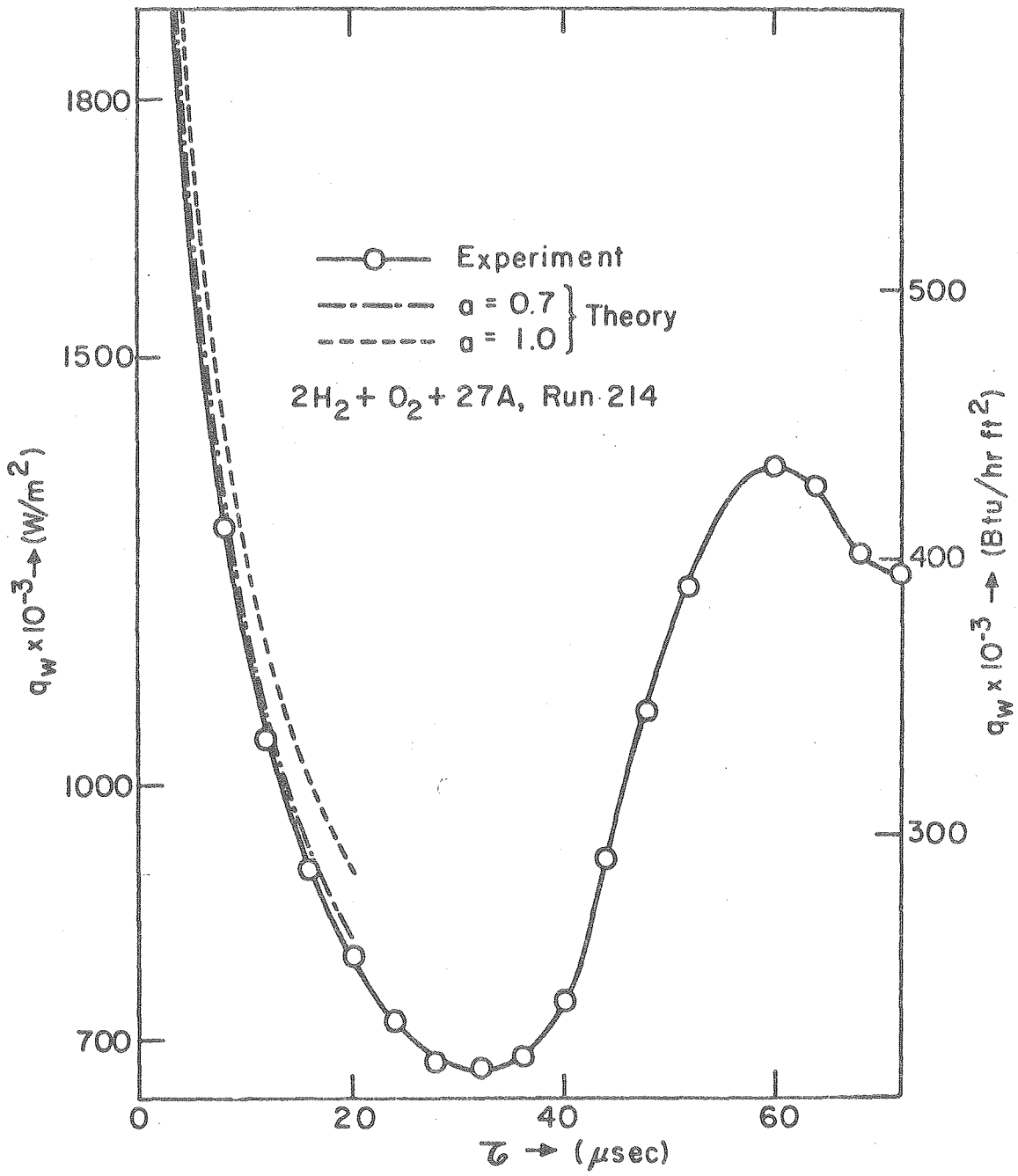

Figure 5.1. Heat flux variation.

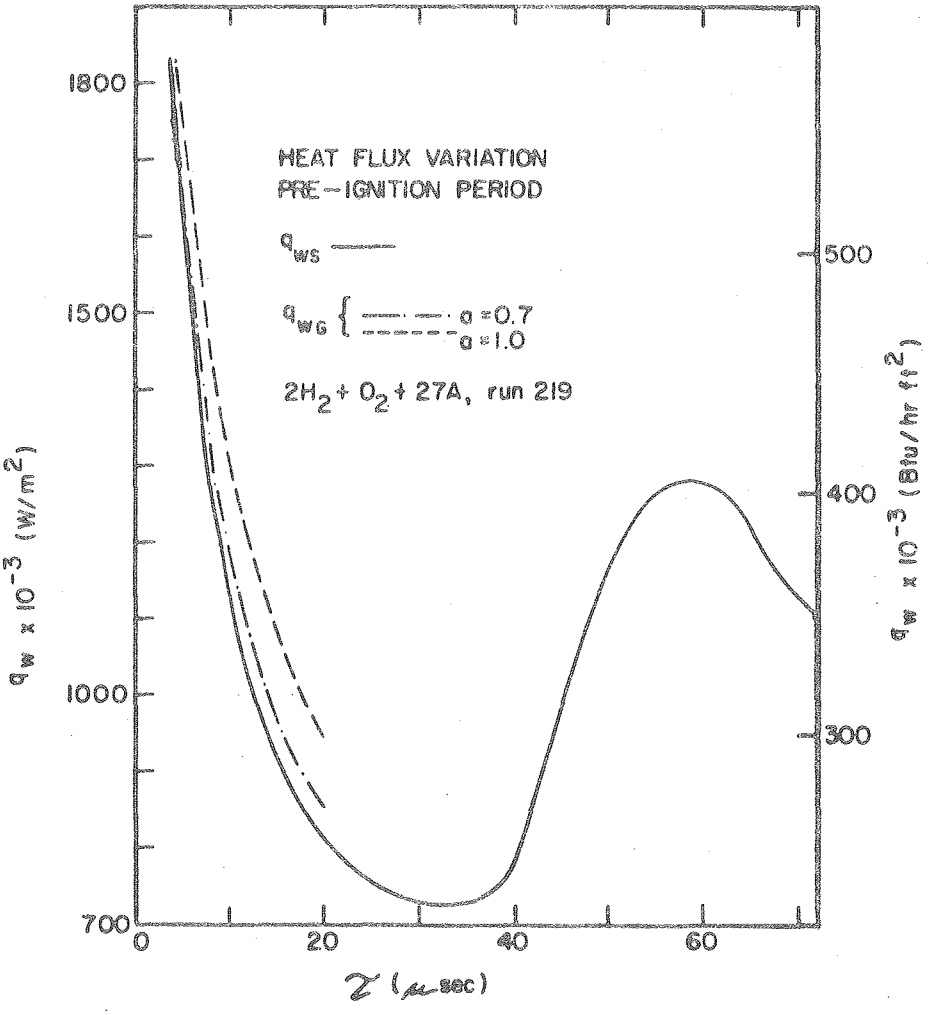

Figure 5.2. Heat flux variation.

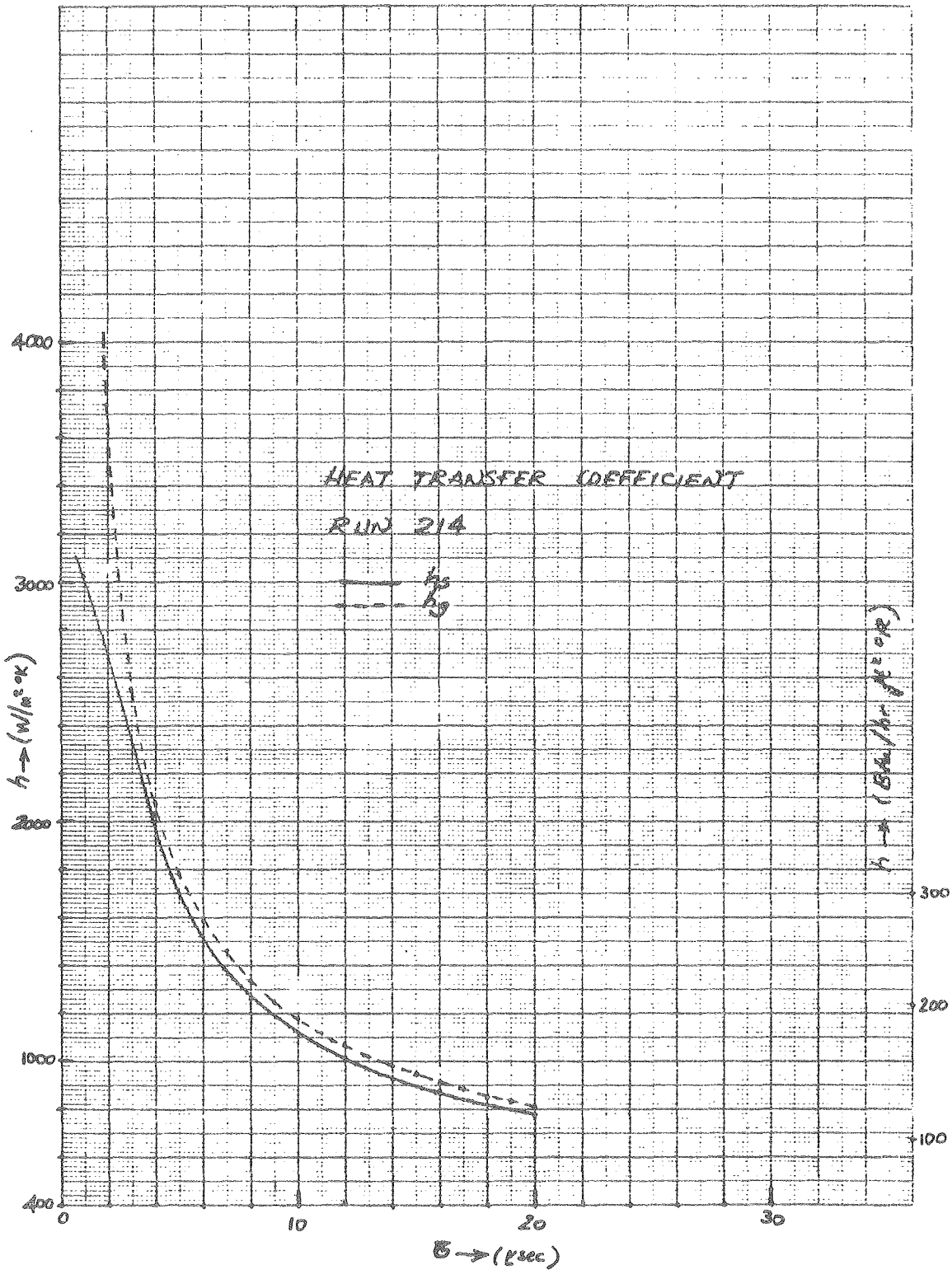

Figure 5.3. Heat transfer coefficient.

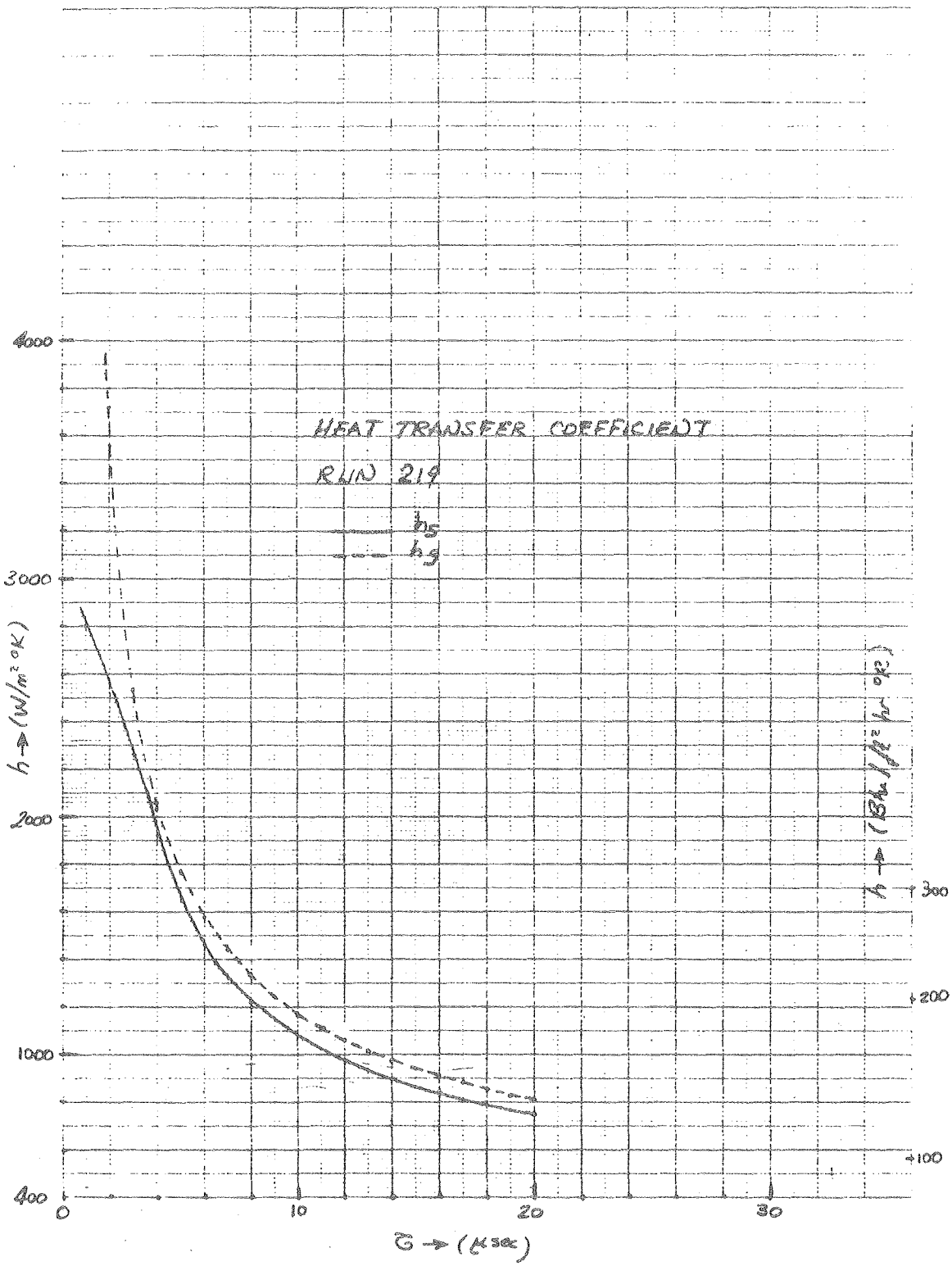

Figure 5.4. Heat transfer coefficient.

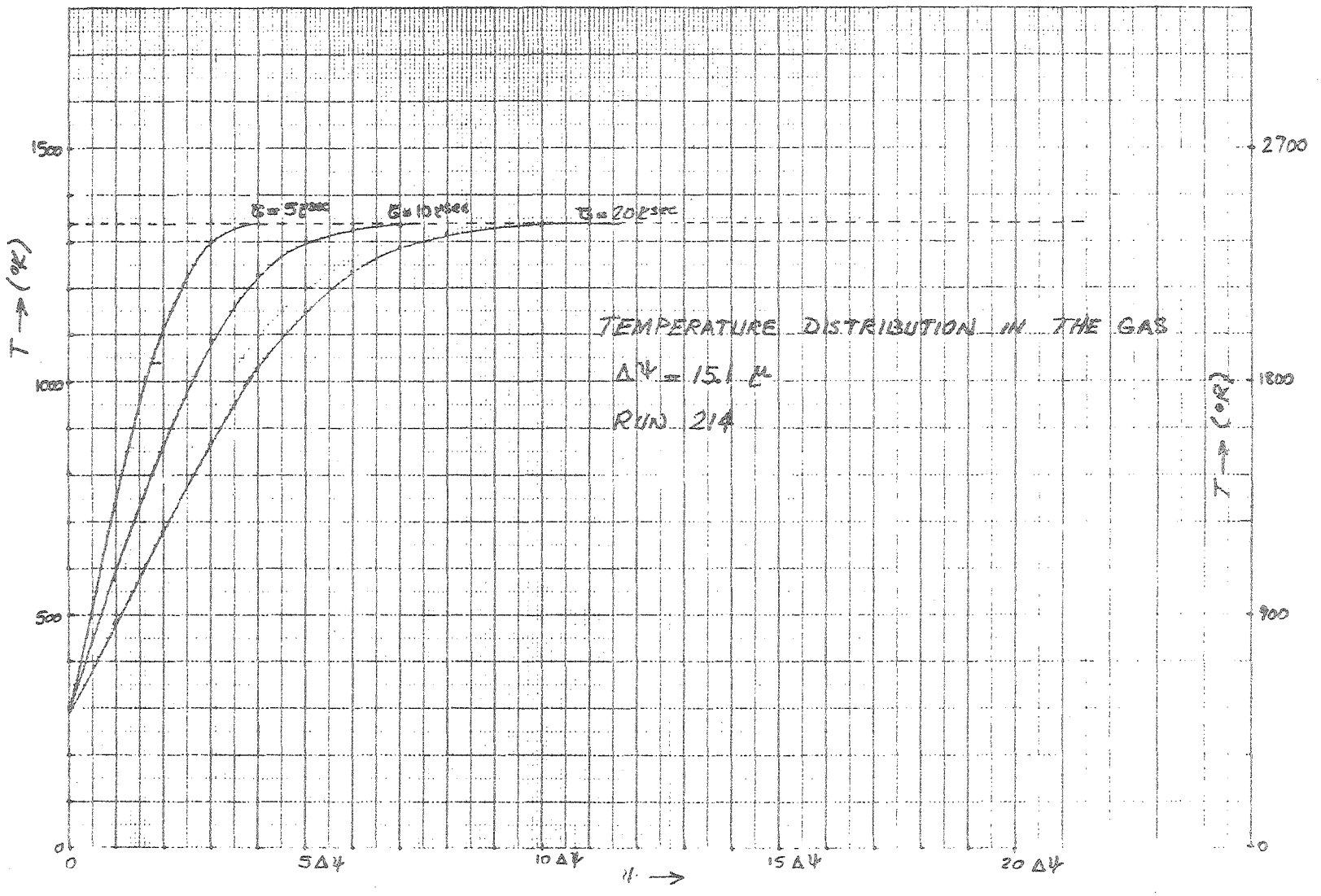

Figure 5.5. Temperature distribution.

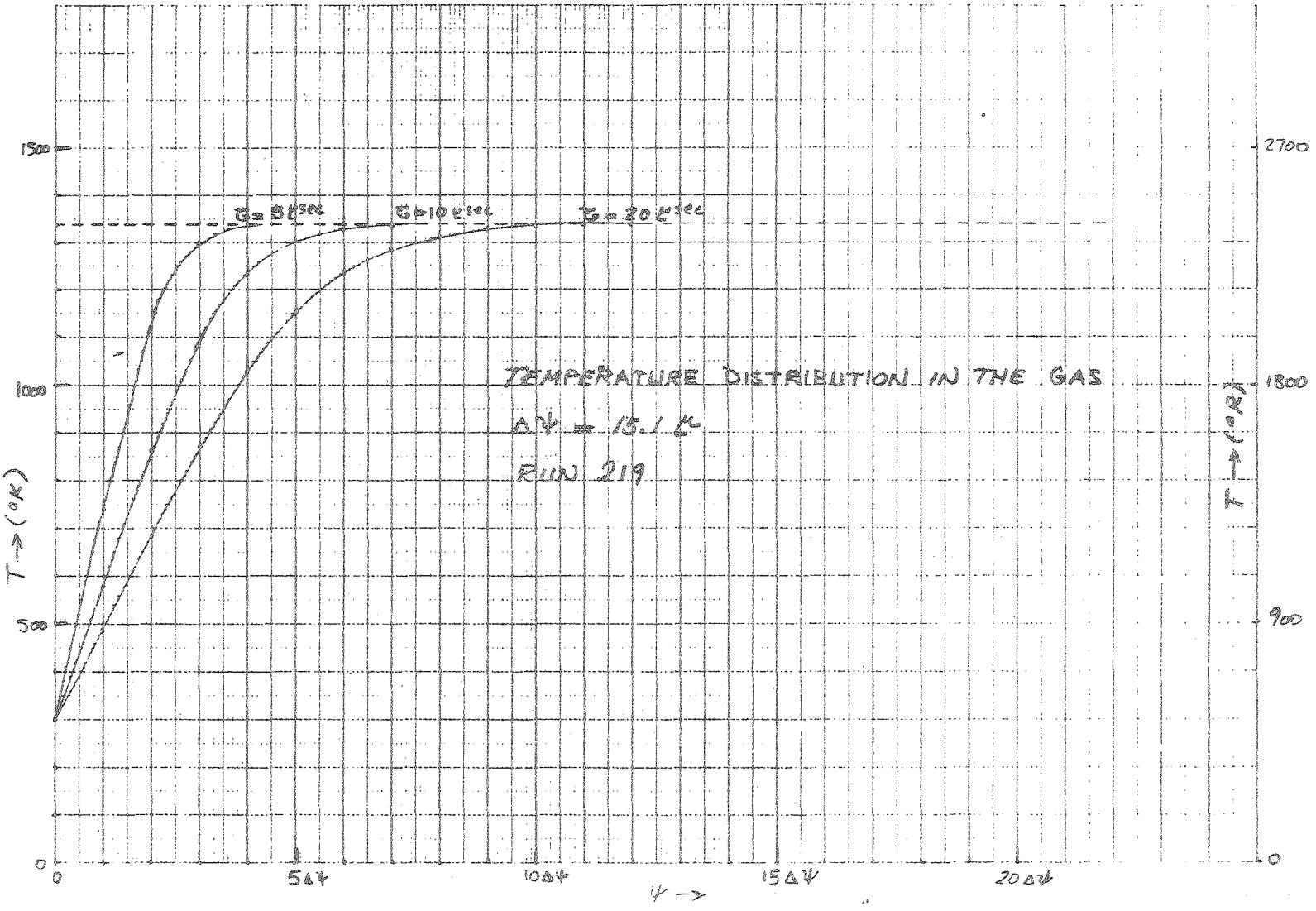

Figure 5.6. Temperature distribution.

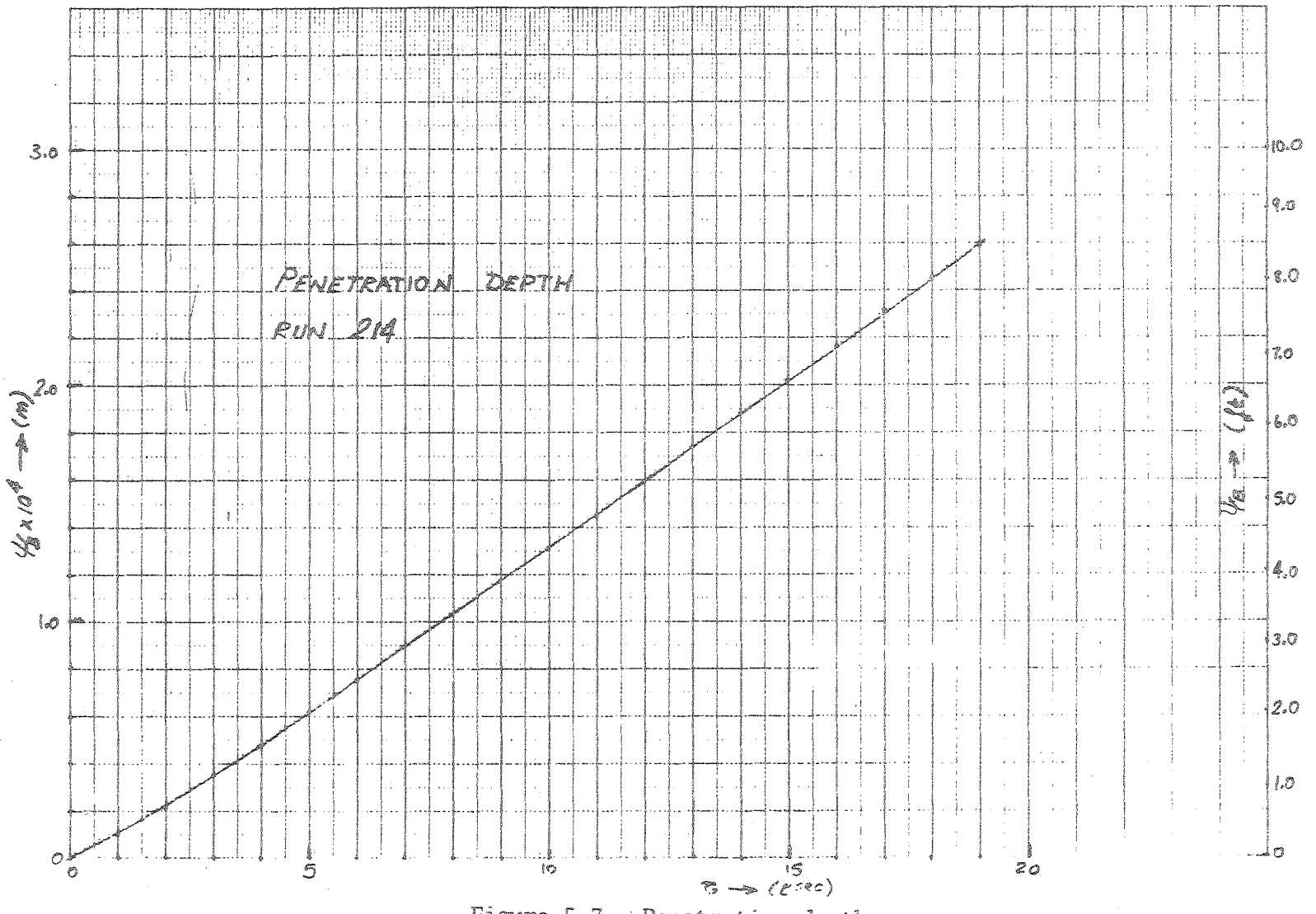

Figure 5.7. Penetration depth.

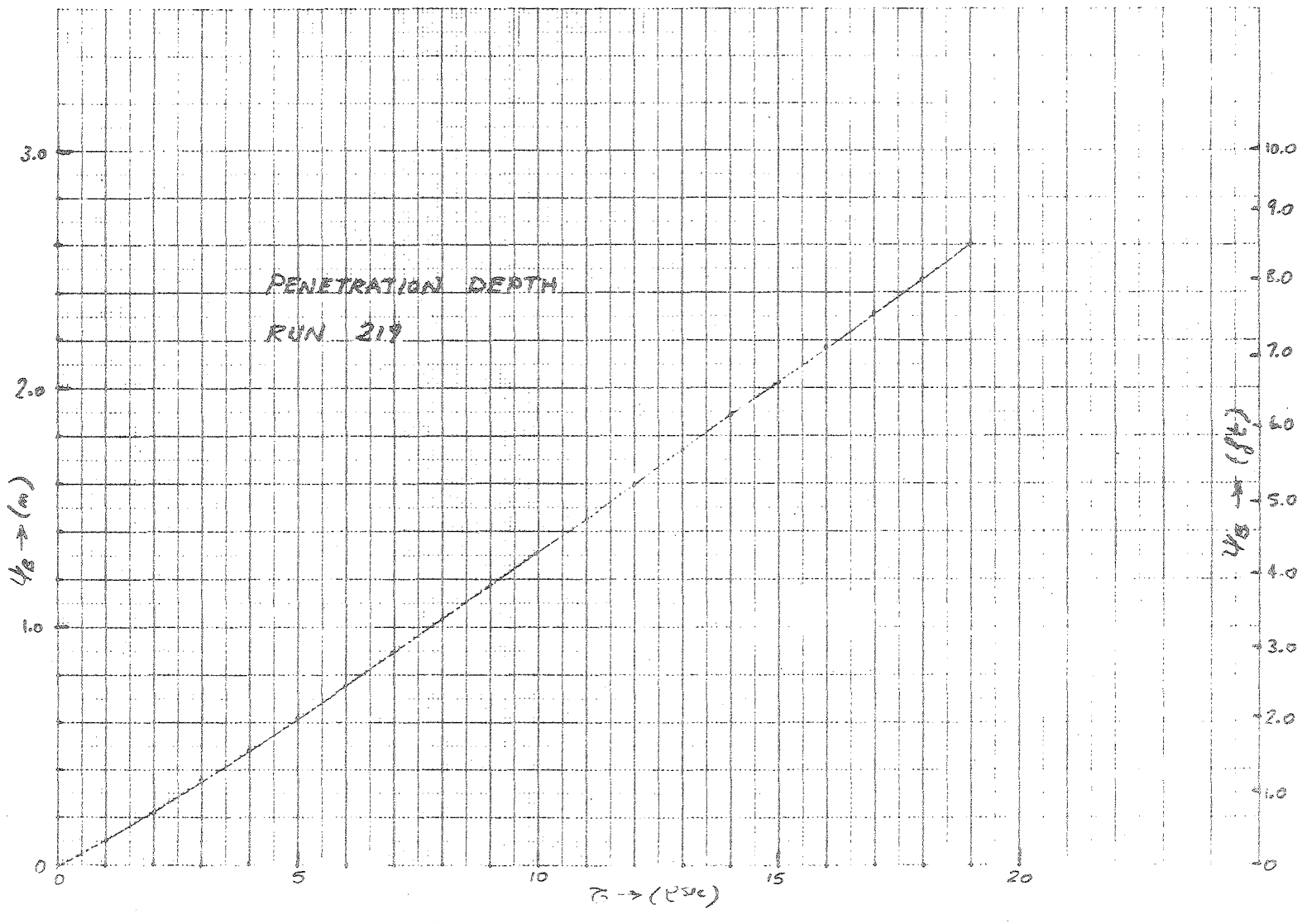

Figure 5.8. Penetration depth.

VI. HEAT TRANSFER IN THE GAS: COMBUSTION PERIOD

The gas mixture in the end wall region undergoes a rapid increase in temperature due to shock wave heating from both the incident and the reflected shock waves. In Chapter V we restricted our considerations to the pre-ignition, non-reacting interval corresponding to the first 20 microseconds after the shock wave reflection. The present chapter considers the combustion interval.

The ignition starts in a plane close to the end wall. The burned gases from the initial deflagration have a specific volume that is of the order of 5 to 15 times the values of the unburned gases. Since one end of the tube is closed there is an increasing pressure which acts like a gas piston generating compression waves away from the end wall. Thus a wave moves down the tube through the unburned gases ahead of the flame. The succeeding waves travel at higher speeds due to preheating by the previous waves and catch up with the initial one. Thus a shock front called a detonation wave is formed which continues to ignite the gas mixture and sustain itself [9]. This detonation wave moves away from the wall while the combustion zone penetrates slowly primarily by diffusion towards the end wall. The region between the end wall and the combustion zone does not have heat generation in it. An analysis in this region is made based on one-dimensional transport normal to the end wall.

6.1. Analysis

The unsteady, one-dimensional equations of continuity, energy and mass diffusion with no heat or species generation as applied to the end wall region are:

$$\frac{\partial \rho}{\partial t} + \frac{\partial}{\partial x}(\rho u) = 0 \tag{6.1.1}$$

$$\rho \frac{\partial h}{\partial t} + \rho u \frac{\partial h}{\partial x} = \frac{dp}{dt} + \frac{\partial}{\partial x}\left(k \frac{\partial T}{\partial x}\right) - \frac{\partial}{\partial x}\left(\sum_i \rho Y_i V_i h_i\right) \tag{6.1.2}$$

$$\rho \frac{\partial Y_i}{\partial t} + \rho u \frac{\partial Y_i}{\partial x} - \frac{\partial}{\partial x}\left(\rho D \frac{\partial Y_i}{\partial x}\right) = 0 \tag{6.1.3}$$

where Y_i is the mass fraction and h_i is the enthalpy of species i,

$$h_i = \int C_{p_i}\, dT + h_i^o \tag{6.1.4}$$

h_i^o being the enthalpy of formation. The diffusion in the end wall region arises from the combustion products which diffuse to the end wall. This effect will be discussed in Appendix G. In this section the analysis will be carried out omitting the last term in the energy equation. The initial and boundary conditions for the energy equation are:

$$T(x, o) = T_g(x) \tag{6.1.2.a}$$

$$T(o, t) = T_w \tag{6.1.2.b}$$

$$T(\delta, t) = T_\delta(t) \tag{6.1.2.c}$$

The momentum equation yields that the pressure may be taken to be constant in space. Thus the pressure will only be a function of time.

A stream function ψ is defined according to:

$$\frac{\partial \psi}{\partial x} = \frac{\rho}{\rho_{ig}} \tag{6.1.5}$$

$$\frac{\partial \psi}{\partial t} = -\frac{\rho u}{\rho_{ig}} \tag{6.1.6}$$

where ρ_{ig} is the initial constant density of the gas, ρ_5. Making a transformation from x, t coordinates to ψ, t coordinates the partial derivatives can be expressed as:

$$\left.\frac{\partial}{\partial x}\right|_t = \frac{\rho}{\rho_{ig}} \left.\frac{\partial}{\partial \psi}\right|_t \tag{6.1.7}$$

$$\left.\frac{\partial}{\partial t}\right|_x = -\frac{\rho u}{\rho_{ig}} \left.\frac{\partial}{\partial \psi}\right|_t + \left.\frac{\partial}{\partial t}\right|_\psi \tag{6.1.8}$$

The stream function satisfies the continuity equation and the energy equation is given in terms of temperature by:

$$\rho c_p \frac{\partial T}{\partial t} = \frac{dp}{dt} + \frac{\rho}{\rho_{ig}} \frac{\partial}{\partial \psi}\left[k \frac{\rho}{\rho_{ig}} \frac{\partial T}{\partial \psi}\right] \tag{6.1.9}$$

A number of assumptions have been made in solving the equations. The specific heat of the gas is taken constant equal to the mass averaged value for the mixture. Radiation effects are neglected. The change of the wall temperature is small compared to the change of the temperature at the combustion zone and is assumed to be constant. The gas is assumed to have a power law dependence on temperature.

$$\frac{k}{k_{ig}} = \left[\frac{T}{T_{ig}}\right]^a \tag{6.1.10}$$

For an ideal gas we have

$$\frac{\rho}{\rho_{ig}} = \frac{T_{ig}}{T} \frac{p}{p_{ig}} \tag{6.1.11}$$

Then using Equations (6.1.10) and (6.1.11) the energy equation becomes

$$\frac{\partial T}{\partial t} = \frac{1}{\rho C_p}\frac{dp}{dt} + \frac{k_{ig}}{\rho_{ig} C_p}\frac{p}{p_{ig}}\frac{\partial}{\partial \psi}\left(\left[\frac{T}{T_{ig}}\right]^{(a-1)}\frac{\partial T}{\partial \psi}\right) \tag{6.1.12}$$

From the ideal gas law and the definition of the specific heat we have:

$$\rho C_p = \frac{\gamma}{\gamma-1}\frac{p}{T} \tag{6.1.13}$$

$$\alpha_{ig} = \frac{k_{ig}}{\rho_{ig} C_p} \tag{6.1.14}$$

The pressure is only a function of time, so that

$$p(x, t) = p(t) \tag{6.1.15}$$

The following form of the energy equation is obtained:

$$\frac{\partial T}{\partial t} = \frac{\gamma-1}{\gamma}\frac{T}{p}\frac{dp}{dt} + \alpha_{ig}\frac{p}{p_{ig}} T_{ig}^{(1-a)}\frac{\partial}{\partial \psi}\left[T^{(a-1)}\frac{\partial T}{\partial \psi}\right] \tag{6.1.16}$$

It is convenient to introduce the following non-dimensional variable.

$$V = \left[\frac{T}{T_{ig}}\right]^{a}\left[\frac{p}{p_{ig}}\right]^{\frac{a(1-\gamma)}{\gamma}} \tag{6.1.17}$$

The partial derivatives in terms of the new variable are given by:

$$\frac{\partial T}{\partial t} = \frac{T_{ig}}{a}\left[\frac{T}{T_{ig}}\right]^{(1-a)}\left[\frac{p}{p_{ig}}\right]^{\frac{a(\gamma-1)}{\gamma}}\frac{\partial V}{\partial t} - \frac{T}{p}\frac{(1-\gamma)}{\gamma}\frac{dp}{dt} \tag{6.1.18}$$

$$\frac{\partial T}{\partial \psi} = \frac{T_{ig}}{a}\left[\frac{T}{T_{ig}}\right]^{(1-a)}\left[\frac{p}{p_{ig}}\right]^{\frac{a(\gamma-1)}{\gamma}}\frac{\partial V}{\partial \psi} \tag{6.1.19}$$

The energy equation can then be written as:

$$\frac{\partial V}{\partial t} = \alpha_{ig}\left[\frac{p}{p_{ig}}\right]^{\frac{a\gamma-a+1}{\gamma}} V^{\frac{a-1}{a}}\frac{\partial^2 V}{\partial \psi^2} \tag{6.1.20}$$

Defining a new time variable

$$d\tau = \left[\frac{P}{P_{ig}}\right]^{\frac{a\gamma - a + 1}{\gamma}} dt \tag{6.1.21}$$

yields,

$$\frac{\partial V}{\partial \tau} = \alpha_{ig} V^{\frac{a-1}{a}} \frac{\partial^2 V}{\partial \psi^2} \tag{6.1.22}$$

The initial and boundary conditions are:

$$V(\psi, \tau_I) = F(\psi) \tag{6.1.22.a}$$

$$V(0,\tau) = \left[\frac{T_w}{T_{ig}}\right]^a \left[\frac{P}{P_{ig}}\right]^{\frac{a(1-\gamma)}{\gamma}} \tag{6.1.22.b}$$

$$V(\delta,\tau) = \left[\frac{T_\delta}{T_{ig}}\right]^a \left[\frac{P}{P_{ig}}\right]^{\frac{a(1-\gamma)}{\gamma}} \tag{6.1.22.c}$$

where δ is a specified function of time.

The heat flux at the wall can be evaluated from:

$$q_w = -k \frac{\partial T}{\partial x}\bigg|_w = -k \frac{\partial T}{\partial V} \frac{\partial V}{\partial \psi} \frac{\partial \psi}{\partial x}\bigg|_w$$

$$= -\frac{k_w}{a} \frac{(T_{ig})^{(a+1)}}{T_w^a} \left[\frac{P}{P_{ig}}\right]^{\frac{a(\gamma-1)}{\gamma}+1} \frac{\partial V}{\partial \psi}\bigg|_{\psi=0} \tag{6.1.23}$$

In the same way the heat flux at the combustion zone can be found as:

$$q_\delta = -\frac{k_\delta}{a} \frac{(T_{ig})^{(a+1)}}{T_\delta^a} \left[\frac{P}{P_{ig}}\right]^{\frac{a(\gamma-1)}{\gamma}+1} \frac{\partial V}{\partial \psi}\bigg|_{\psi=\delta} \tag{6.1.24}$$

Using Equation (6.1.10) this becomes:

$$q_\delta = -\frac{k_{ig}}{a} T_{ig} \left[\frac{P}{P_{ig}}\right]^{\frac{a(\gamma-1)}{\gamma}+1} \frac{\partial V}{\partial \psi}\bigg|_{\psi=\psi_B} \tag{6.1.25}$$

Values for p(t) and $T_\delta(t)$ are calculated based on the work of Cohen [12], (See Appendix D). The initial temperature distribution T_g for the combustion period is equal to the calculated temperature distribution at the end of the pre-ignition period. A penetration depth similar to the pre-ignition period can also be evaluated for this period using Equation (6.1.5) as explained in Appendix H.

6.2. Numerical Method

An explicit forward finite difference scheme has been used. Equation (6.1.22) can be written in finite difference form as:

$$V_{j,k+1} = M V_{j,k}^{\frac{a-1}{a}} \left(V_{j+1,k} + V_{j-1,k} \right) + \left(1 - 2M V_{j,k}^{\frac{a-1}{a}} \right) V_{j,k} \qquad (6.2.1)$$

where

$$M = \frac{\alpha_{ig} \Delta \tau}{(\Delta \psi)^2} \qquad (6.2.2)$$

The initial and boundary conditions are:

$$V(j=1,\ldots,m,\ k=1) = F(\psi) \qquad (6.2.2.a)$$

$$V(j=1,\ k=1,\ldots,n) = \left[\frac{T_w}{T_{ig}}\right]^a \left[\frac{P}{P_{ig}}\right]^{\frac{a(1-\gamma)}{\gamma}} \qquad (6.2.2.b)$$

$$V(j=m,\ k=1,\ldots,n) = \left[\frac{T_\delta}{T_{ig}}\right]^a \left[\frac{P}{P_{ig}}\right]^{\frac{a(1-\gamma)}{\gamma}} \qquad (6.2.2.c)$$

For stability the following condition should be satisfied:

$$1 - 2M V_{j,k}^{\frac{a-1}{a}} \geq 0 \qquad (6.2.3)$$

or

$$M \leqslant \frac{V_{j,k}^{\frac{1-a}{a}}}{2} \tag{6.2.4}$$

$V_{j,k}$ takes the minimum value at the wall, therefore the stability condition is:

$$M \leqslant \frac{1}{2}\left[\frac{T_w}{T_{ig}}\right]^{(1-a)}\left[\frac{P}{P_{ig}}\right]^{\frac{(1-a)(1-\gamma)}{\gamma}} \tag{6.2.5}$$

The heat flux at the end wall can be evaluated from Equation (6.1.23), and at infinity from Equation (6.1.24). This requires the evaluation of the derivative of V with respect to ψ at $\psi = 0$ and $\psi = \delta$. Three different relations have been used to obtain these derivatives [8],

$$\left.\frac{\partial V}{\partial \psi}\right|_{\psi=0} = \frac{V_{2,k} - V_{1,k}}{\Delta\psi} \tag{6.2.6}$$

$$\left.\frac{\partial V}{\partial \psi}\right|_{\psi=0} = \frac{-V_{3,k} + 4V_{2,k} - 3V_{1,k}}{2\Delta\psi} \tag{6.2.7}$$

$$\left.\frac{\partial V}{\partial \psi}\right|_{\psi=0} = \frac{2V_{4,k} - 9V_{3,k} + 18V_{2,k} - 11V_{1,k}}{6\Delta\psi} \tag{6.2.8}$$

$$\left.\frac{\partial V}{\partial \psi}\right|_{\psi=\delta} = \frac{V_{m-1,k} - V_{m,k}}{\Delta\psi} \tag{6.2.9}$$

$$\left.\frac{\partial V}{\partial \psi}\right|_{\psi=\delta} = \frac{-V_{m-2,k} + 4V_{m-1,k} - 3V_{m,k}}{2\Delta\psi}$$

$$\left.\frac{\partial V}{\partial \psi}\right|_{\psi=\delta} = \frac{2V_{m-3,k} - 9V_{m-2,k} + 18V_{m-1,k} - 11V_{m,k}}{6\Delta\psi} \tag{6.2.10}$$

When solving Equation (6.2.1), the initial temperature distribution at the time of ignition and the combustion zone location are required. The temperature distribution as discussed in Chapter 5 is obtained from

the results at the end of the pre-ignition period. The location of the combustion zone is assumed to be at the penetration depth at 20 μsec, the end of the pre-ignition period. The combustion zone then diffuses toward the end wall. The trajectory of the zone was determined by reassuring the two calculated heat fluxes at the end wall to be equal. This will be discussed in more detail in Section 6.3.

An approximate solution can also be found for the location of the combustion zone using an integral method. This procedure is discussed in Appendix K.

The computer listing for the solution of Equation (6.2.1) is given in Appendix F.

6.3. Results and Discussion

In Chapter 3 the experimental variation of the end wall temperature, including pre-ignition and ignition, was given for runs 214 and 219 in Figure 3.1. These values were plotted in Figures 3.2.a and 3.2.b. Also, in the same chapter, the heat flux, q_{ws}, was calculated using the wall temperature, based on an analysis in the solid.

Then, in Chapter 5, q_{ws} was compared with the heat flux obtained from solving the conservation equations in the gas during the pre-ignition period, that is for the first 20 μsec.

In this chapter the analysis is extended to the period after ignition has occurred ($t \geqslant 20$ μsec). The pressure, p and the temperature, T_δ, at the gas boundary layer are now no longer constants due to the effects of combusion. The temporal variations of the pressure and the

temperature were calculated from a study of the chemical kinetics and thermodynamics of the combustion zone by Cohen [12]. This study is discussed in Appendix D. The computer listing is also given in Appendix D. The values for T_δ and p for run 214 are plotted as a function of time in Figures 6.1 and 6.2. For run 219 T_δ and p are plotted in Figures 6.3 and 6.4.

At the end of Chapter 5, the temperature distribution and the penetration depth at the time of ignition, $\tau = 20$ μsec, were calculated. Note that the time variable, τ, used in the pre and past-ignition periods are defined differently. During the pre-ignition period, $p = p_{ig}$ = constant and there is also no difference between t and τ. At the initiation of the combustion period, $\tau = \tau_I$, the pressure is p_{ig} from the pre-ignition period.

For stability, the increment of the space variable, $\Delta\psi$, must be chosen in conjuntion with the increment of the time variable, $\Delta\tau$. The stability factor is chosen to be the same for both periods and as explained above there is no difference between t and τ at the time of ignition. Therefore the space increments, $\Delta\psi$, at the time of ignition are also identical. The temperature distribution and the penetration depth from the pre-ignition period can be directly used at the time of ignition, $\tau = \tau_I$. This temperature distribution is plotted as a function of ψ in Figure 6.5 for run 214 and in Figure 6.6 for run 219. Also shown on the figures is the value of the penetration depth at $\tau = 20$ μsec for that specific run.

The combustion zone is initially assumed to be at the penetration depth which was calculated during the pre-ignition period. This zone

then diffuses toward the end wall. The trajectory of the zone is unknown. Calculations were made for four different trajectories in conjunction with Equation (6.2.1) in order to determine q_{wg} numerically. The diffusion from the combustion zone to the wall proceeded in the same manner for all the cases considered; the difference was solely that the propagation was stopped at different final distances from the end wall. The calculations were carried out with the temperature T_δ at the same location for two consecutive time increments. In detail, for run 214, values of T_δ equal to 1338°K and 1339°K were applied at 196 μ for two consecutive time steps; T_δ = 1342°K and 1343°K were applied at 181 μ for the next two consecutive time steps, etc. {In order to obtain some information about the shape of the trajectories an integral method was used as described in Appendix K. This was done by requiring the two calculated heat fluxes at the end wall, q_{ws} and q_{wg}, to be equal. The variation of the location of the combustion zone is shown in Figure 6.7. It can be seen from this figure that the penetration depth increases slightly at the beginning of the combustion period and then decreases rapidly.} The heat flux at the wall, q_{wg}, obtained from each trajectory is compared with q_{ws} in Figure 6.8 for run 214 and in Figure 6.9 for run 219. From the comparison of the heat fluxes it is seen that the best match is for the case $\psi_{BF} = 6\ \Delta\psi$, which means that the combustion zone diffused toward the end wall until it reached a final distance equal to $6\Delta\psi$ from the end wall. This distance may be considered to be a "quenching distance" since the flame does not come closer than this distance to the end wall. For emphasis the heat flux

calculated from the solution of the conservation equations in the gas for the case of $\psi_{BF} = 6\,\Delta\psi$ is plotted again with the heat flux obtained from the solid analysis in Figure 6.10 for run 214 and in Figure 6.11 for run 219. Also shown on these figures are curves for the heat flux obtained from the approximation a = 1.0. As discussed in Appendix E, this yields an exact solution. The heat flux curve for a = 0.7 is closer to the heat flux curve obtained from the solid analysis because the thermal conductivity of argon, which constitutes 90% by volume of the mixture, depends on temperature to the 0.7 power approximately [10, 11]. The two heat fluxes q_{ws} and q_{wg} are in good agreement with maximum errors of 5% for both cases. Comparisons are made until $\tau = 45$ μsec. At this instant the detonation wave overtakes the reflected shock wave and we can no longer calculate T_δ and p. [12].

A penetration depth, δ_B, as defined in Chapter 5 ($T = 0.99\ T_\delta$) was calculated for each trajectory by a back transformation from the ψ coordinate to the real space coordinate x. This transformation is discussed in Appendix H. The variation of ψ with x is plotted for $\tau = 20$ μsec and 40 μsec in this appendix. The relation between ψ and x is different for every time step due to the character of the transformation. The penetration depths are shown in Figure 6.12 for run 214 and in Figure 6.13 for run 219.

Temperature profiles in the gas boundary layer next to the end wall for different times, $\tau = 5$ μsec, 20 μsec, 35 μsec and 45 μsec are given in Figure 6.14 for run 214 and in Figure 6.15 for run 219.

A heat transfer coefficient can be defined for this period too, based on the wall heat flux by:

$$h = \frac{(-q_w)}{T_\delta - T_w} \tag{6.3.1}$$

For the combustion period, T_δ is a function of time and the heat transfer coefficient, h, and the heat flux do not have similar shapes. Heat transfer coefficient curves are given in Figure 6.16 for run 214 and in Figure 6.17 for run 219.

From the solution of Equation (6.2.1) the slopes at the edge of the gas layer can be evaluated and the heat flux can be calculated. The heat flux curve, q_δ, is shown in Figure 6.18 for run 214 and in Figure 6.19 for run 219. This heat flux is related to the heat release in the combustion zone at the edge of the gas layer.

In order to obtain more accurate heat fluxes, the heat storage in the gas was considered in the evaluation of the derivative of the temperature with respect to distance. This is discussed in Appendix I. The results showed that the contribution was small.

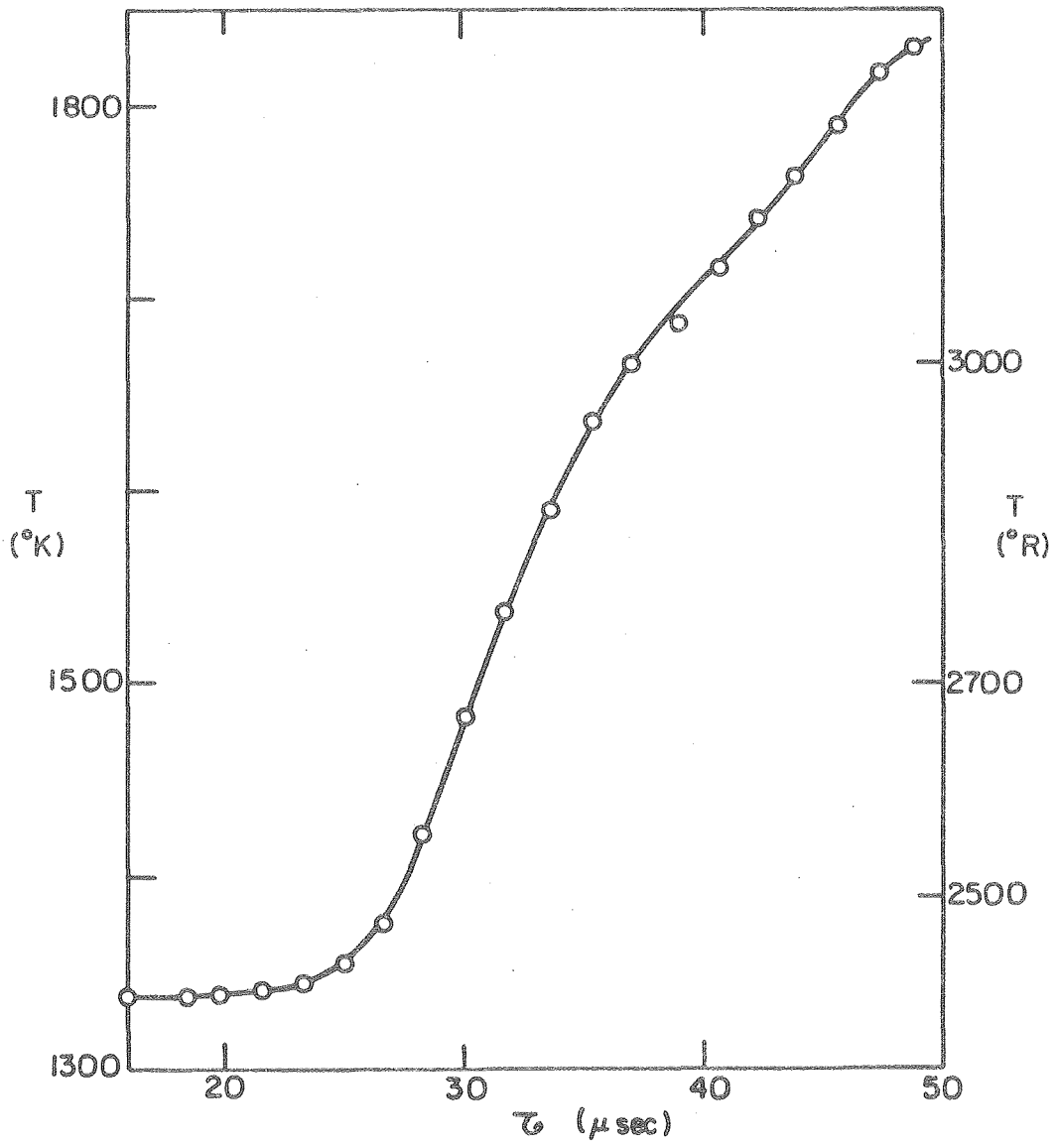

Figure 6.1. Temperature variation for the gas. Run 214

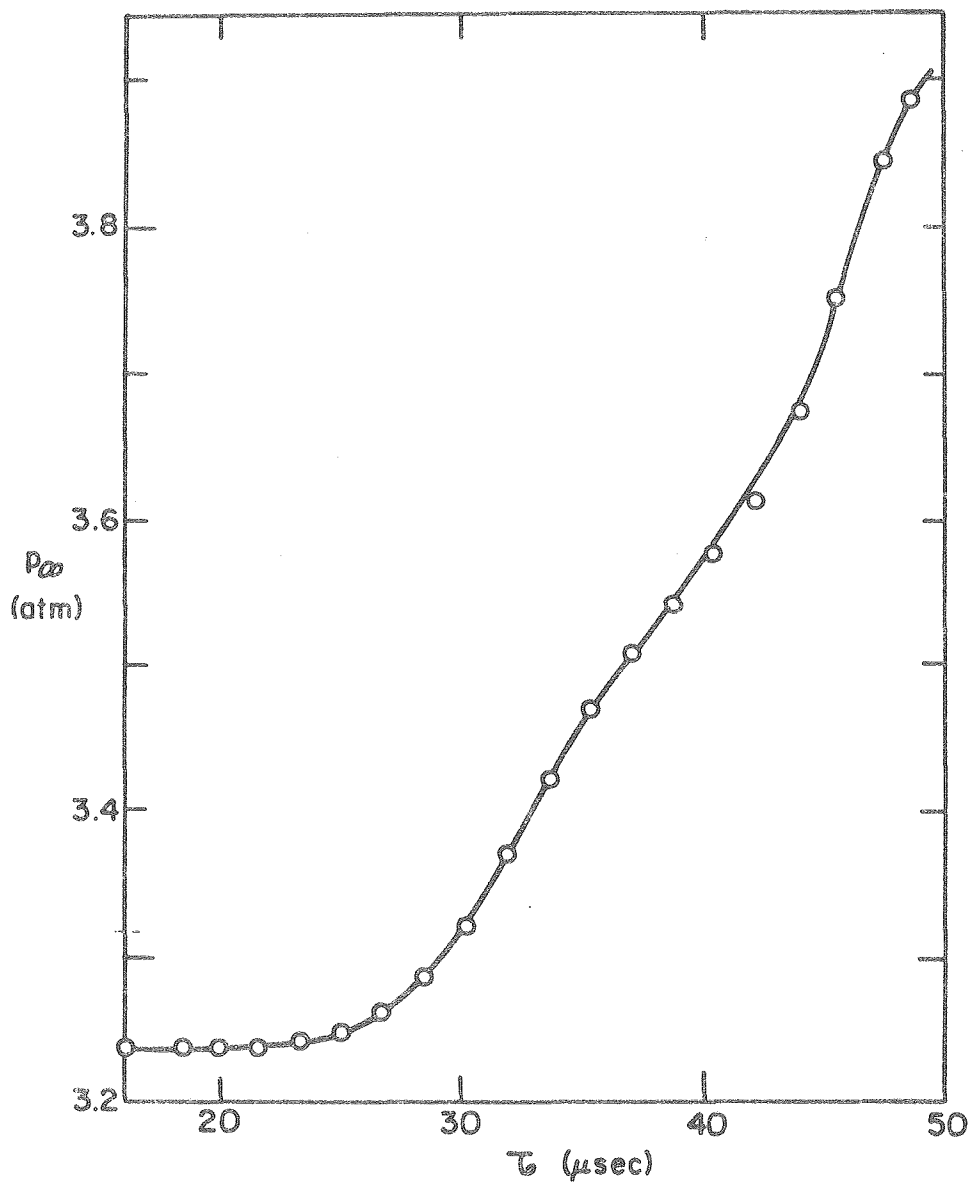

Figure 6.2. Pressure variation for the gas. Run 214

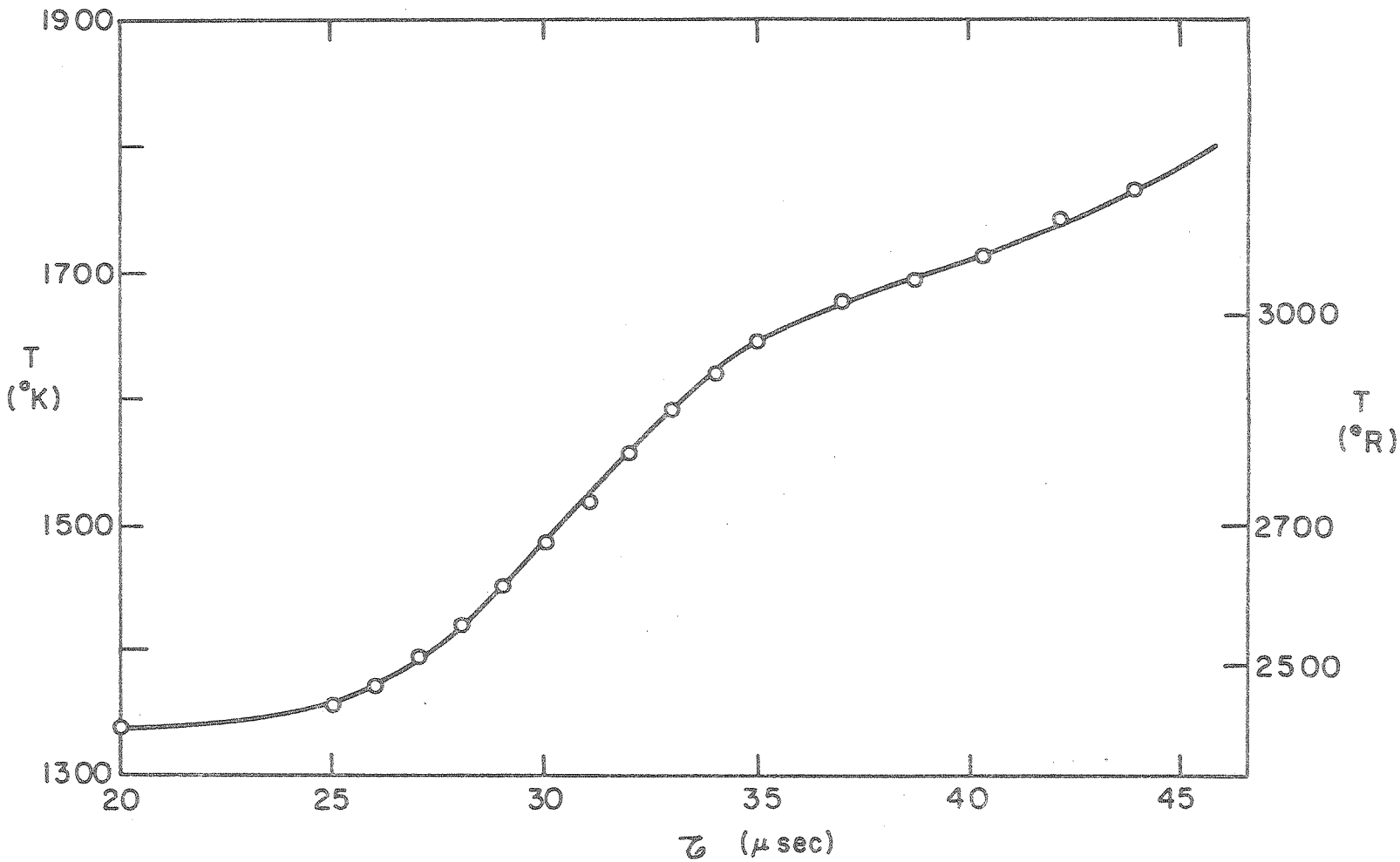

Figure 6.3. Temperature variation for the gas. Run 219

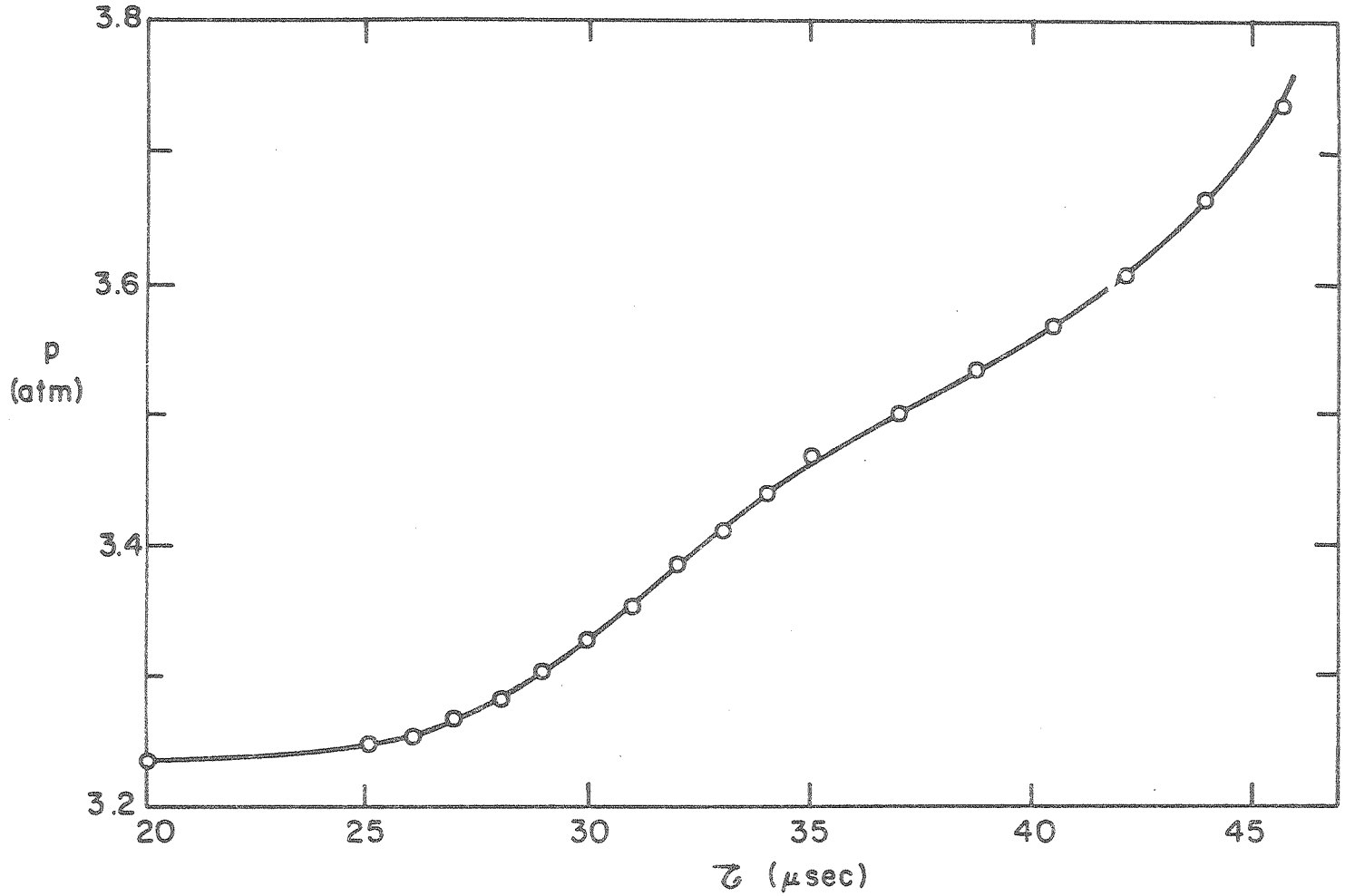

Figure 6.4. Pressure variation for the gas. Run 219

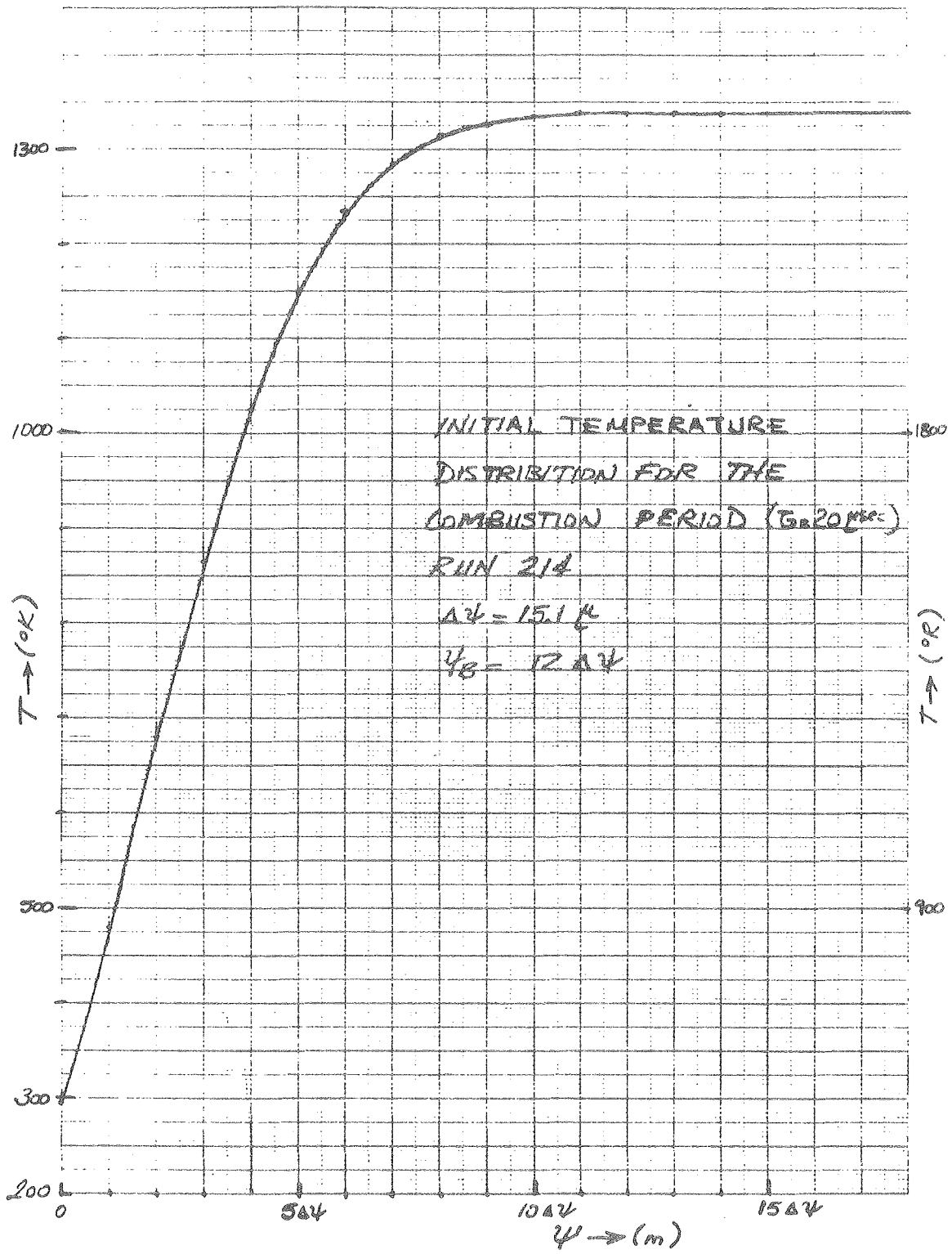

Figure 6.5. Initial temperature distribution.

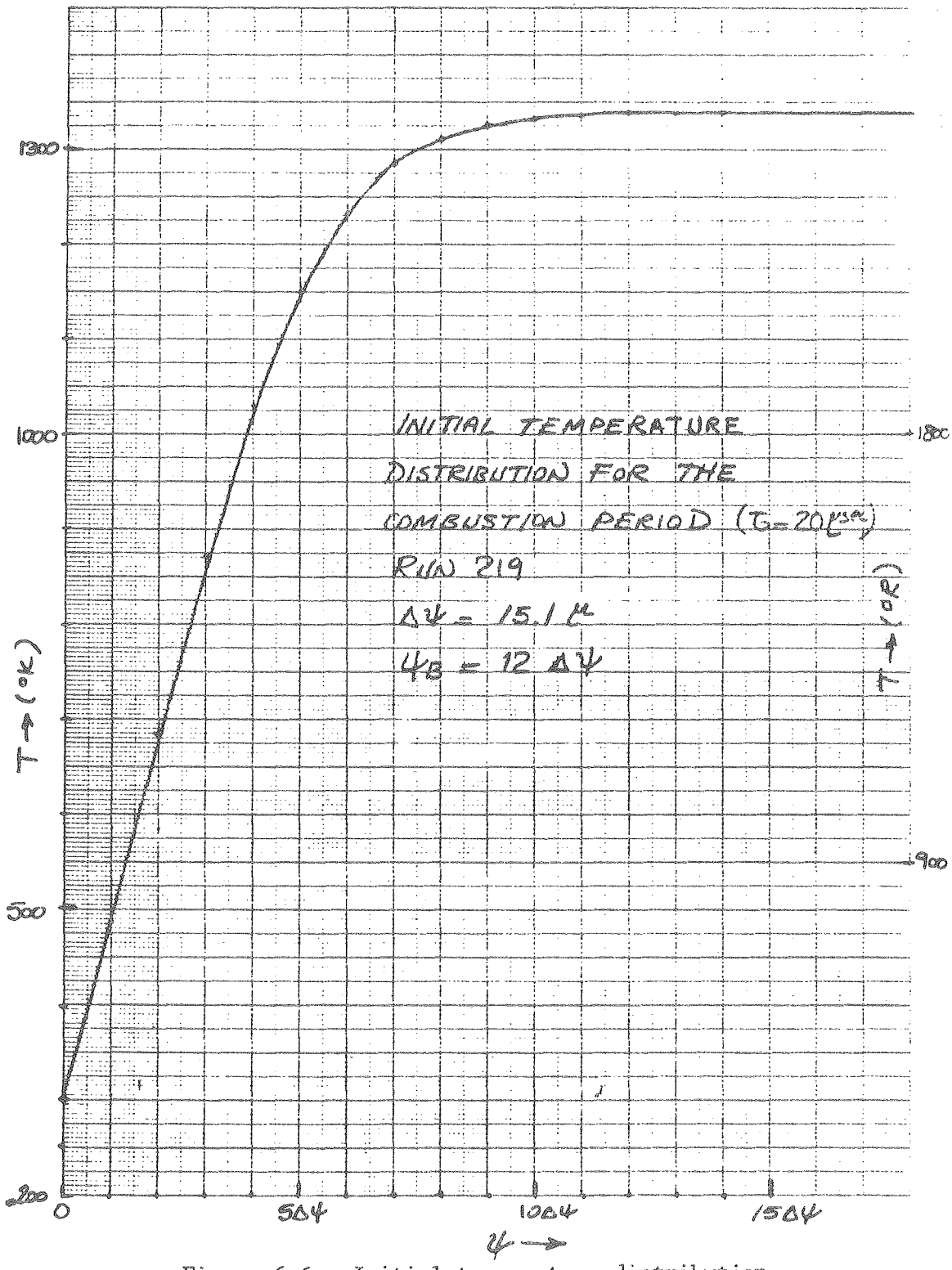

Figure 6.6. Initial temperature distribution.

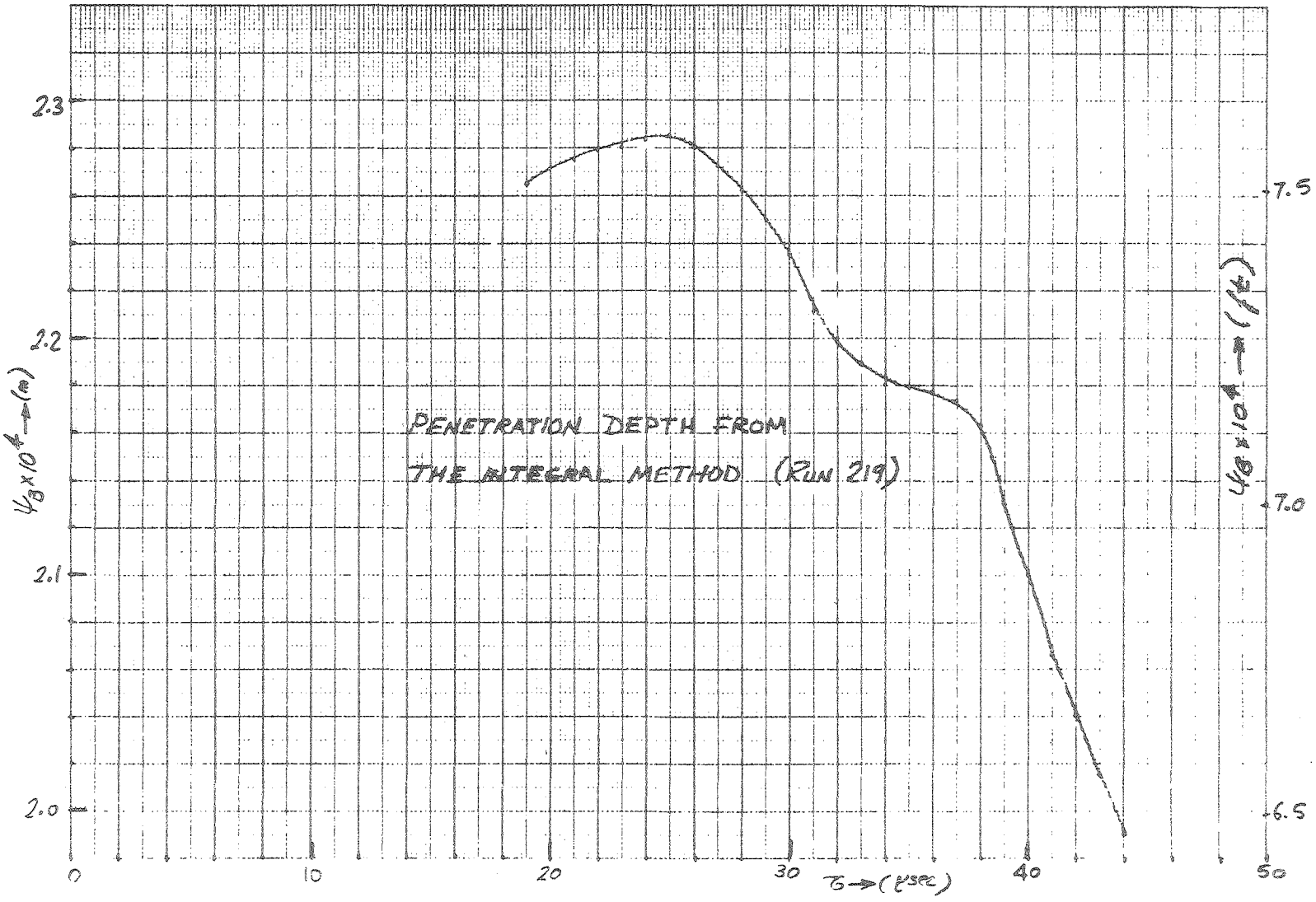

Figure 6.7. Penetration depth.

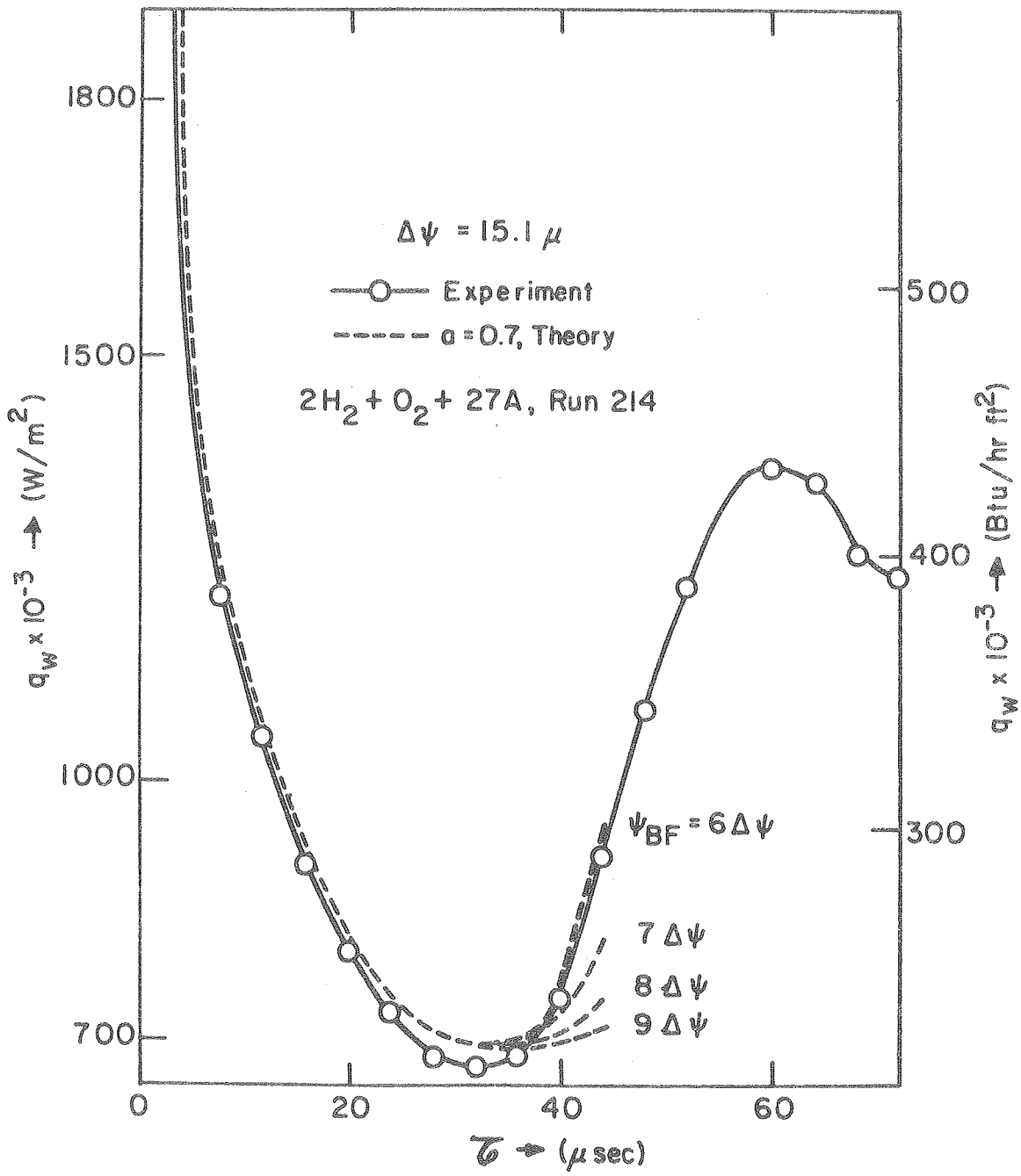

Figure 6.8. Heat flux variation for different trajectories.

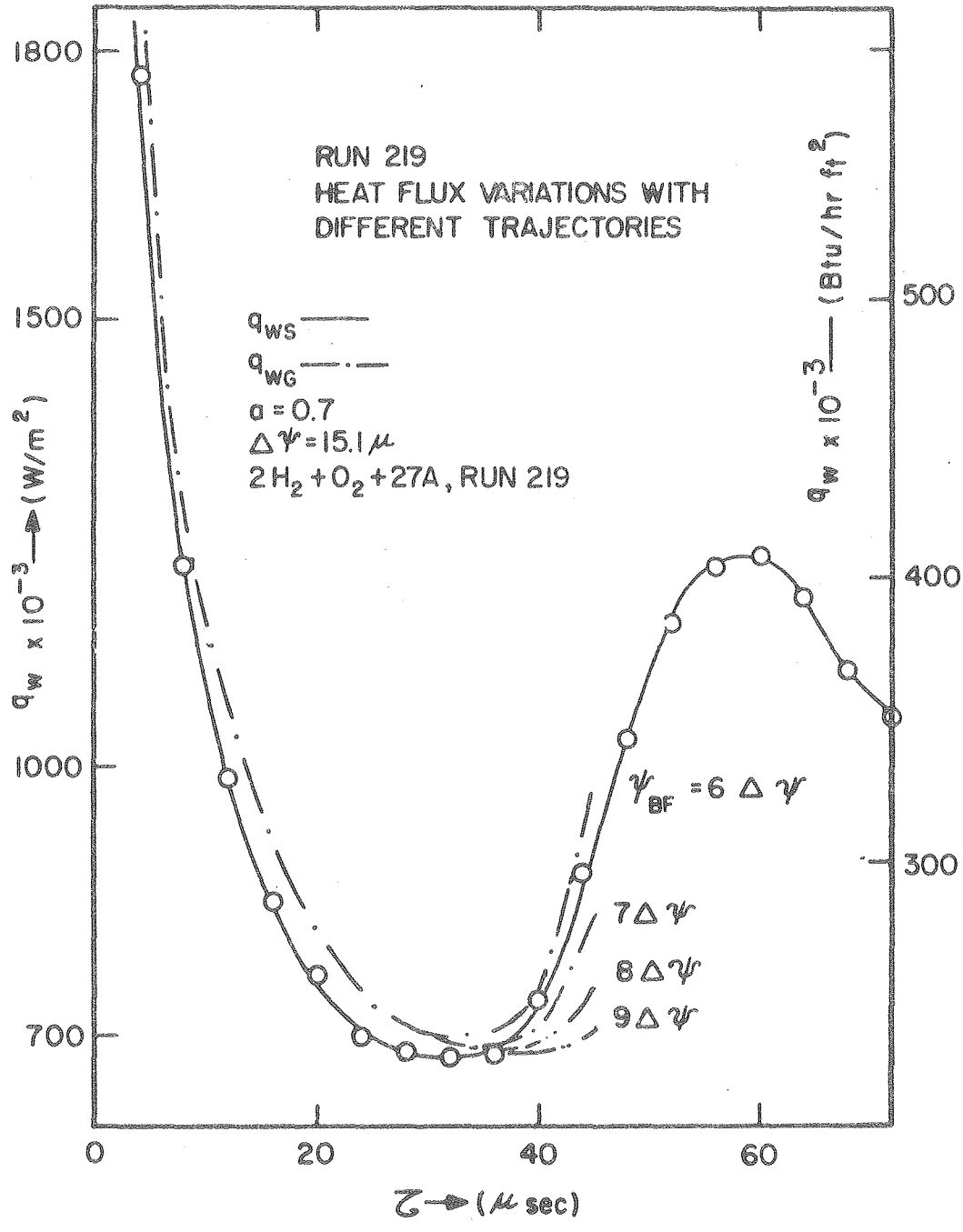

Figure 6.9. Heat flux variation for different trajectories.

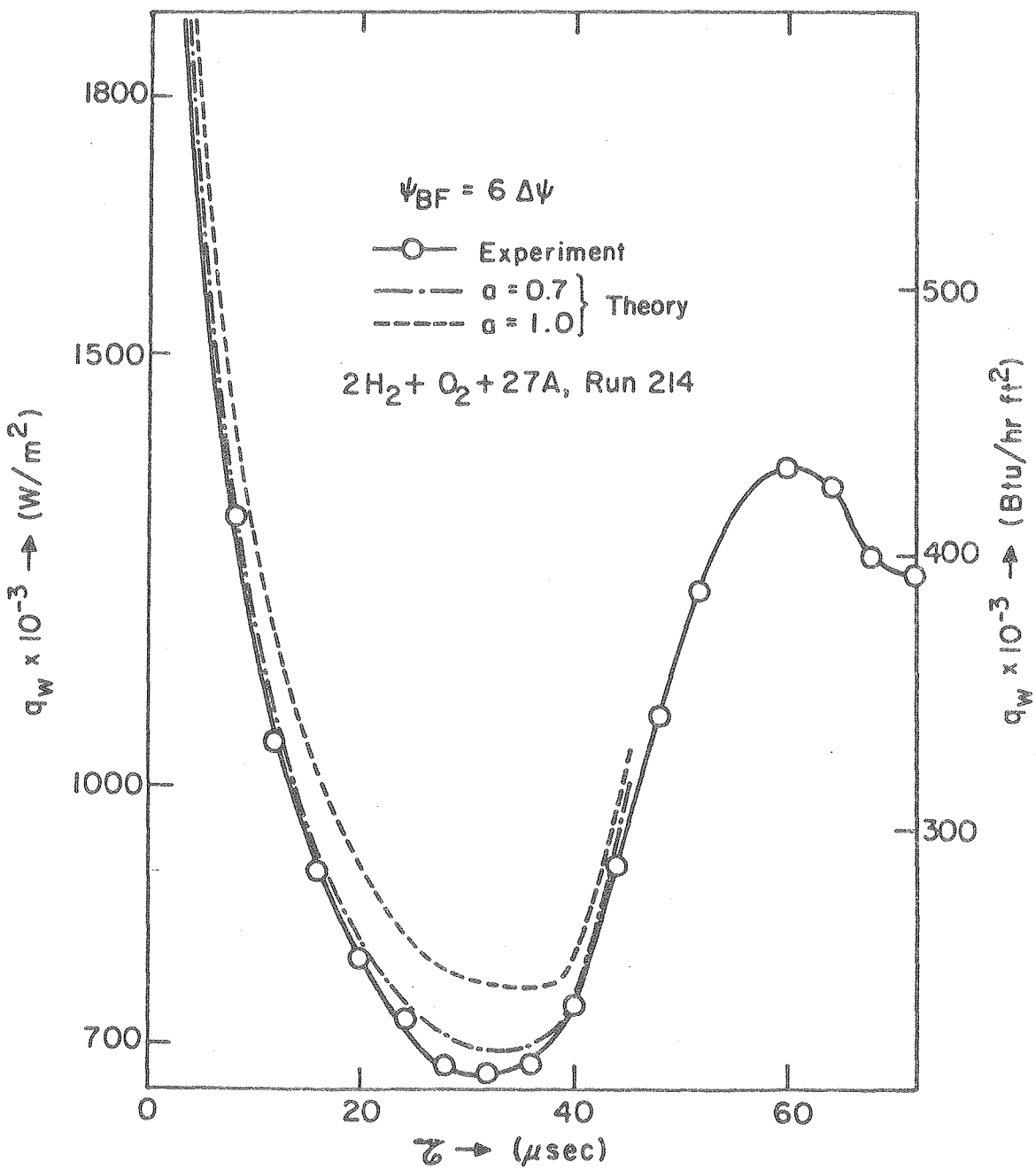

Figure 6.10. Heat flux variation.

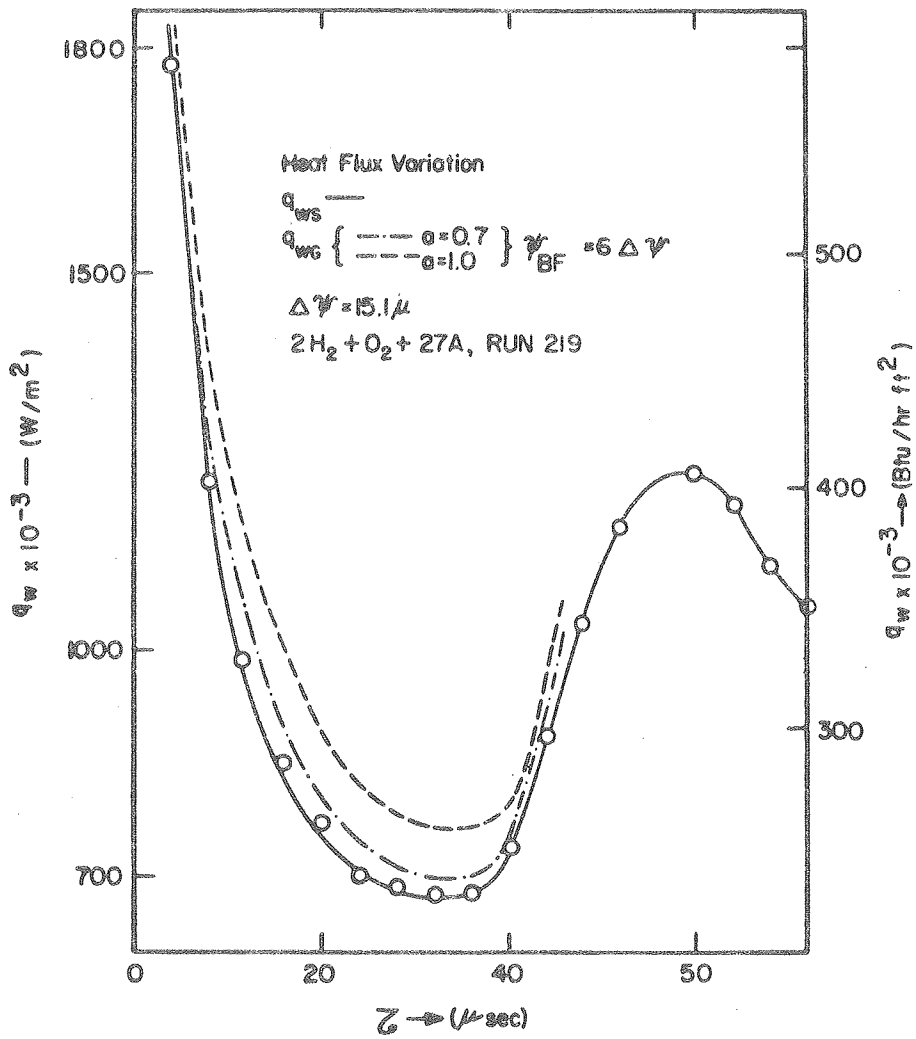

Figure 6.11. Heat flux variation.

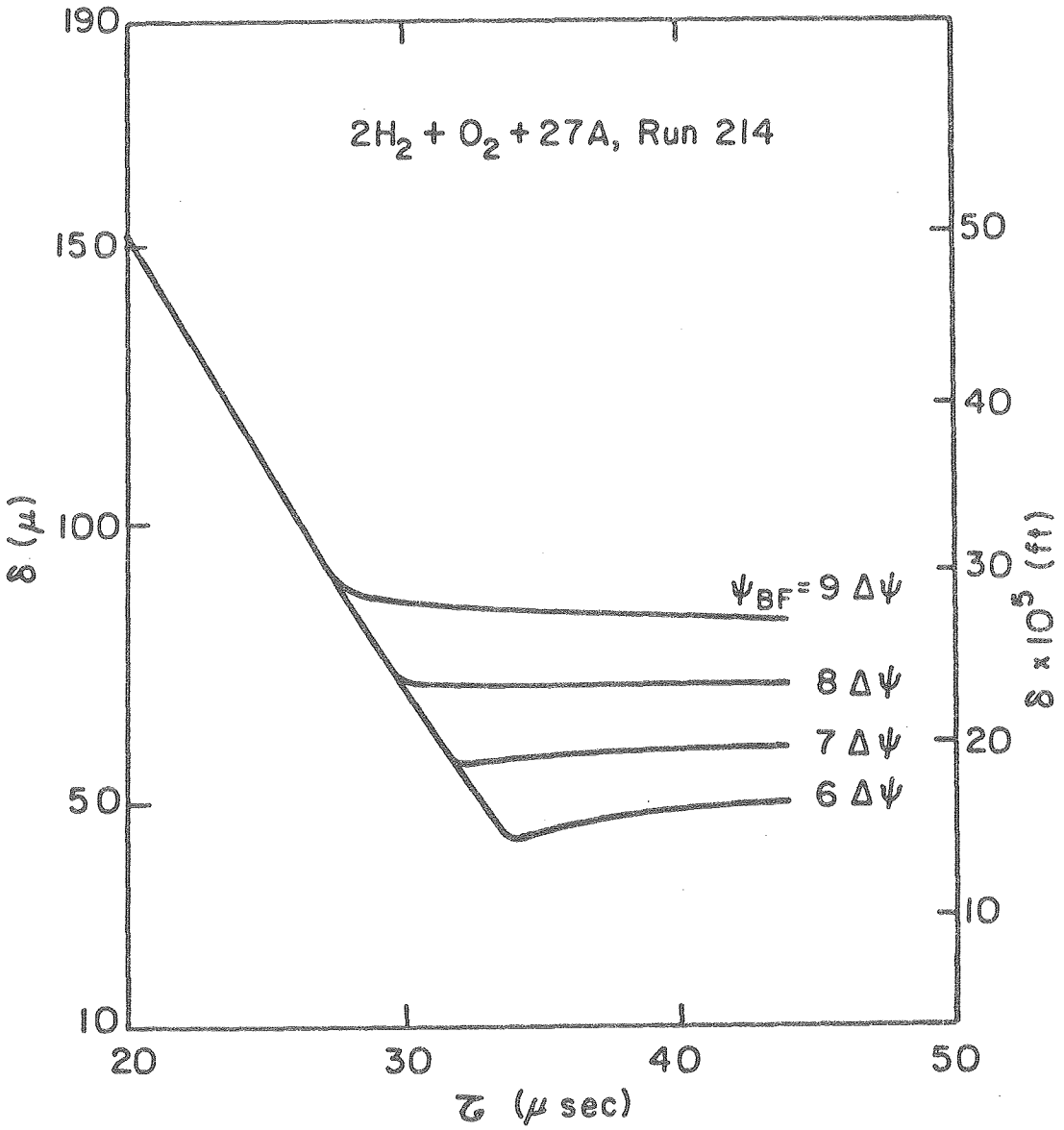

Figure 6.12. Location of the combustion zone.

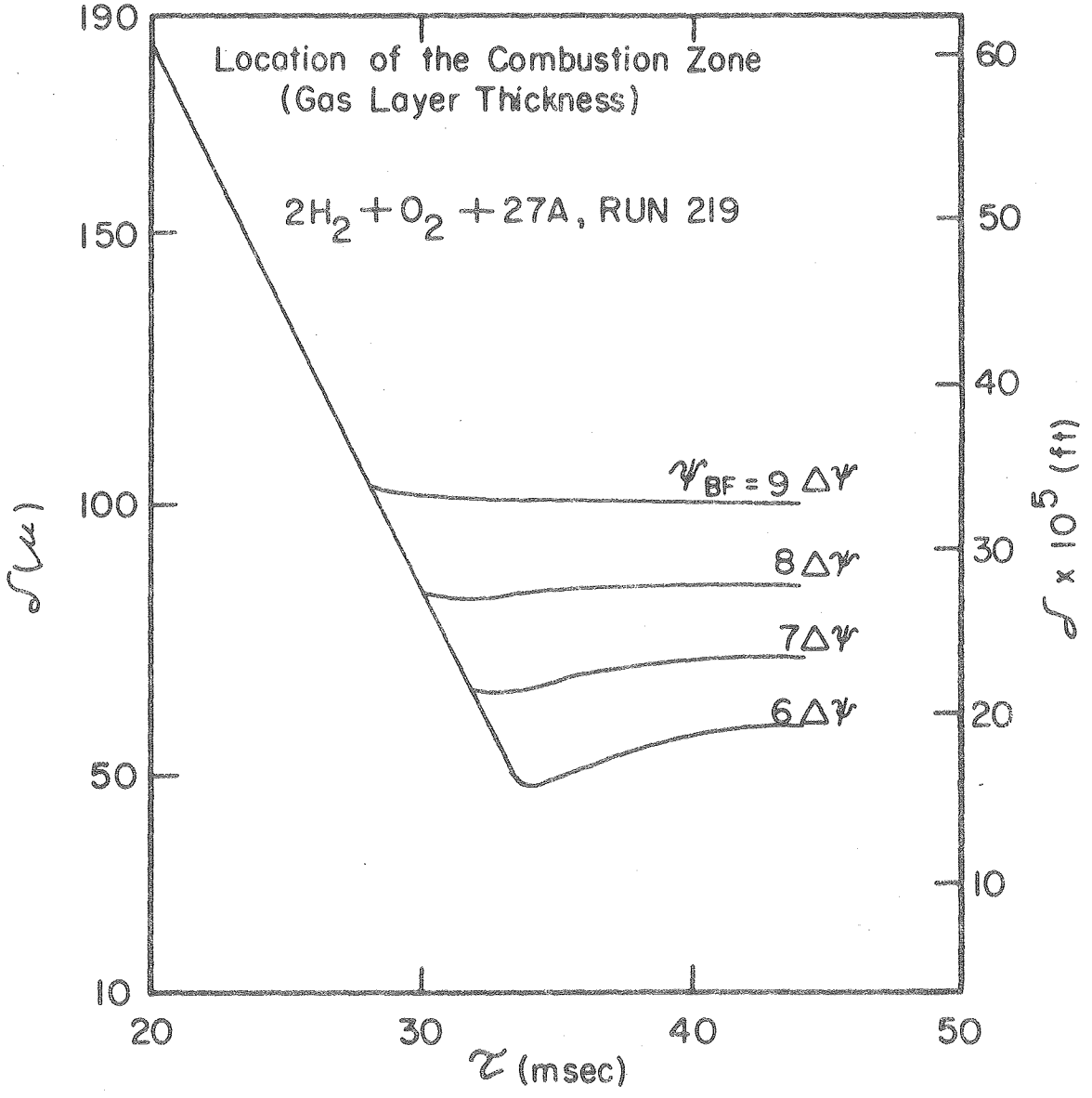

Figure 6.13. Location of the combustion zone.

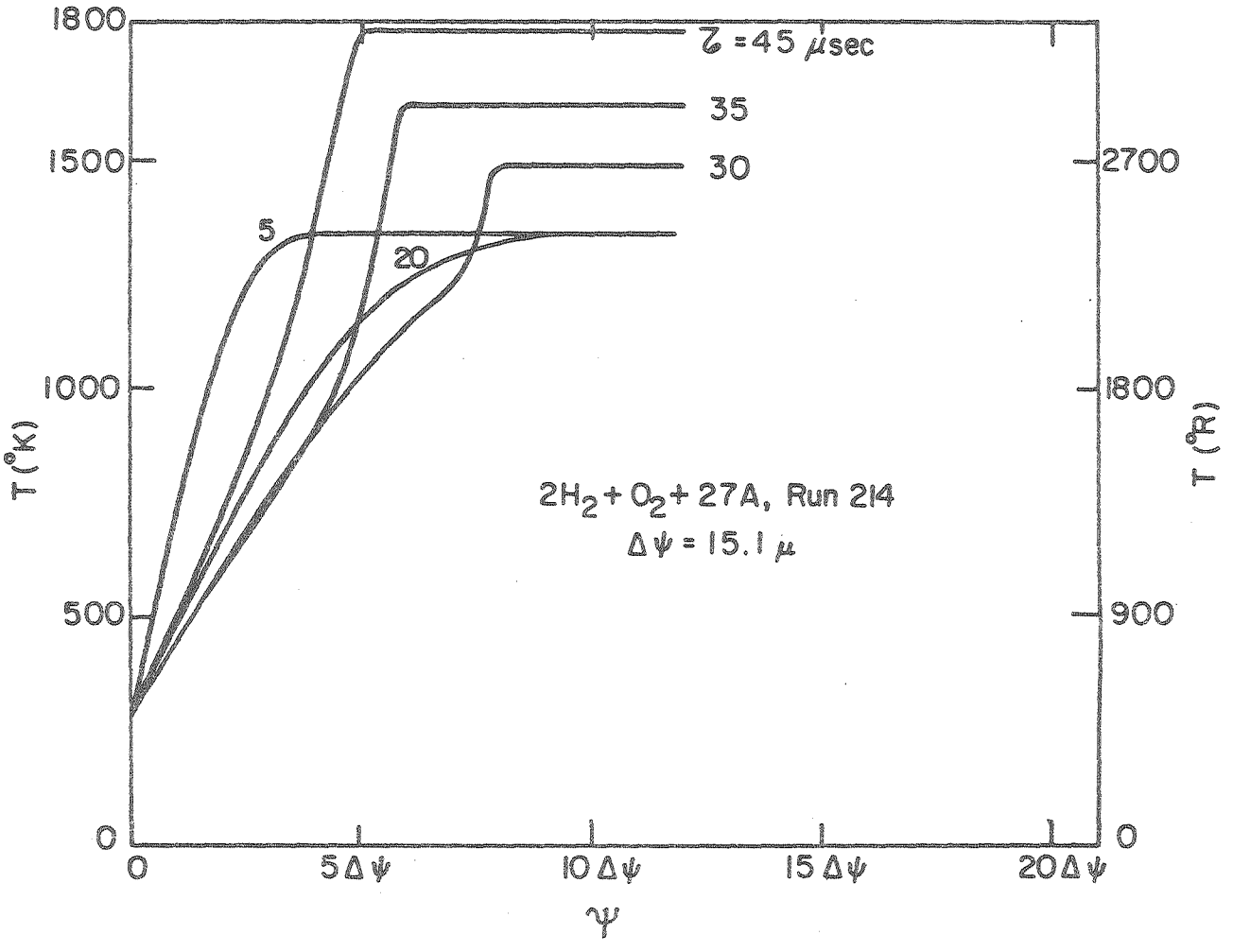

Figure 6.14. Temperature distributions.

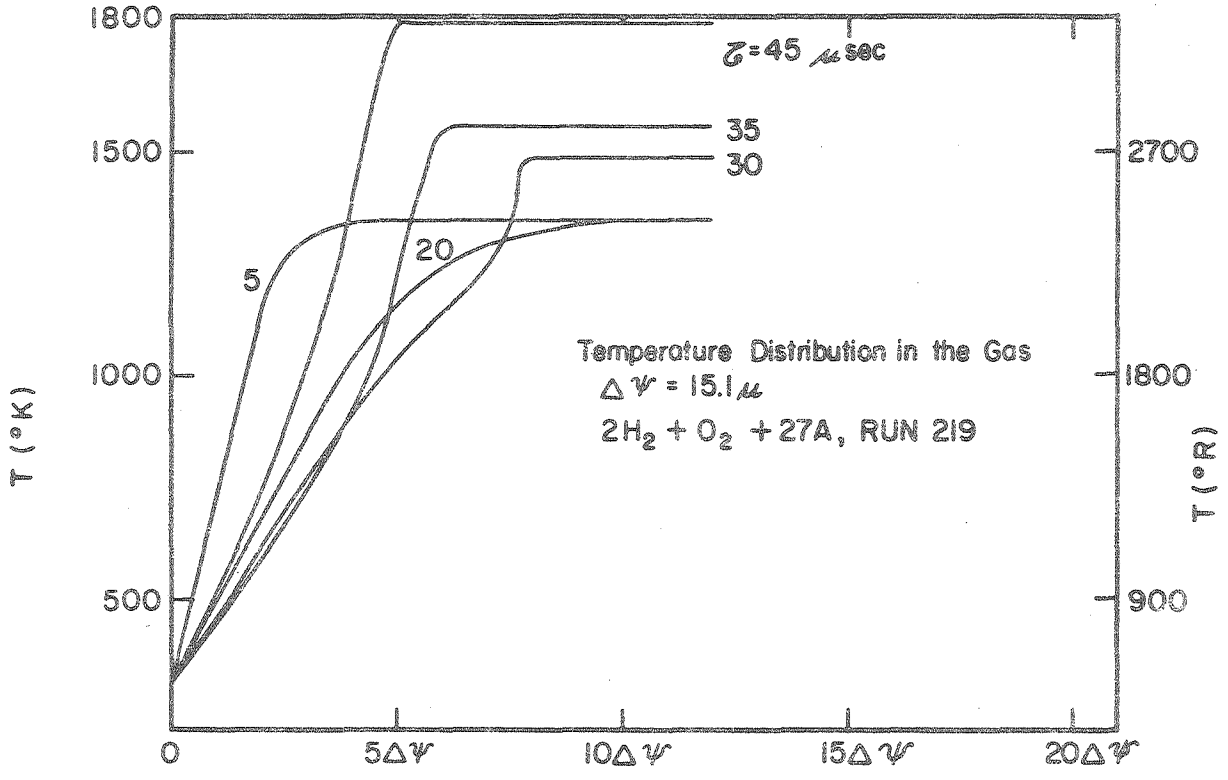

Figure 6.15. Temperature distribution.

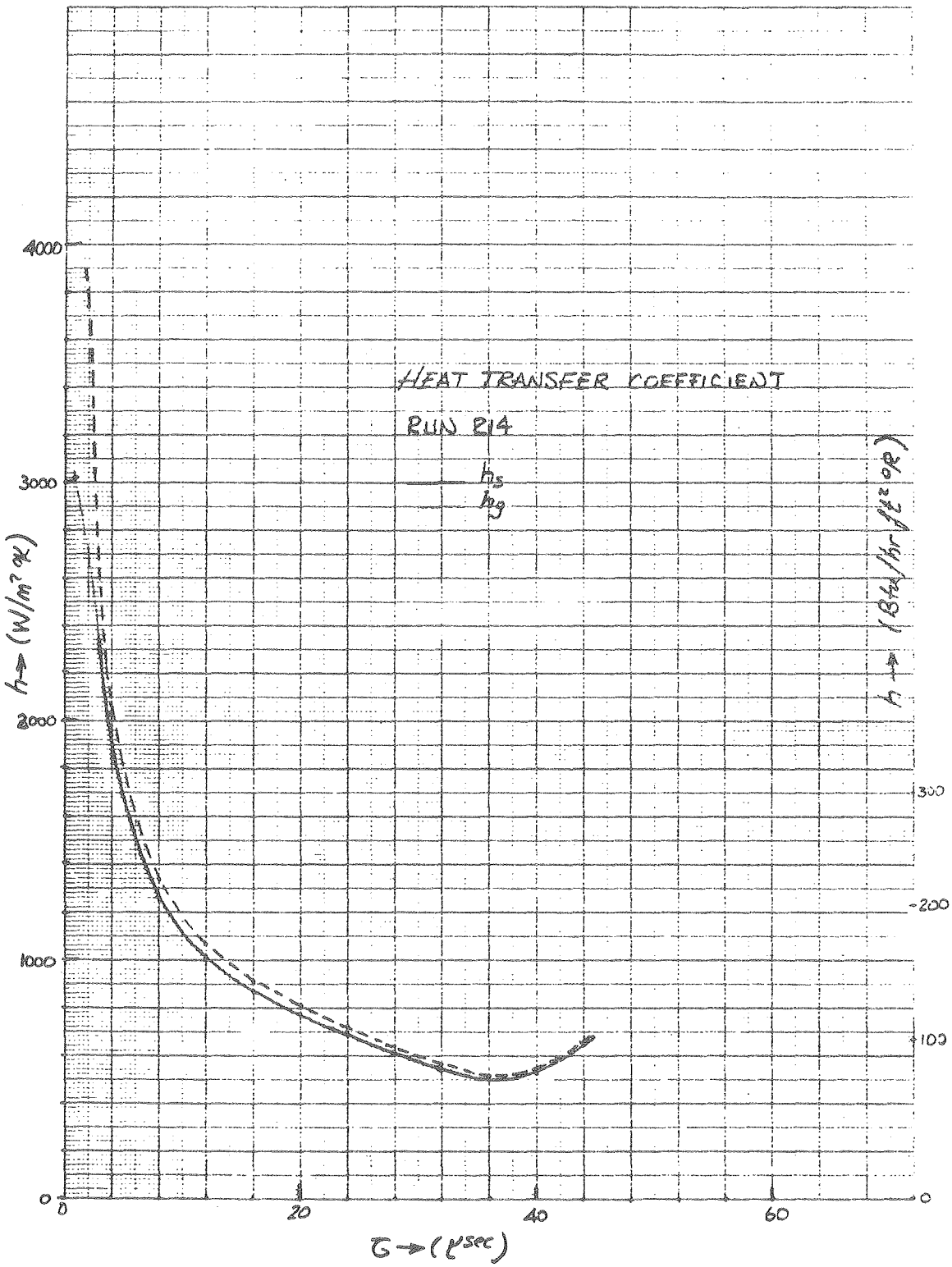

Figure 6.16. Heat transfer coefficient.

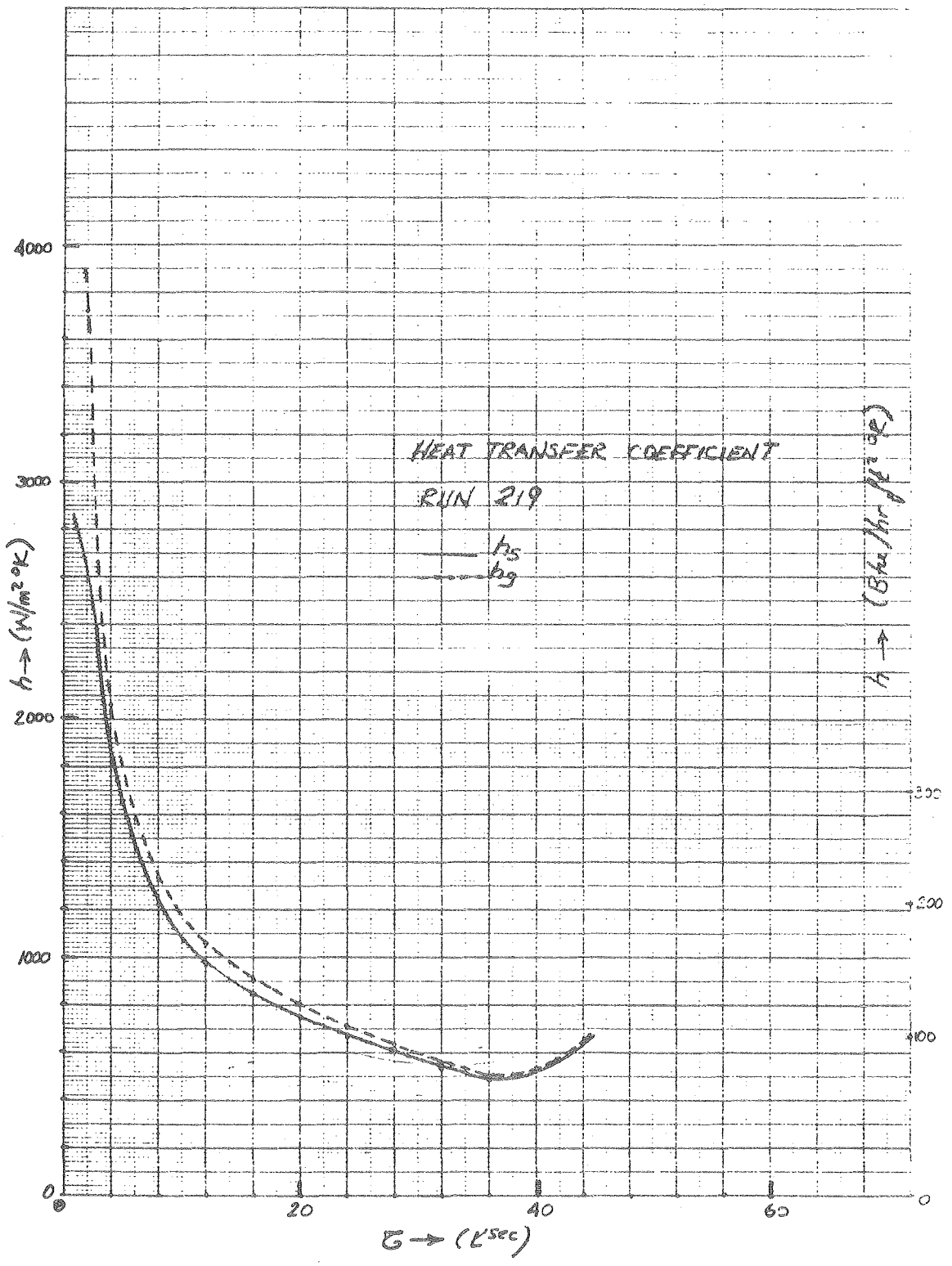

Figure 6.17. Heat transfer coefficient.

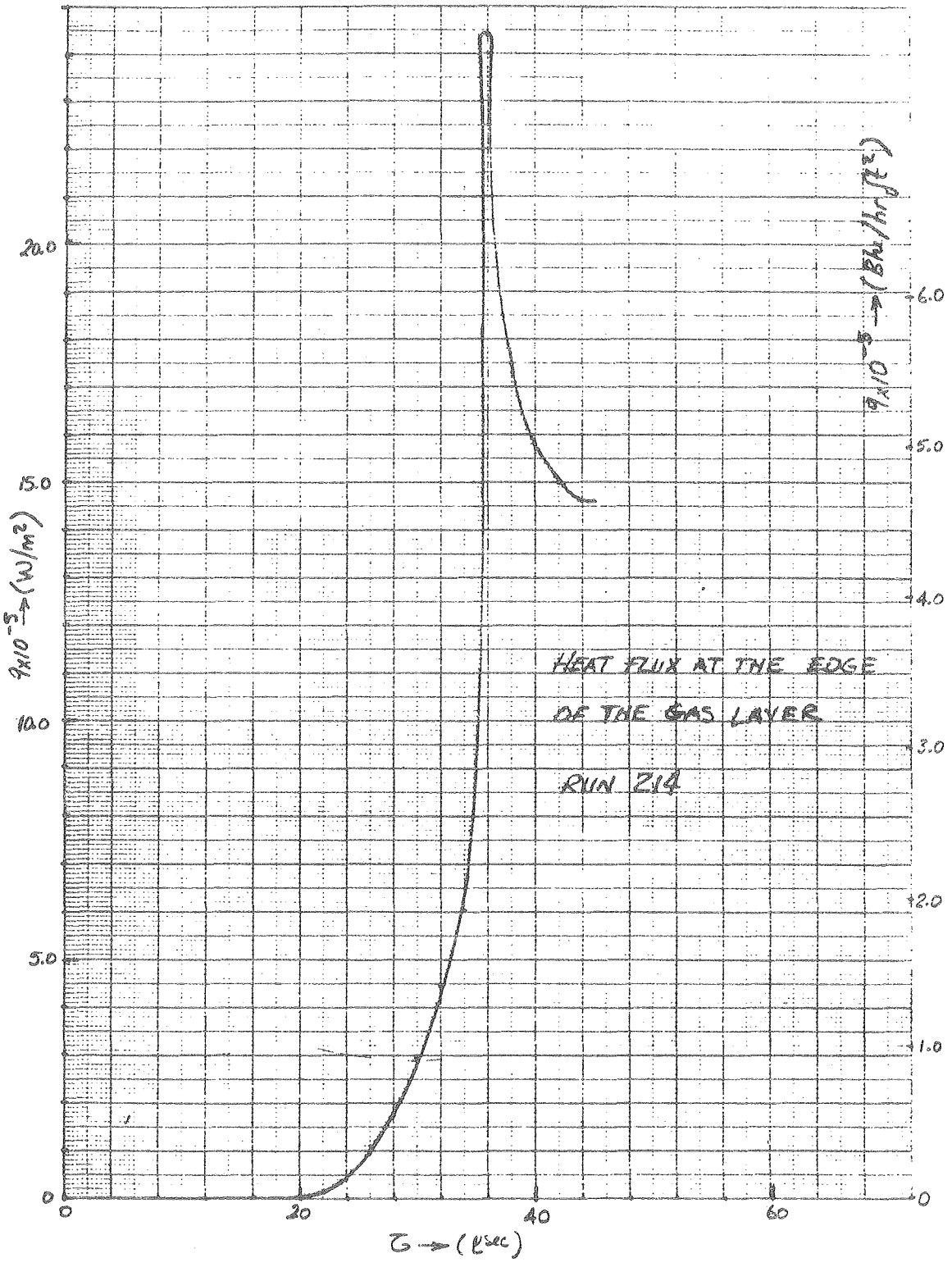

Figure 6.18. Heat flux at the edge of the gas layer.

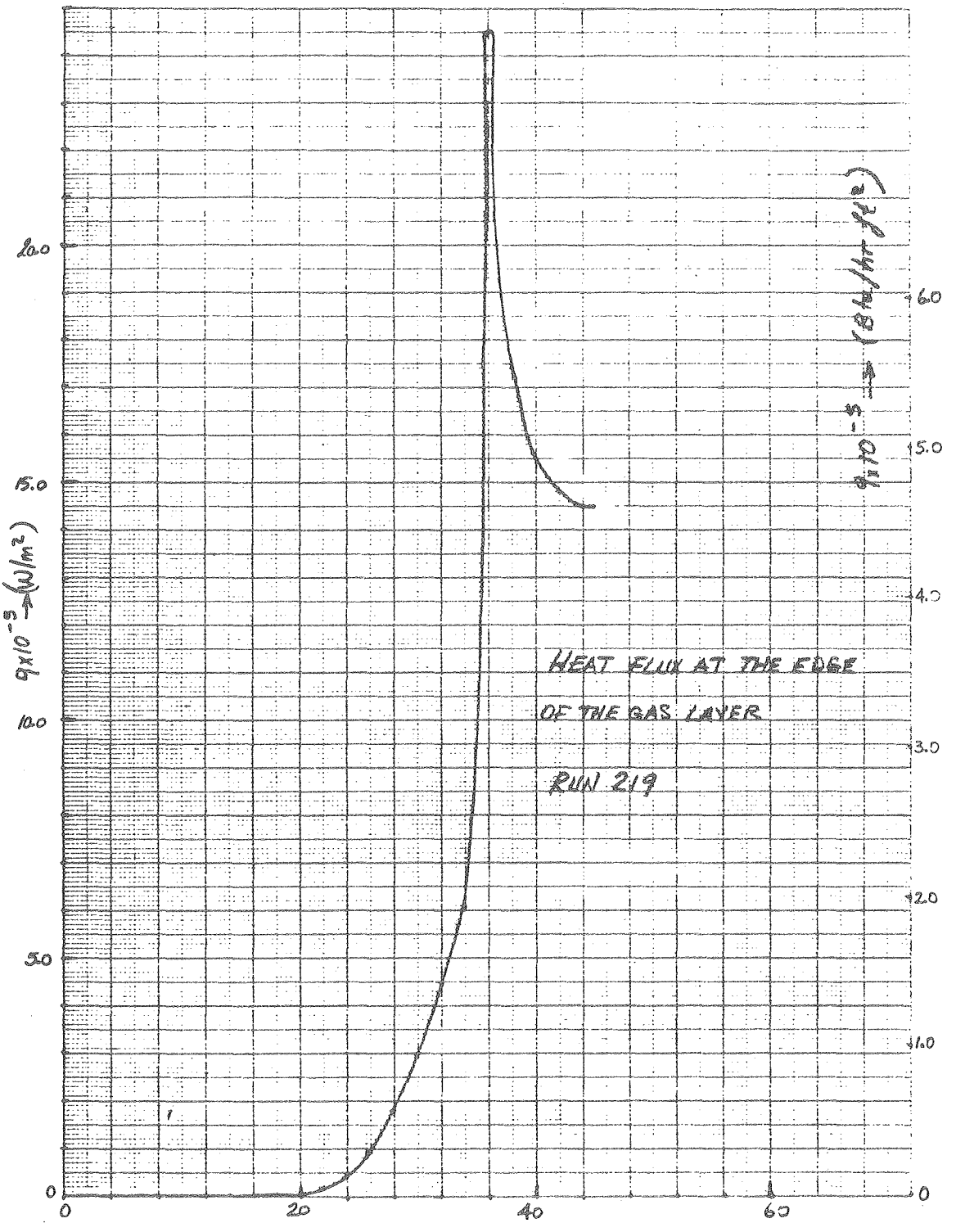

Figure 6.19. Heat flux at the edge of the gas layer.

VII. DETERMINATION OF THE HEAT FLUX IN A CONSTANT VOLUME CHAMBER

The determination of the heat flux to the wall in the presence of a flame propagating towards the wall is of interest in combustion chambers. The study in the previous chapters considered the heat transfer from a combustion zone behind a detonation wave with the diffusion of the combustion zone towards the wall. The flame was moving away from the wall. In this chapter a set of experiments which was performed in a constant volume chamber is discussed. A methane, air mixture at an equivalence ratio of unity was used.

7.1. Experimental Apparatus and Measurements

Experiments were performed in a cylindrical, stainless steel explosion vessel, fitted with optical glass windows suitable for schlieren photography, [22], Figure 7.1. The total volume of the vessel was 530.6 cm^3. Four instrument plugs were fitted on the sides of the vessel. One of them was used to purge the burnt gases out of the chamber after the experiment was completed. The two plugs on the sides were used to hold the spark plug, Figure 7.2, which was used to ignite the mixture and to hold the thin film resistance thermometer, Figure 7.3. The top plug held a Kistler Nr. 601 pressure transducer, Figure 7.4, to record the pressure variation with time. A schematic diagram of the experimental apparatus is shown in Figure 7.5 which shows the locations of the instruments.

The heat transfer gauge was designed and prepared in a manner similar to that described in Chapter II. An additional hole is present in the gauge which was used to fill the vessel with the test gas, Figure 7.6. Only one thermocouple junction was placed on the surface of the gauge. This was used for recording the initial temperature of the gas. The calibration curve of the gauge is shown in Figure 7.7. The signal from the gauge was amplified and recorded on the screen of a Tektronix dual beam oscilloscope (Model 551). The signal has first a gradual increase which is followed by a very sharp increase corresponding to the time when the flame is very close to the wall. To more accurately analyze the high heat flux interval the same signal was delayed and recorded on the screen of a second oscilloscope, Tektronix Nr. 549 storage oscilloscope, which was set to a higher sweep speed. This expanded the signal over the range where there was a rapid change in the temperature.

The signal from the pressure transducer was amplified through a charge amplifier and recorded on the screen of the dual beam oscilloscope using its second channel. The calibration constant for the pressure transducer was 9.95 psi (6.8×10^4 Pa.) per volt. The signals from the heat transfer gauge and the pressure transducer are shown in Figure 7.8 for run 7 and in Figure 7.9 for run 10. The oscillogram on top is the delayed temperature signal with a 0.5 msec/cm sweep speed. The sensitivity is 0.5 v/cm. The picture at the bottom contains two signals. The one on top is the temperature signal with a sensitivity of 1 v/cm,

the other one is for the pressure with a sensitivity of 2 v/cm. The sweep speed is 10 msec for both signals.

The vessel was filled with a methane (CH_4)-air mixture with an equivalence ratio of 1 at room temperature, 74.2°F and atmospheric pressure, 14.80 psia. The mixture was ignited by a spark at the wall. The spark also triggered the instruments. The flame that formed, propagated toward the thin film resistance thermometers as the surface temperature of the Macor gauge increased slowly until the flame came close to the surface. At that time a very rapid increase in the surface temperature was recorded. After the mixture was completely burned the temperature started to decrease due to the cooling of the hot gases in the vessel.

7.2. Results, Discussion and Recommendations

Using the signals from the oscilloscope and the calibration curves, the variation of the wall temperature with respect to time and the pressure of the vessel as a function of time were obtained. The wall temperatures are plotted in Figure 7.10 for run 7 and in Figure 7.11 for run 10. The pressure variation is plotted in Figures 7.12 and 7.13 for runs 7 and 10 respectively.

Using a conduction analysis in the thermally semi-infinite solid, as described in Chapter III, the heat flux at the wall, q_{ws}, was calculated. The heat flux variations q_{ws}, are shown in Figures 7.14 and 7.15 for runs 7 and 10. The heat flux increases slowly at first due to the compression of the unburned gases resulting from the burning

gases. The heat transfer gauge is placed on the wall opposite the spark plug, hence it gives us the heat flux from the unburned gases until the flame comes close to the wall. At this time the heat flux starts to increase rapidly due to the proximity of the flame. The heat flux reaches a maximum and then decreases due to the cooling of the hot gases near the wall [23]. These variations can be seen in Figures 7.14 and 7.15.

Further work should analyze the phenomena in the gas. An analysis should be made which would yield the heat flux at the wall. The knowledge of the temperature of the unburned gases is very important for the study. The experiments should be modified to include the direct measurement of the unburned gas temperature.

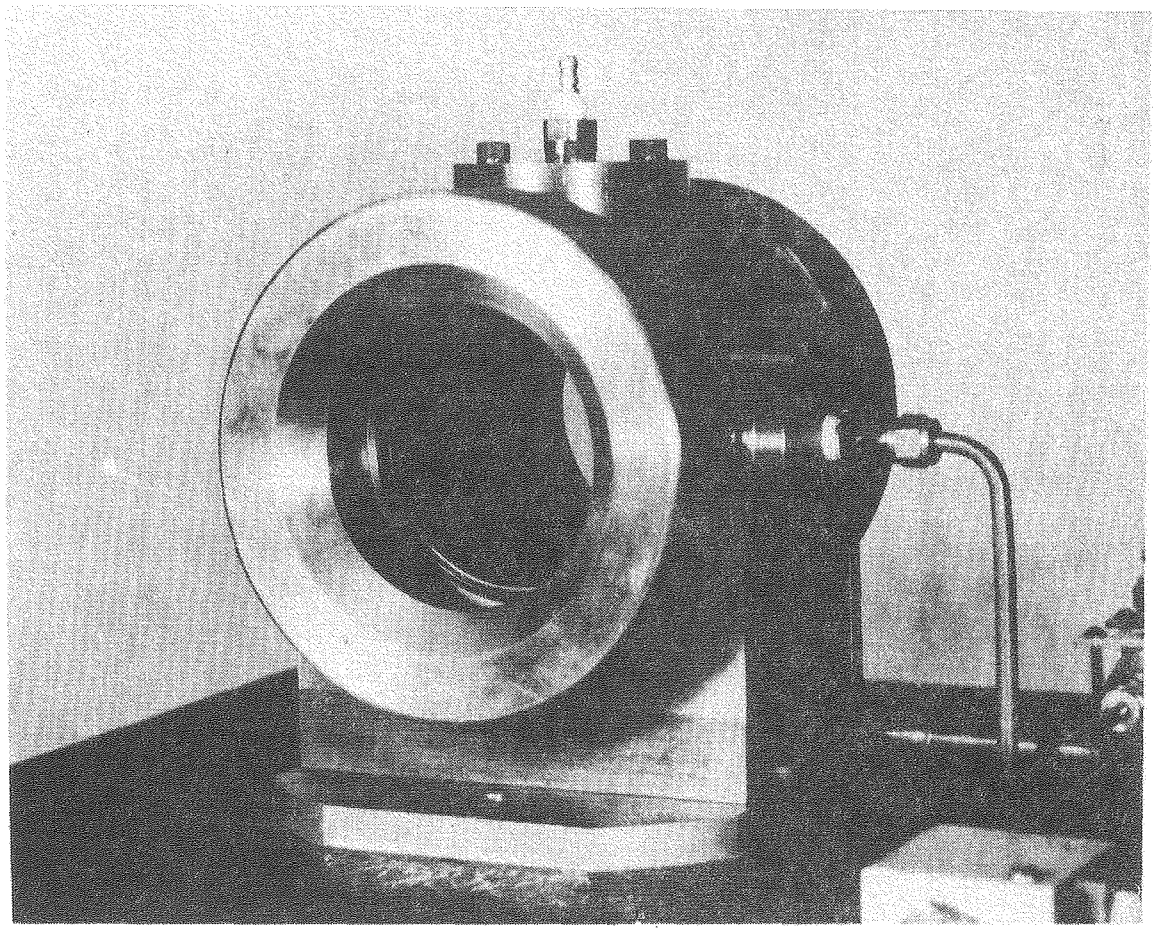

XBB805 6250

Figure 7.1. Constant volume bomb.

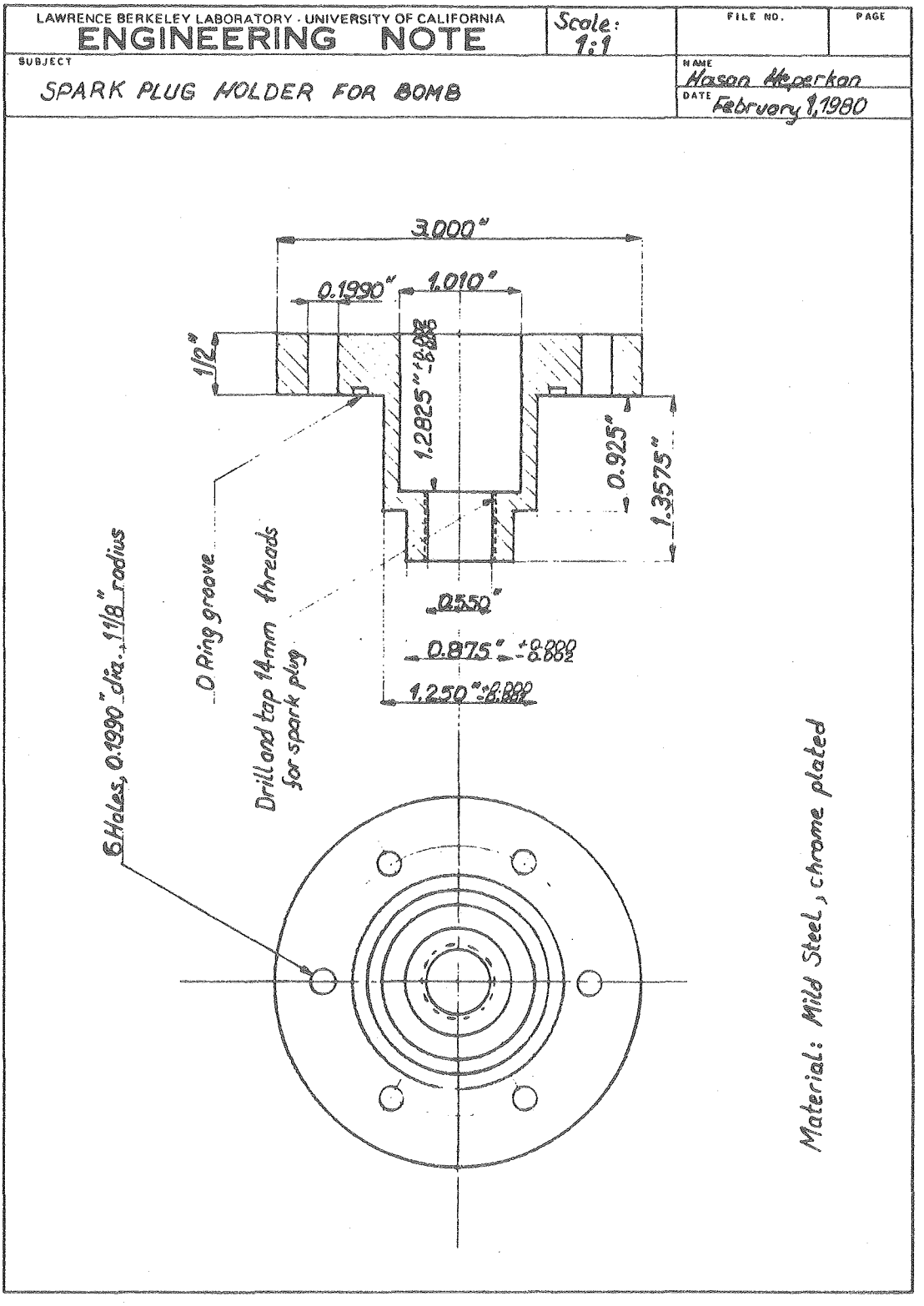

Figure 7.2. Spark plug holder.

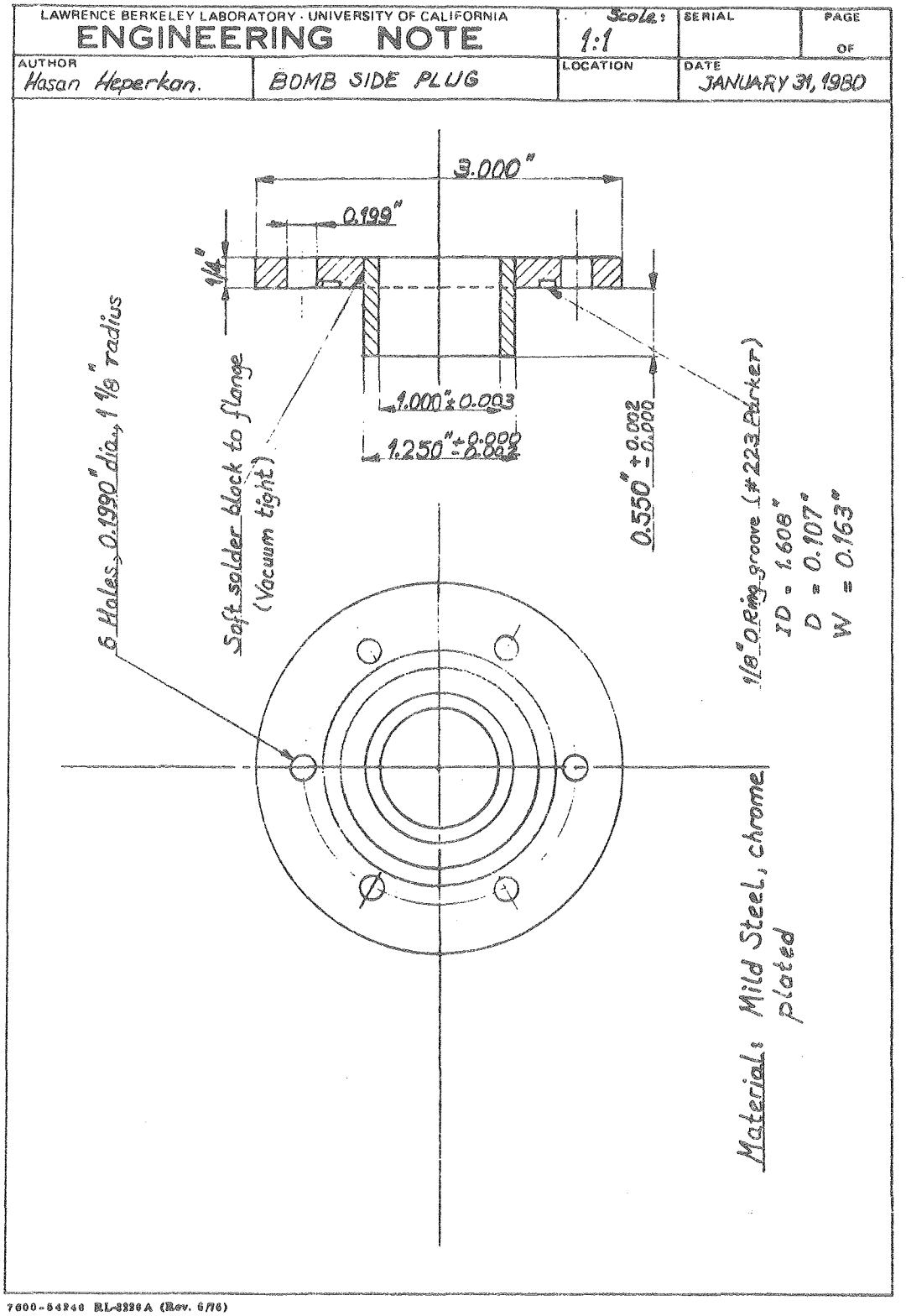

Figure 7.3. Temperature gauge holder.

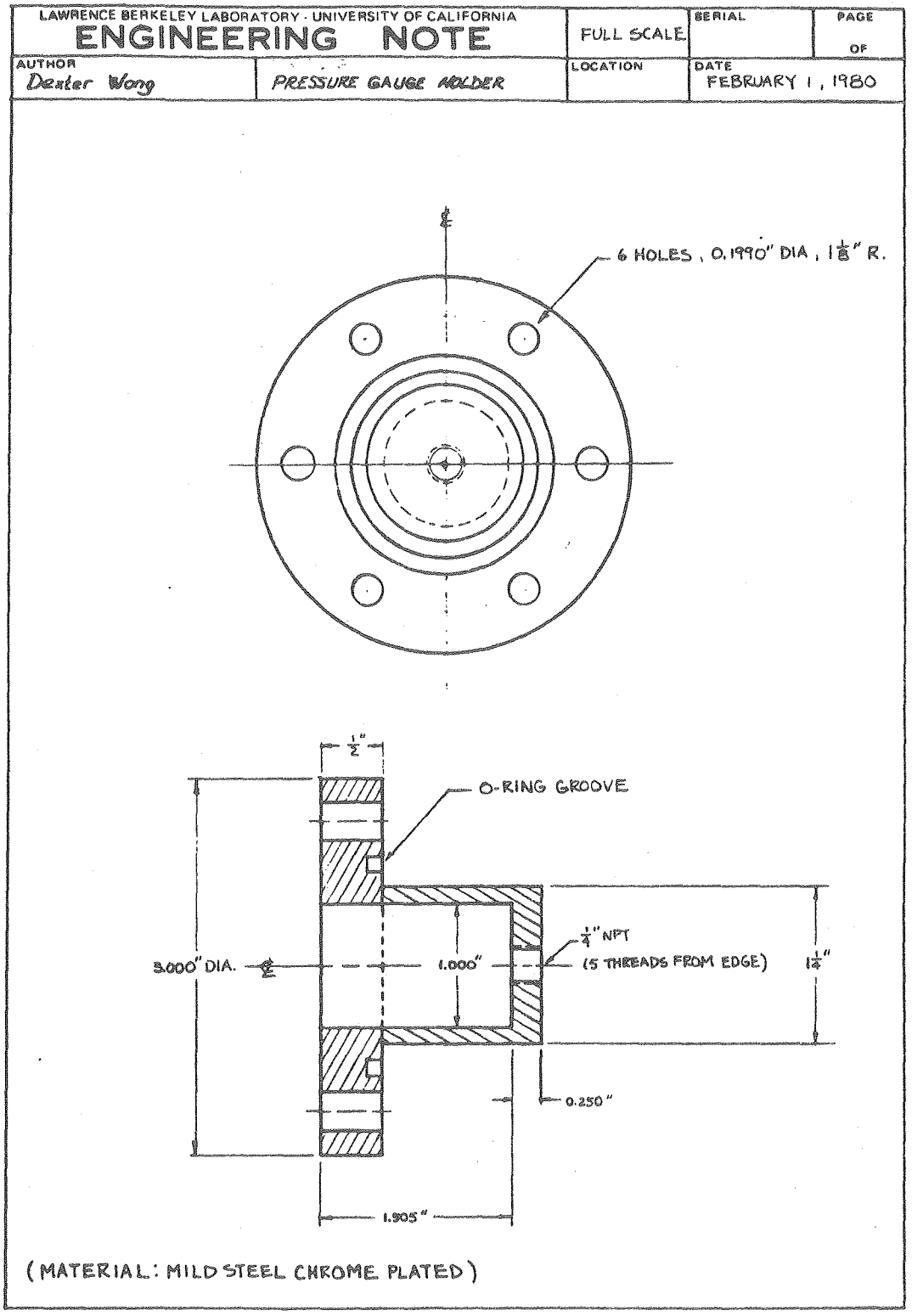

7000-84846 BL-8230 A (Rev. 6/76)

Figure 7.4. Pressure gauge holder.

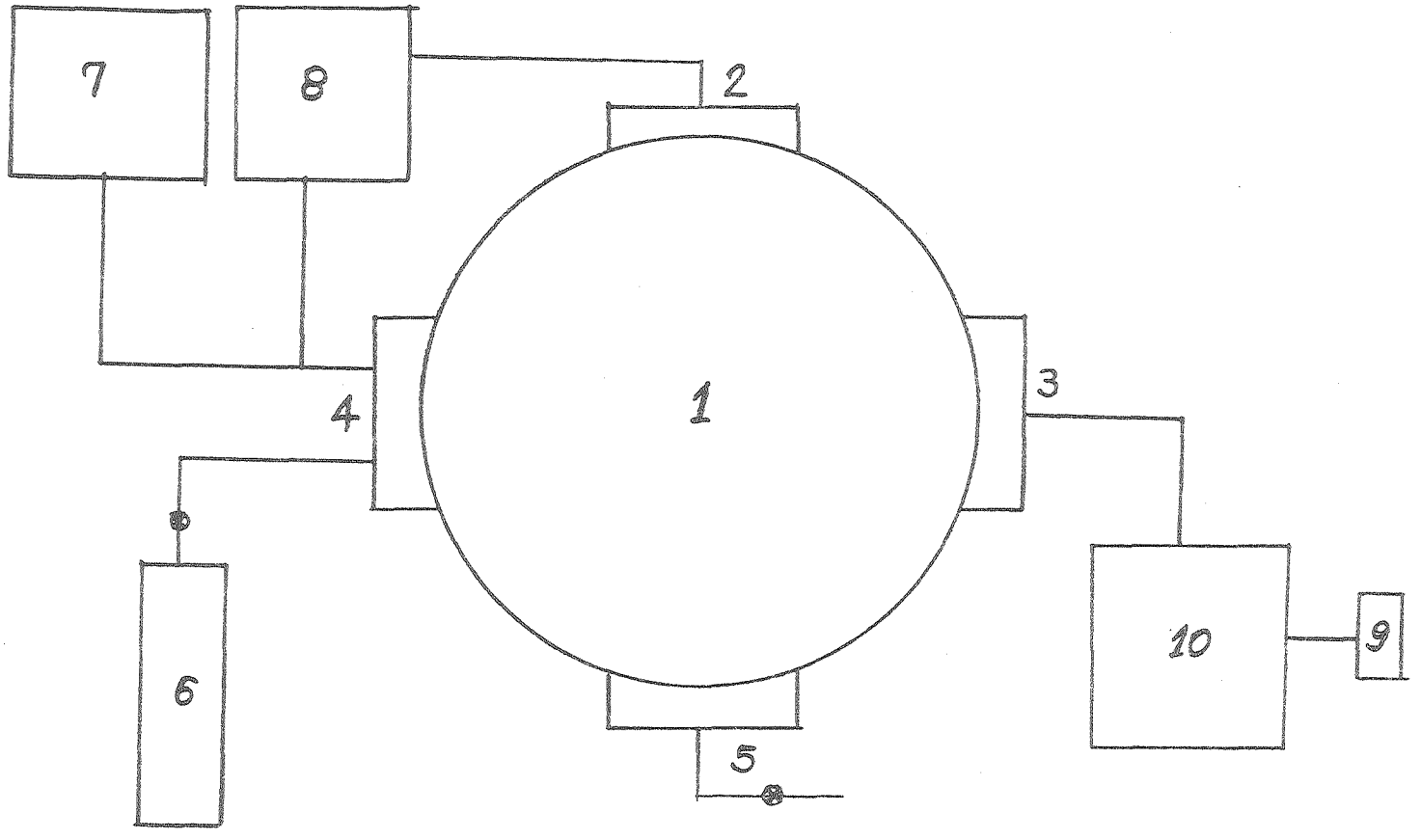

1. Constant Volume Bomb
2. Pressure Transducer
3. Spark Plug
4. Thin Film Gauge
5. Exhaust Valve
6. Methane - Air Mixture
7. Oscilloscope (Storage)
8. Oscilloscope (Dual Beam)
9. Trigger
10. Spark Power Supplier

Figure 7.5. Experimental apparatus.

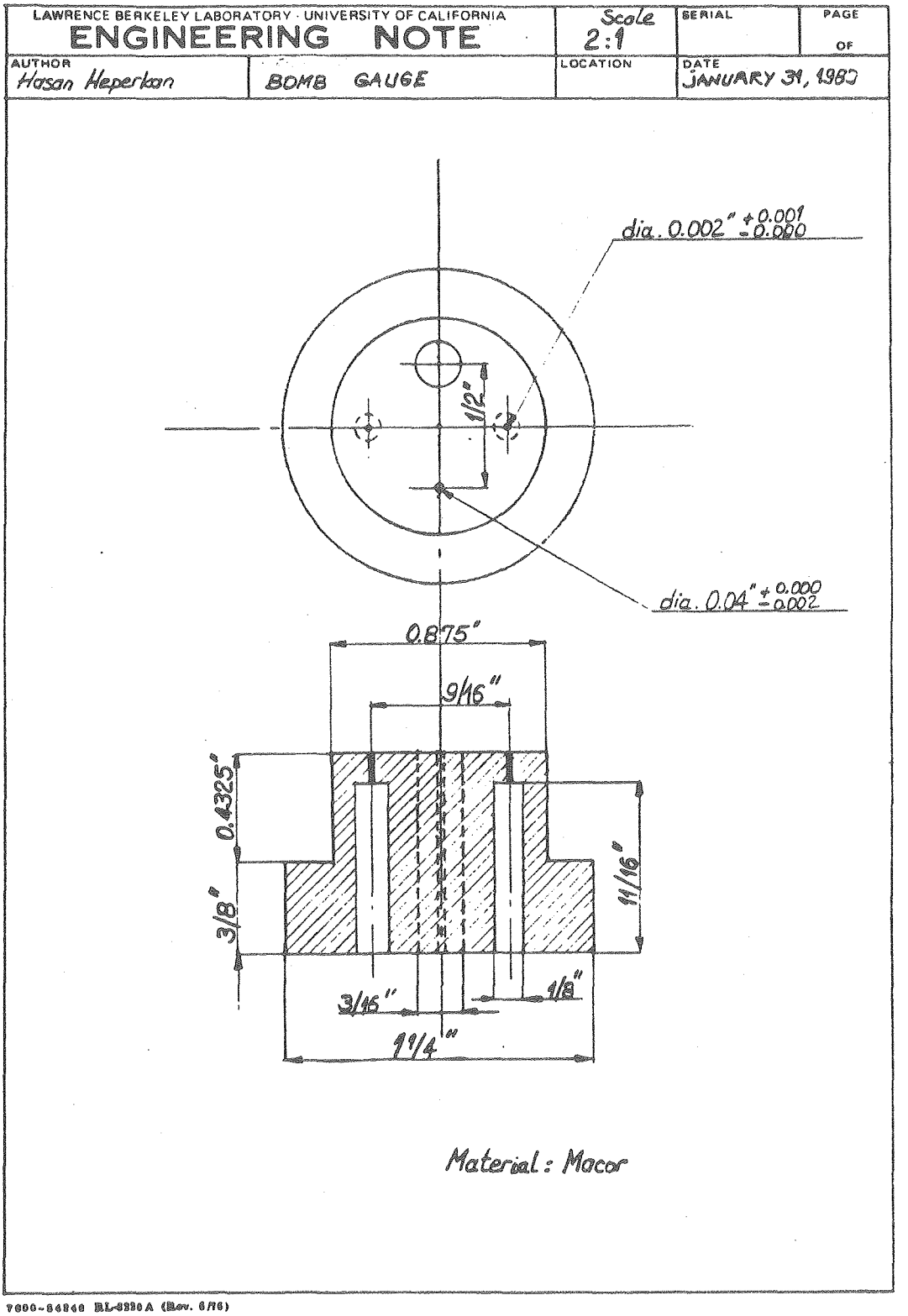

Figure 7.6. Thin film heat transfer gauge.

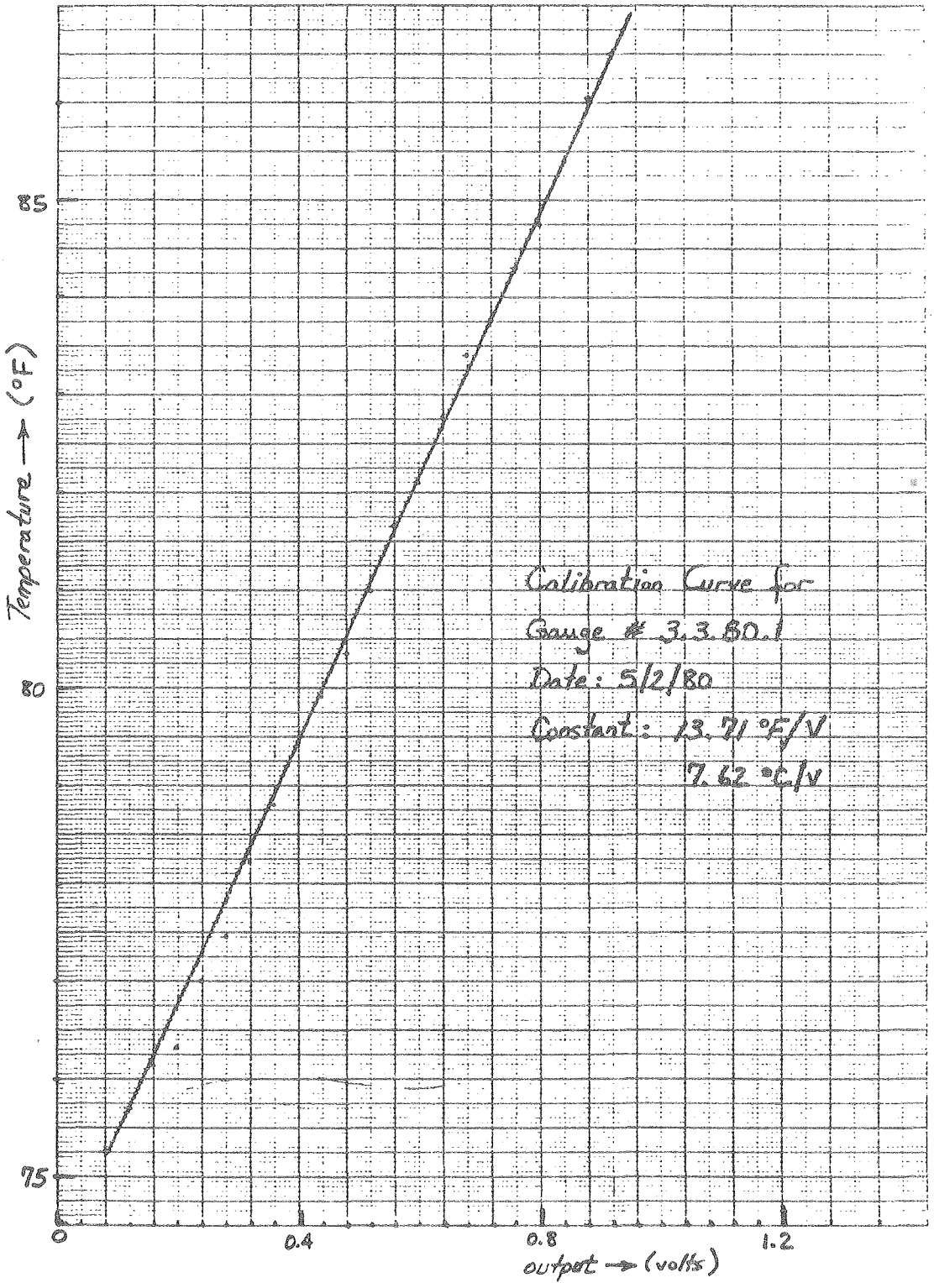

Figure 7.7. Calibration curve.

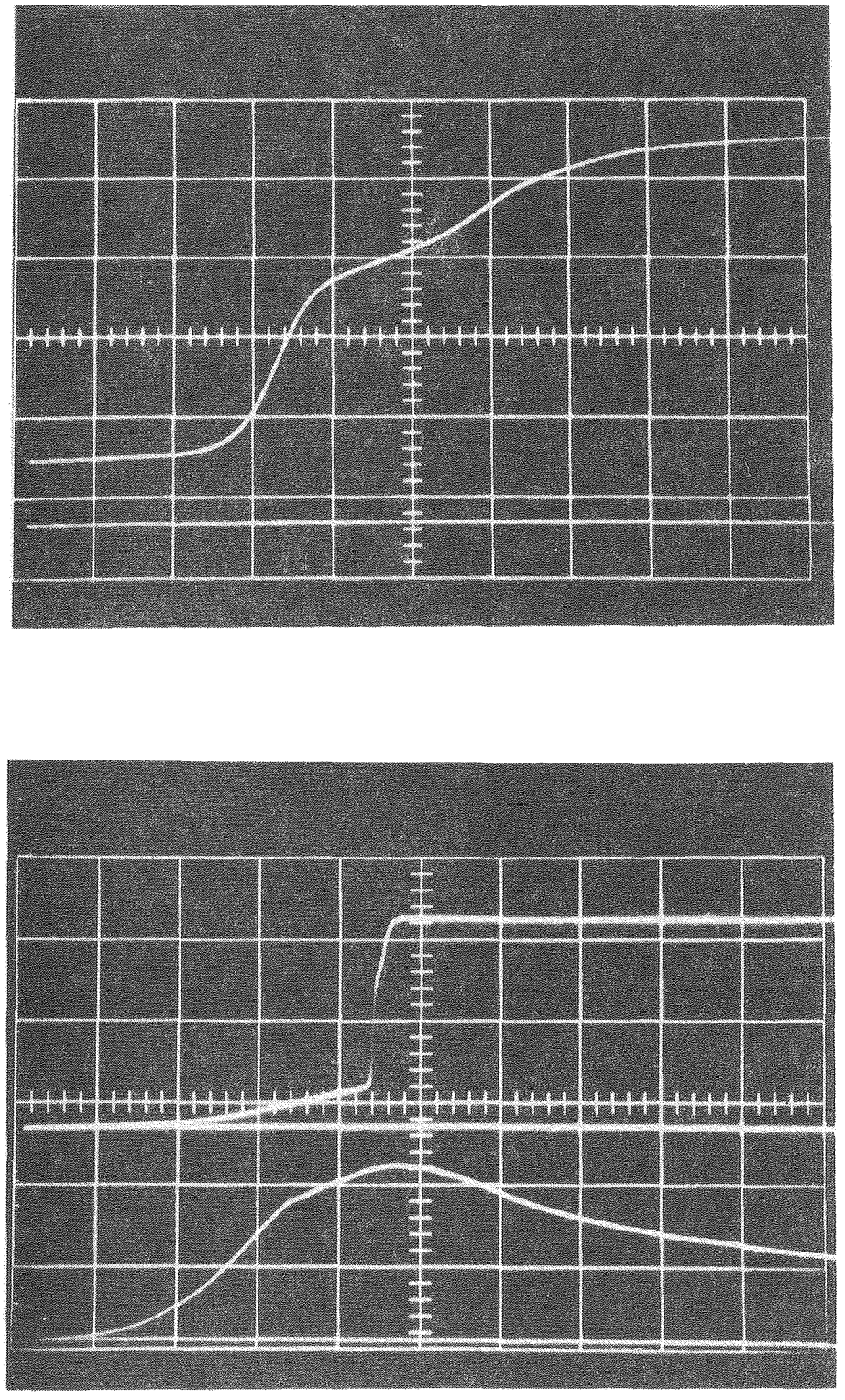

XBB805 6644

Figure 7.8. Surface temperature and pressure measurement, Run 7.
Time scale: 0.5 msec/cm and 10 msec/cm.
Vertical scale: 0.5v/cm and 1v/cm (temp.), 2v/cm (press).

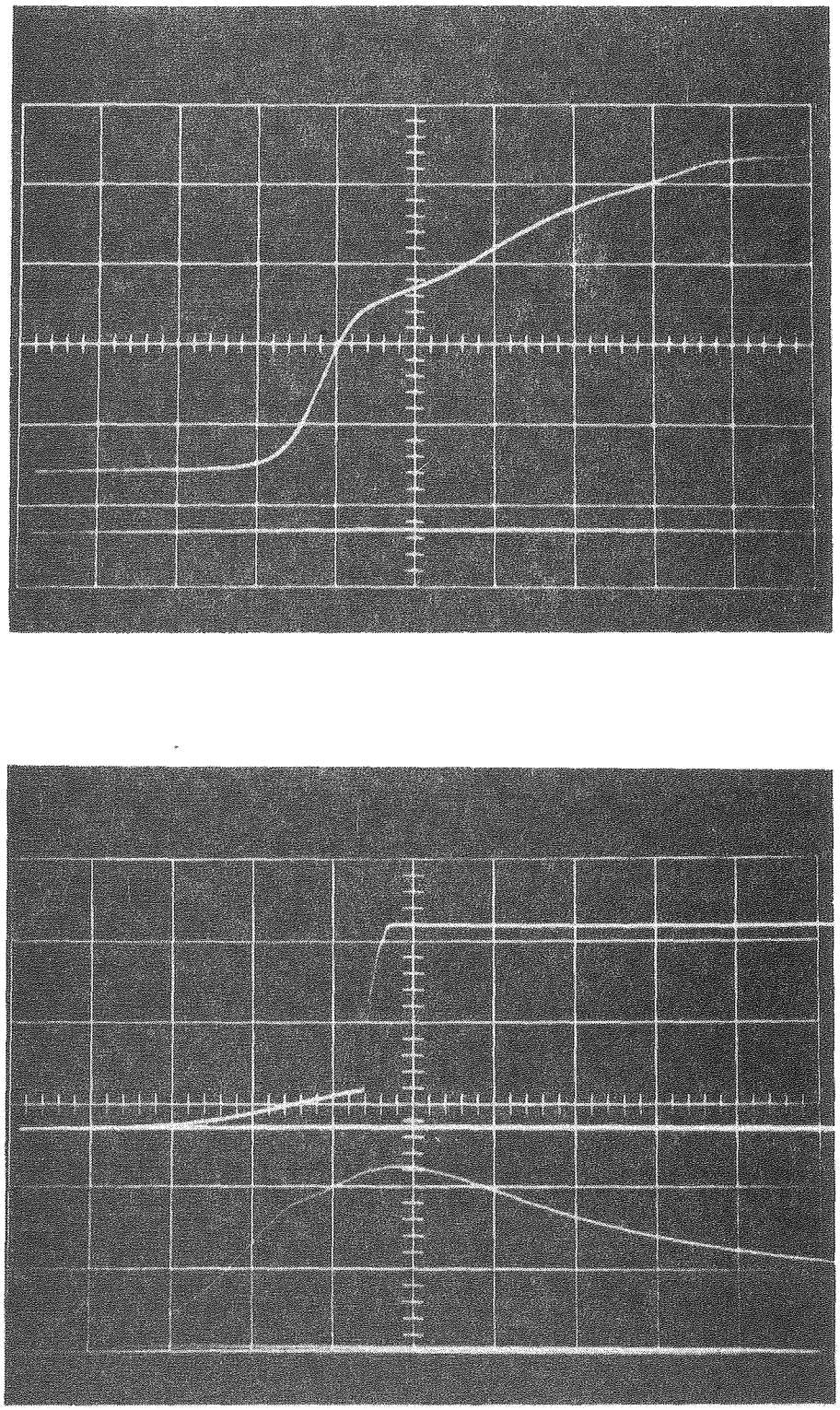

XBB805 6646

Figure 7.9. Surface temperature and pressure measurements. Run 10
Time scale: 0.5 msec/cm and 10 msec/cm.
Vertical scale: 0.5v/cm and 2v/cm (temp.), 2v/cm (press).

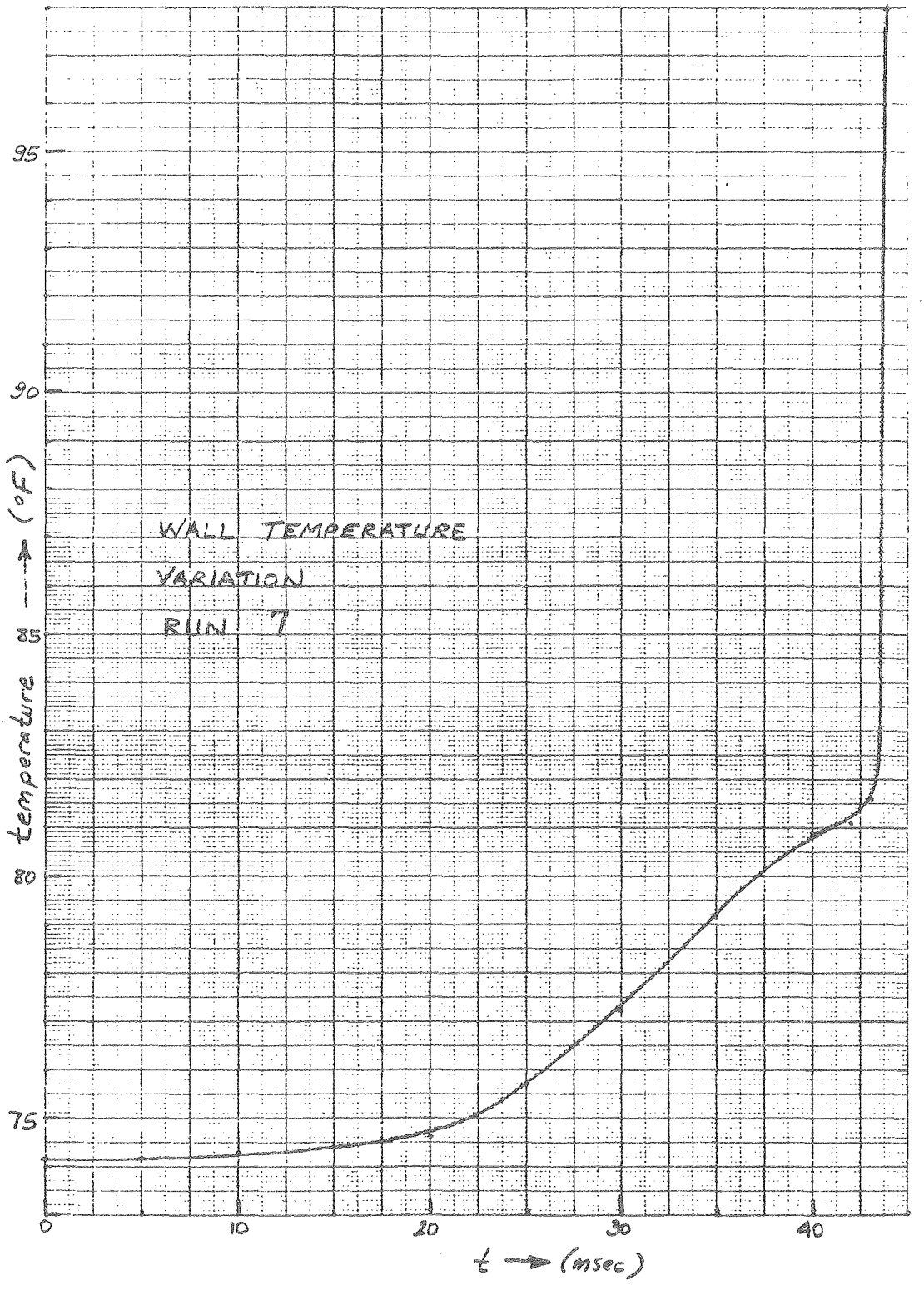

Figure 7.10. Wall temperature.

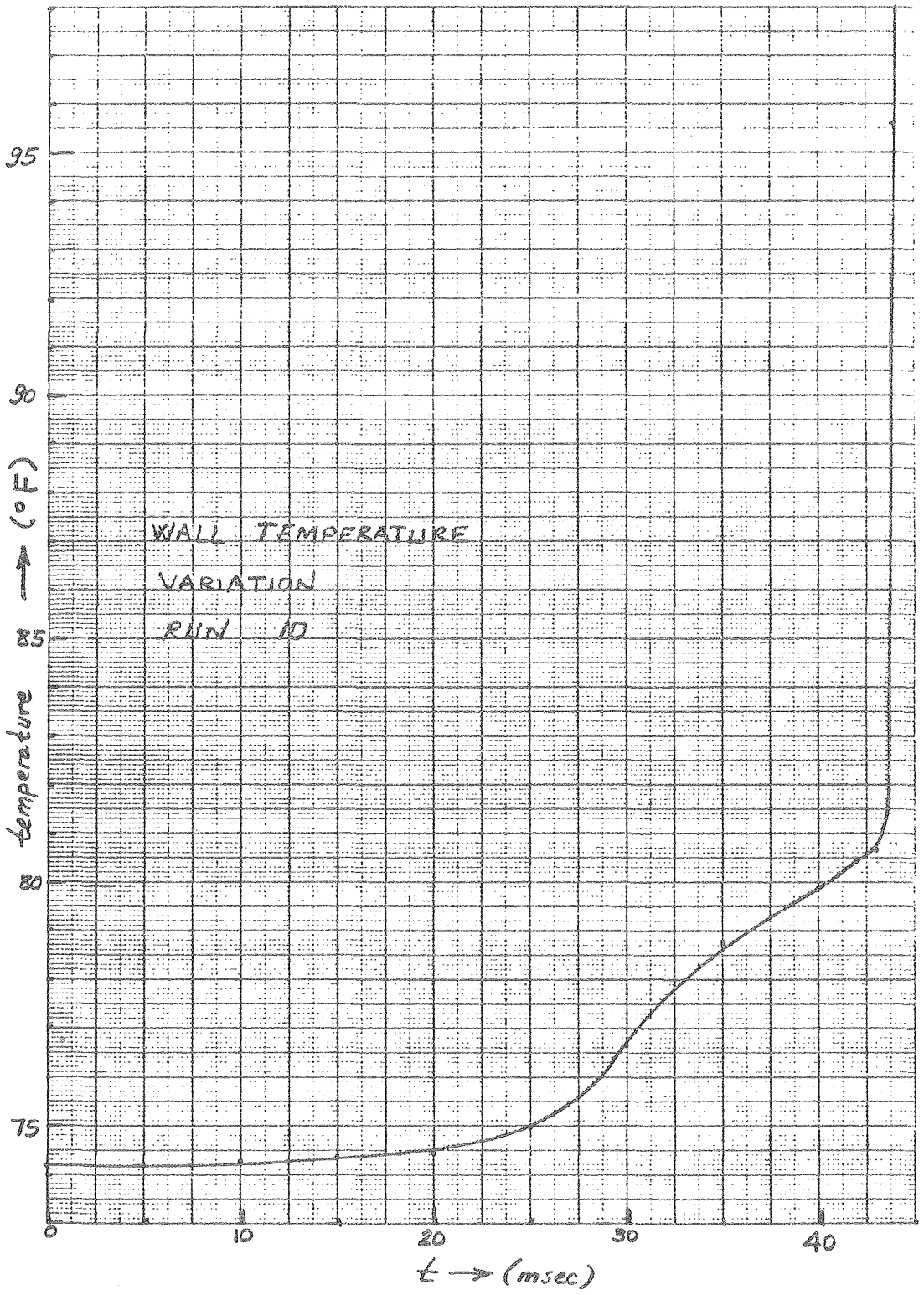

Figure 7.11. Wall temperature.

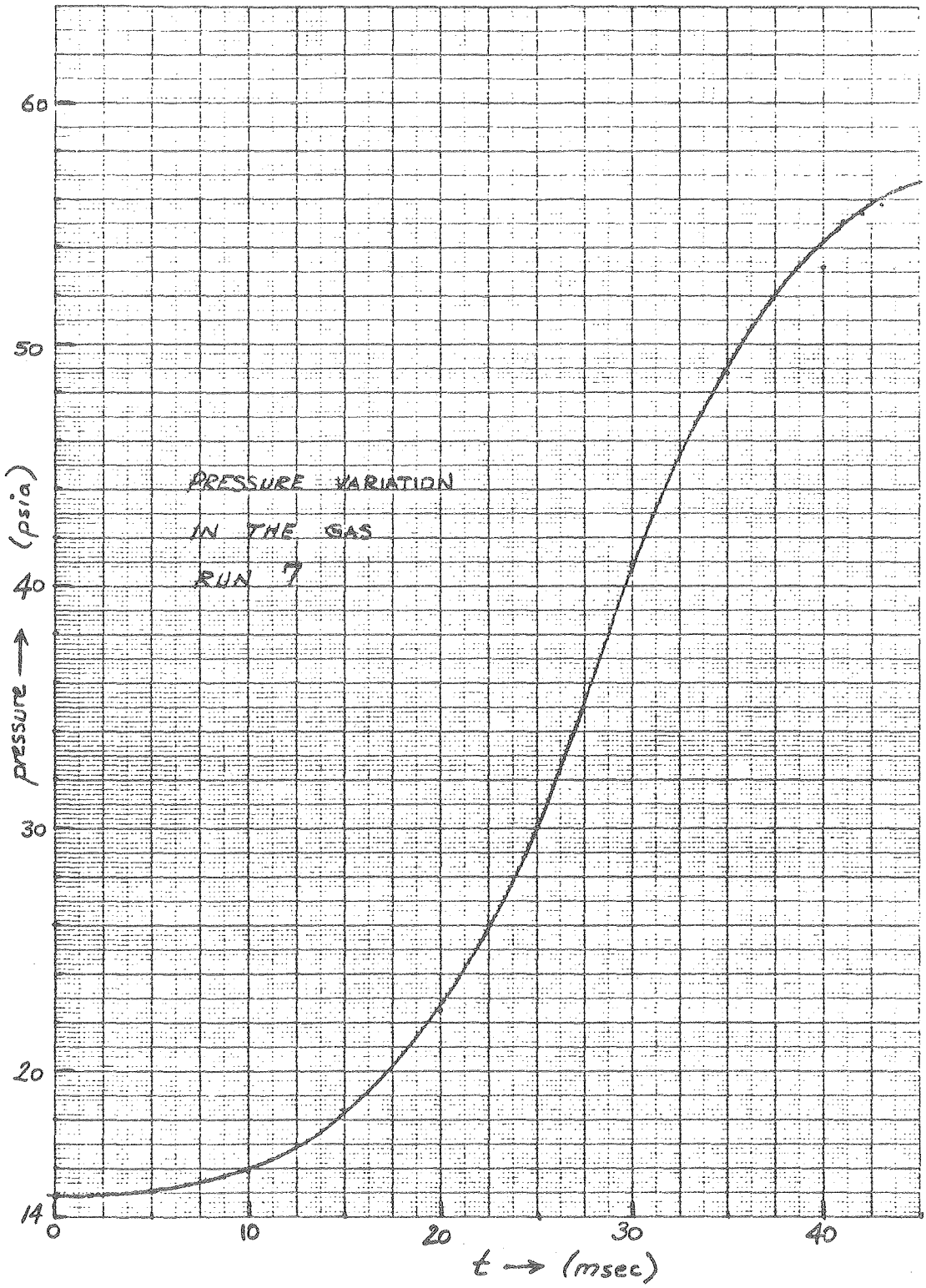

Figure 7.12. Pressure of the gas.

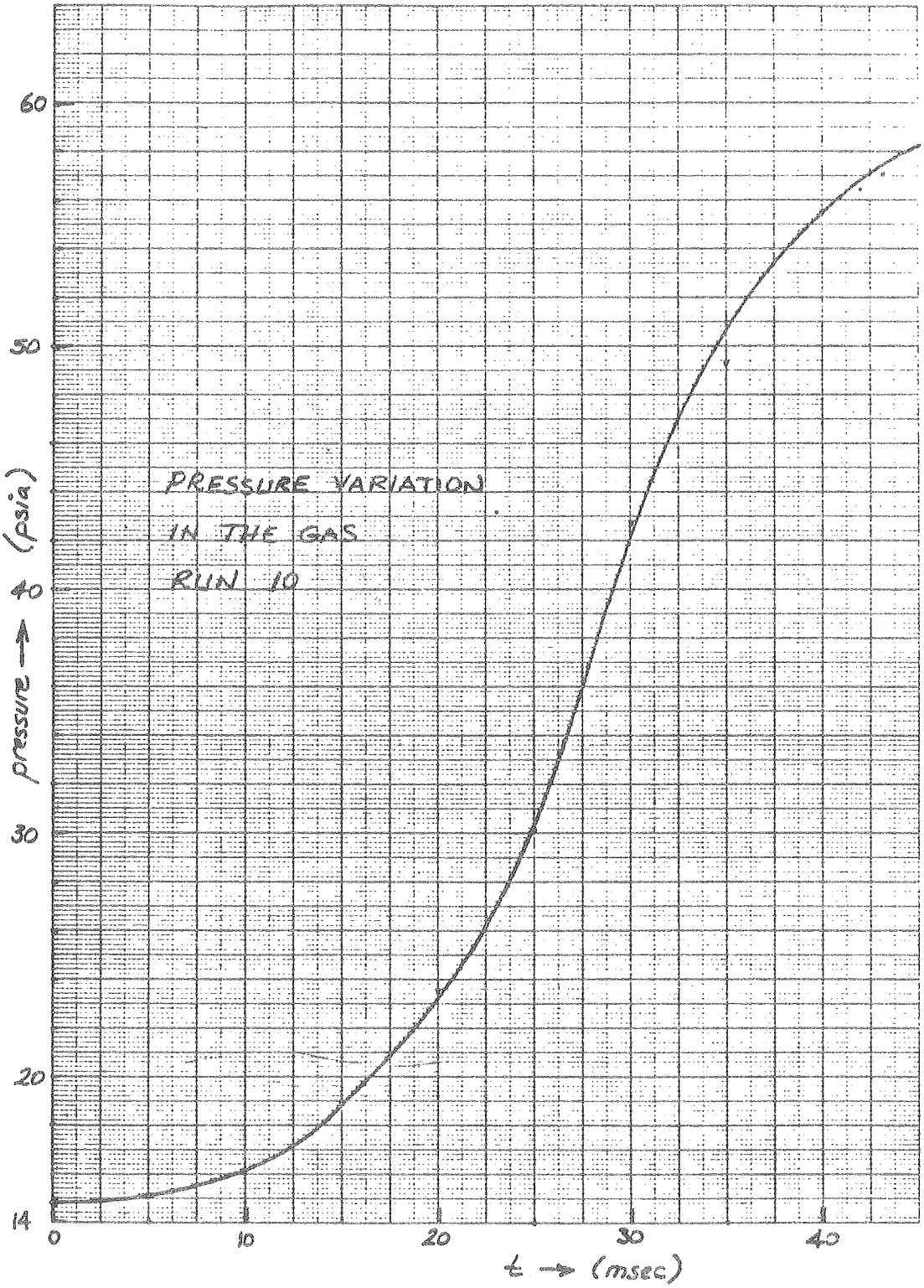

Figure 7.13. Pressure of the gas.

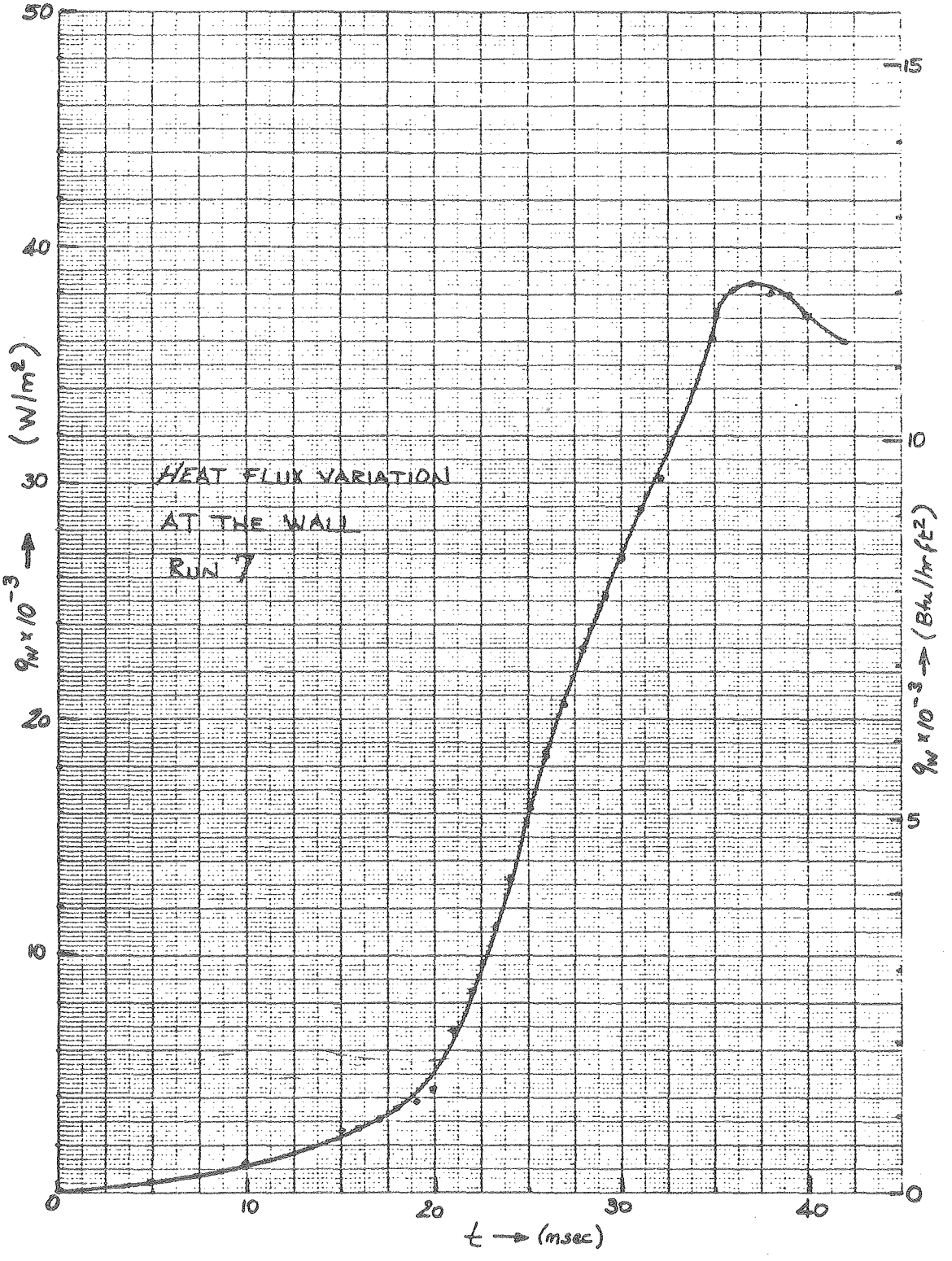

Figure 7.14. Wall heat flux.

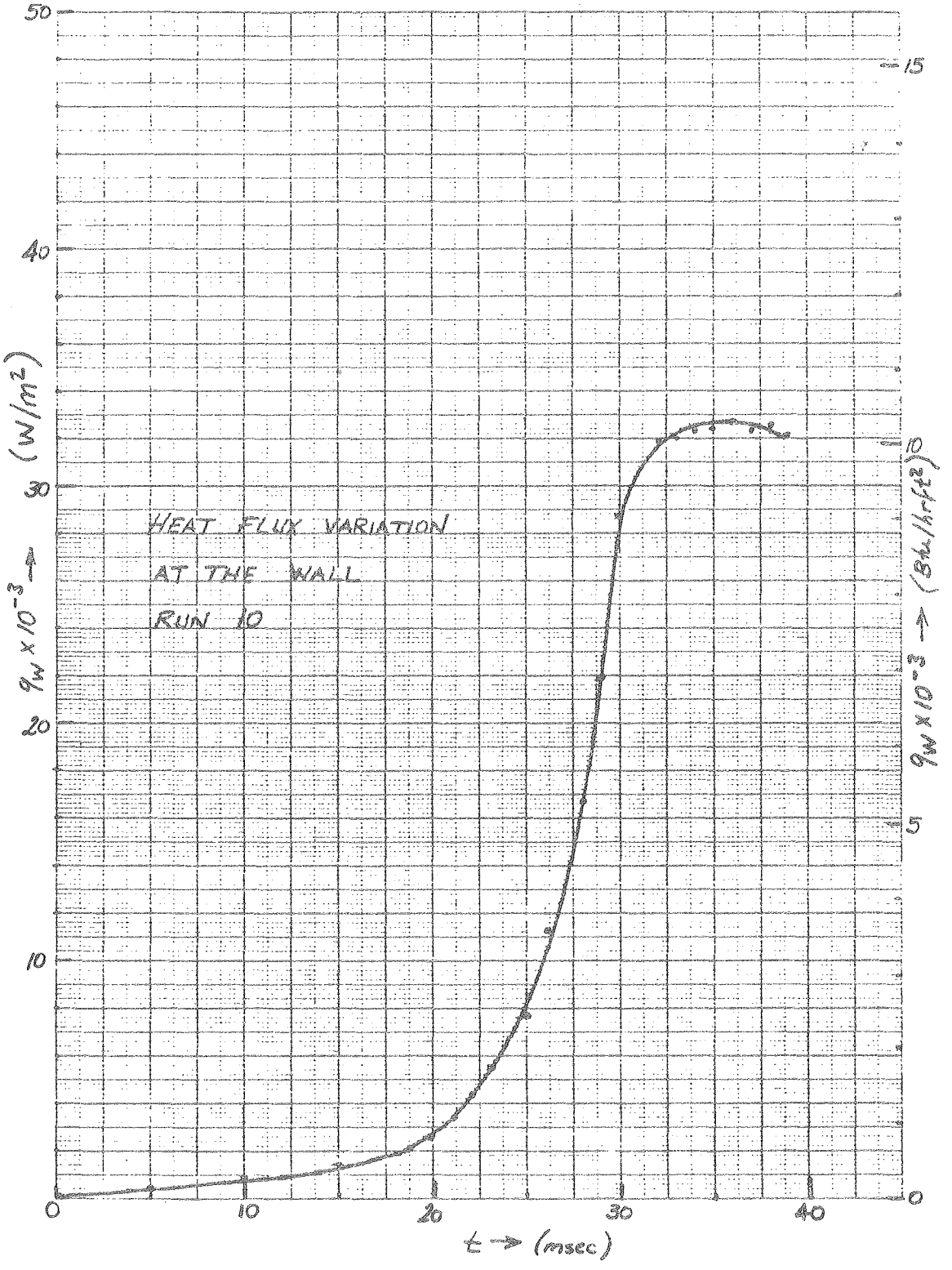

Figure 7.15. Wall heat flux.

APPENDIX A

NUMERICAL CALCULATION OF THE DUHAMEL INTEGRAL

In Chapter 3 the heat flux at the end wall, q_{ws}, was calculated based on an analysis in the solid. q_{ws} was given by:

$$q_{ws} = -\sqrt{\frac{k_s \rho_s c_s}{\pi}} \left[\frac{T_w(t) - T_{is}}{\sqrt{t}} + \frac{1}{2} \int_0^t \frac{T_w(t) - T_w(\xi)}{(t-\xi)^{3/2}} \, d\xi \right] \tag{A.1}$$

The numerical evaluation of the last integral shows some difficulty since at $\xi = t$ the integrand is undefined.

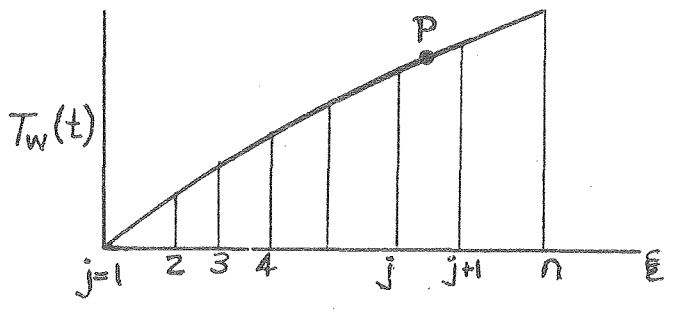

Let us assume that the temperature varies linearly between j and j + 1. Then the temperature at point P can be expressed as:

$$T_p(\xi) = A_{j,j+1} + B_{j,j+1}\,\xi \tag{A.2}$$

and from comparing the two slopes,

$$\frac{T_p - T(\xi = j)}{\xi - \xi(j)} = \frac{T(\xi = j+1) - T(\xi = j)}{\xi(j+1) - \xi(j)} \tag{A.3}$$

or

$$T_p(t) = T(\xi=j) - \xi(j)\left[\frac{T(\xi=j+1) - T(\xi=j)}{\xi(j+1) - \xi(j)}\right] + \left[\frac{T(\xi=j+1) - T(\xi=j)}{\xi(j+1) - \xi(j)}\right]\xi \quad \text{(A.4)}$$

The coefficients, $A_{j,j+1}$ and $B_{j,j+1}$ can be obtained by comparing Equations (A.2) and (A.4). The coefficients are given by:

$$A_{j,j+1} = T(\xi=j) - \xi(j)\left[\frac{T(\xi=j+1) - T(\xi=j)}{\xi(j+1) - \xi(j)}\right] \quad \text{(A.5)}$$

$$B_{j,j+1} = \frac{T(\xi=j+1) - T(\xi=j)}{\xi(j+1) - \xi(j)} \quad \text{(A.6)}$$

The first term in Equation (A.1) does not present any difficulty. The second term which is an integral can be expressed as a summation of integrals.

$$\int_0^t \frac{T(t) - T(\xi)}{(t-\xi)^{3/2}}\, d\xi = \int_{\xi=1}^{\xi=n} \frac{T(\xi=j) - T(\xi)}{(\xi(j) - \xi)^{3/2}}\, d\xi \quad \text{(A.7)}$$

or

$$\int_0^t \frac{T(t) - T(\xi)}{(t-\xi)^{3/2}}\, d\xi = \sum_{j=1}^{j=n} \int_{\xi=j}^{\xi=j+1} \frac{T(\xi=j) - T(\xi)}{(\xi(j) - \xi)^{3/2}}\, d\xi \quad \text{(A.8)}$$

All the terms in the summation in Equation (A.8) have the same form except the last term where the integrand is undefined. The common

terms can be evaluated as follows:

$$\int_{\xi=j}^{\xi=j+1} \frac{T(\xi=j)-T(\xi)}{(\xi(j)-\xi)^{3/2}}\, d\xi = \int_{\xi=j}^{\xi=j+1} \frac{T(\xi=j)-A_{j,j+1}-B_{j,j+1}\xi}{(\xi(j)-\xi)^{3/2}}\, d\xi \quad \text{(A.9)}$$

or

$$\int_{\xi=j}^{\xi=j+1} \frac{T(\xi=j)-T(\xi)}{(\xi(j)-\xi)^{3/2}}\, d\xi = (T(\xi=j)-A_{j,j+1}) \int_{\xi=j}^{\xi=j+1} \frac{d\xi}{(\xi(j)-\xi)^{3/2}} - B_{j,j+1} \int_{\xi=j}^{\xi=j+1} \frac{\xi\, d\xi}{(\xi(j)-\xi)^{3/2}} \quad \text{(A.10)}$$

The quantities $T(\xi = j)$, $A_{j,j+1}$, $B_{j,j+1}$ and $\xi(j)$ are known quantities. Therefore the integrals can easily be evaluated. To find the last integral we can express $T(\xi = j)$ and $T(\xi)$ in the form given in Equation (A.2). This yields:

$$\int_{\xi=n-1}^{\xi=n} \frac{T(\xi=n)-T(\xi)}{(\xi(n)-\xi)^{3/2}}\, d\xi = \int_{\xi=n-1}^{\xi=n} \frac{A_{n-1,n}+B_{n-1,n}\xi(n)-A_{n-1,n}-B_{n-1,n}\xi}{(\xi(n)-\xi)^{3/2}}\, d\xi$$

(A.11)

or

$$\int_{\xi=n-1}^{\xi=n} \frac{T(\xi=n)-T(\xi)}{(\xi(n)-\xi)^{3/2}}\, d\xi = \int_{\xi=n-1}^{\xi=n} \frac{B_{n-1,n}\left(\xi(n)-\xi\right)}{\left(\xi(n)-\xi\right)^{3/2}}\, d\xi$$

$$= B_{n-1,n} \int_{\xi=n-1}^{\xi=n} \frac{d\xi}{\left(\xi(n)-\xi\right)^{1/2}} \qquad \text{(A.12)}$$

The integral in Equation (A.12) can now be evaluated.

A computer code was used based on the above analysis to obtain the heat flux from the temporal wall temperature variation. The code was developed by M. Nikanjam [18]. A computer listing of this program is given at the end of this Appendix.

```
      PROGRAM ENGINE(INPUT,OUTPUT)
      DIMENSION T(99), V(99), U(99), B(99), Q(99), H(99), A(99), DV(99)
      REAL K
C     T=TIME
C     V=ACTUAL TEMPERATURE
C     U=TEMPERATURE - INITIAL TEMPERATURE
C     B=SLOPE OF THE TEMP. PROFILE AT THE BOUNDARY FOR A SMALL INCREMENT
C     Q= HEAT FLUX AT TIME T
C     K=THERMAL CONDUCTIVITY
C     RHO=DENSITY
C     CP= SPECIFIC HEAT OF MACOR
C     TTH=NUMBER OF TEETH
C     VOL=VOLUME AT TIME T
C     VIN= INITIAL VOLUME
      N=44
      TTH=70
      VIN=12.8059
      PI=4.0*ATAN(1.0)
      RHO=146.9
      CP=0.11
      K=0.00026897
      GAMA=1.4
      G1=GAMA-1.0
      CONST=SQRT(RHO*CP*K/PI)
      PRINT4
    4 FORMAT(5X,*TIME*,10X,*TW*,10X,*Q*,10X,*VDISP*,10X,*DISP*,10X,*VOL*
     1,10X,*TG*,10X,*H*,/)
      PRINT5
    5 FORMAT(5X,*SEC*,11X,*F*,5X,*BTU/(HR-FT2)*,5X,*VOLT*,11X,*INCH*,9X,
     1*INCH3*,9X,*F*,4X,*BTU/(HR-FT2-F)*,///)
      READ 1, (T(I), I=1,N)
    1 FORMAT(8F10.6)
      READ 2, (V(I), I=1,N)
    2 FORMAT (8F10.5)
      READ6, (DV(I), I=1,N)
    6 FORMAT(10F8.5)
      FR=TTH/DV(N)
      DO 10 I=1,N
   10 U(I)=V(I)-V(1)
      DO 20 I=2,N
      A(I)=U(I-1)-T(I-1)*(U(I)-U(I-1))/(T(I)-T(I-1))
   20 B(I)=(U(I)-U(I-1))/(T(I)-T(I-1))
      T(1)=0.
      Q(1)=0.
      DIN=0.
      VOL=VIN
      TG=V(1)
      HT=0.0
      PRINT 3, T(1), V(1), Q(1), DV(1), DIN, VOL, TG, HT
    3 FORMAT(1X,F10.6,4X,F9.4,3X,F12.4,3X,F10.4,5X,F10.5,6X,F10.5,2X,F9.
     13,3X,F10.4,/)
      Q(2)=CONST*(U(1)/SQRT(T(2))+B(2)*SQRT(T(2)-T(1)))
      Q(2)=3600.*Q(2)
      Q(2) = Q(2)*3.1546
      DIN=DV(2)*FR*.0645
      DELV=2.25*DIN
      VOL=VIN-DELV
      TG=(VIN/VOL)**G1*(V(1)+460.)-460.
      HT=Q(2)/(TG-V(2))
      PRINT3, T(2), V(2), Q(2), DV(2), DIN, VOL, TG, HT
      H(1)=0.0
```

```
      DC 40 I=3,N
      I1=I-1
      DC 30 J=2,I1
      DD=U(I)-A(J)-2.0*B(J)*T(I)
      AA=DD+B(J)*T(J)
      T1=1.0/SQRT(T(I)-T(J))
      BB=DD+B(J)*T(J-1)
      T2=1.0/SQRT(T(I)-T(J-1))
   30 H(J)=H(J-1)+AA*T1-BB*T2
      CC=B(I)*SQRT(T(I)-T(I-1))
      H(I)=H(I-1)+CC
      Q(I)=CONST*(U(I)/SQRT(T(I))+H(I))
      Q(I)=360C.*Q(I)
      Q(I) = Q(I)*3.1546
      DIN=DV(I)*FR*.0645
      DELV=2.25*DIN
      VOL=VIN-DELV
      TG=(VIN/VCL)**G1*(V(I)+460.)-460.
      HT=Q(I)/(TG-V(I))
      PRINT3, T(I), V(I), Q(I), DV(I), DIN, VOL, TG, HT
   40 CCNTINUE
      STCP
      END
```

APPENDIX B

SAMPLE CALCULATION FOR ARGON

In this Appendix the evaluation of the reference values for pressure and temperature is presented. The procedure is the same for the pre-ignition period and the argon run. To help understanding, the details for run 108 with argon is considered. In the pre-ignition period the property values for the mixture will be used instead of values for argon.

For this run the increase in the wall temperature was 4.1 °F or 2.28°C. The initial temperature of the gas was 536.8°R or 292.2°K, the initial pressure on the low pressure side, p_1, was 0.775 psia. The high pressure side was He, p_4, at 15 psia.

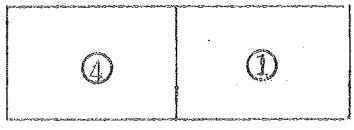

diaghragm

$$T_1 = 298.2°K$$

$$p_1 = 0.053 \text{ atm.}$$

$$p_4 = 1.020 \text{ atm.}$$

The speed of sound in the low pressure side which is filled with argon is [14]:

$$a_1 = \sqrt{\gamma R T_1} = 321.6 \text{ m/sec}$$

$\gamma = 5/3$ for argon which is an inert gas and R is the universal gas constant. The speed of the incident shock wave is calculated from the measured time between the two pressure transducers as explained in Chapter 2.

$$v_s = 710.5 \text{ m/sec.}$$

The mach number of the incident shock wave is [13. 14]:

$$M_s = \frac{v_s}{a_1} = 2.21.$$

Then from the shock wave equations [13, 14] the following can be calculated:

$$\frac{p_2}{p_1} = 5.88$$

$$\frac{p_5}{p_1} = 20.46$$

$$\frac{T_5}{T_1} = 4.13$$

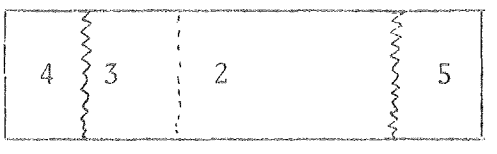

rarefaction wave reflected shock wave

Thus the pressure and temperature behind the reflected shock wave can be calculated.

$$p_5 = 1.079 \text{ atm}$$

$$T_5 = 1231.6°K$$

The thermal conductivity and specific heat at the wall temperature for argon is [15]:

$$k_w = 4.26 \times 10^{-3} \text{ cal/cm sec } ^\circ\text{K}$$

$$C_{pw} = 0.1242 \text{ cal/gm } ^\circ\text{K}$$

The density, ρ_w, can be found from the ideal gas law:

$$\rho_w = \frac{p_5}{RT_w} = 0.00175 \text{ gm/cm}^3$$

Using these values in Equation (4.1.21), the heat flux at the end wall can be calculated.

$$q_{wg} = -\sqrt{\frac{(k\rho c)_w}{2}}\; T_w \cdot \frac{d\theta}{d\eta}\bigg|_{\eta=0} \frac{1}{\sqrt{t}}$$

$$= -\frac{0.044}{\sqrt{t}}$$

In the above equation the heat flux is obtained in cal/cm^{2}sec if the time is used in seconds. The slope of the non-dimensional temperature at $\eta = 0$ is evaluated for $\theta_\infty = 4.1$ as [7]:

$$\frac{d\theta}{d\eta}\bigg|_{\eta=0} = 2.15 \; .$$

APPENDIX C

EVALUATION OF THE PROPERTY VALUES FOR THE MIXTURE

In calculating the reference pressure and temperature which are the pressure and temperature behind the reflected shock wave, property values for the mixture is needed. They are obtained by assuming that the mixture is an ideal gas mixture [16].

At T_{is} = 537.4 °R = 298.3 °K the specific heats for Ar, H_2, O_2 are [15]:

C_{pO_2} = 6.94 Btu/mole °R C_{vO_2} = 4.95 Btu/mole °R

C_{pH_2} = 6.93 Btu/mole °R C_{vH_2} = 4.95 Btu/mole °R

C_{pAr} = 4.97 Btu/mole °R C_{vAr} = 2.98 Btu/mole °R

The gas mixture is composed of 27 Ar + $2H_2$ + O_2, thus:

$$C_p = 6.93\left(\frac{2}{30}\right) + 6.94\left(\frac{1}{30}\right) + 4.97\left(\frac{27}{30}\right)$$

$$= 5.16 \text{ Btu/mole °R}$$

$$C_v = 4.95\left(\frac{2}{30}\right) + 4.95\left(\frac{1}{30}\right) + 2.98\left(\frac{27}{30}\right)$$

$$= 3.18 \text{ Btu/mole °R}$$

$$\gamma = \frac{C_p}{C_v} = 1.625$$

The molecular weight of the mixture is:

$$\left(MW\right)_{mix} = \left(MW\right)_{O_2}\left(\frac{1}{30}\right) + \left(MW\right)_{H_2}\left(\frac{2}{30}\right) + \left(MW_{Ar}\right)\left(\frac{27}{30}\right)$$

$$= 37.2 \text{ lb/lb}_{mole}$$

At $T_\delta = 2407\ ^\circ R = 1337\ ^\circ K$ the specific heats for the components of the mixture are [15]:

$$C_{pO_2} = 8.64 \text{ Btu/mole } ^\circ R$$

$$C_{pH_2} = 7.55 \text{ Btu/mole } ^\circ R$$

$$C_{pAr} = 4.97 \text{ Btu/mole } ^\circ R$$

Thus the specific heat of the mixture is:

$$C_p = 8.64\left(\frac{1}{30}\right) + 7.55\left(\frac{2}{30}\right) + 4.97\left(\frac{27}{30}\right)$$

$$C_p = 0.141 \text{ Btu/lb}_m\ ^\circ R$$

$$C_p = 0.141 \text{ cal/gm } ^\circ C$$

$$C_p = 0.59 \text{ joules/gm}^\circ K$$

The thermal conductivities of H_2, O_2 and Argon at the wall temperature are [15]:

$$k_{Ar} = 3.95 \times 10^{-5} \text{ cal/cm sec } ^\circ K$$

$$k_{H_2} = 42.29 \times 10^{-5} \text{ cal/cm sec } ^\circ K$$

$$k_{O_2} = 6.35 \times 10^{-5} \text{ cal/cm sec } ^\circ K$$

The same values at $T = T_5 = T_{ig}$ are [15]:

$$k_{Ar} = 12.07 \times 10^{-5} \text{ cal/cm sec °K}$$
$$k_{H_2} = 128.33 \times 10^{-5} \text{ cal/cm sec °K}$$
$$k_{O_2} = 21.14 \times 10^{-5} \text{ cal/cm sec °K}$$

Thus the thermal conductivity of the mixture at the wall temperature is:

$$k = 6.35 \times 10^{-5}\left(\frac{1}{30}\right) + 42.29 \times 10^{-5}\left(\frac{2}{30}\right) + 3.95 \times 10^{-5}\left(\frac{27}{30}\right)$$

$$k = 6.58 \times 10^{-5} \text{ cal/cm sec °K}$$

$$k = 2.75 \times 10^{-5} \text{ w/m °K}$$

and at T_{ig} it is:

$$k = 21.14 \times 10^{-5}\left(\frac{1}{30}\right) + 128.33 \times 10^{-5}\left(\frac{2}{30}\right) + 12.07 \times 10^{-5}\left(\frac{27}{30}\right)$$

$$k = 20.12 \times 10^{-5} \text{ cal/cm sec °K}$$

$$k = 8.42 \times 10^{-2} \text{ w/m °K.}$$

APPENDIX D

EVALUATION OF THE PRESSURE AND TEMPERATURE OUTSIDE THE GAS LAYER

The temperature and pressure outside the gas layer was calculated from a computer program BLSTW developed by Cohen [4, 12, 17, 19, 20, 21]. A listing of the program is given at the end of this Appendix.

The input to this program consists of the coefficients of the chemical rate equations, chemical and thermodynamical properties of the components of the mixture, the initial pressure and temperature of the mixture, the Mach numbers of the incident and reflected shock waves.

From the program the pressure and density distributions as functions of time are obtained. For every time step the pressure and density variations with respect to distance are plotted. By extrapolation the values of pressure and density at the edge of the gas layer which is being studied are obtained. Then using the ideal gas law the associated temperatures at the same location were calculated.

```
      PROGRAM BLSTWAV(INPUT,OUTPUT,PUNCH)
      COMMON/ARRAYS/R(2,1001),U(2,1001),P(2,1001),V(2,1001),Q(2,1001),E(
     .2,1001),X(1001),PSII(1001),PSIEX(1001),PV(1001),TAU(1001),DQ(1001)
     .,A(1001),C(1001),AA(1001),BB(1001),CC(1001)
      COMMON/TIME/TERMIN,T,DT,DTL
      COMMON/PARAM/NSTEPS,N,J,G,CL,CO,BTA
 1000 FORMAT(3I5)
 2001 FORMAT(1H0,*COMPUTER TIME IS APPROACHING DESIGNATED MAXIMUM*)
 2002 FORMAT(1H0,*DIMENSION-LIMIT STOP*)
 2003 FORMAT(1H0,*TIME STEPS EQUAL DESIGNATED MAXIMUM*)
 2004 FORMAT(1H0,*NON-POSITIVE TIME STEP*)
C-----DETERMINE INITIAL OR RESTART CONDITIONS
      CALL SECOND(TA)
      INDEX = 0
      READ 1000,LSTART,NCYCLE,NPUNCH
      IF(LSTART.NE.0) GO TO 1
      CALL INITIAL(INDEX,NCYCLE,NFINAL,LSTART,NN)
      GO TO 6
    1 CALL RESTART(INDEX,LSTART,NCYCLE,NFINAL,NN)
    6 LSTART = LSTART + 1
C-----SET INDEX NUMBER
    2 INDEX = INDEX + 1
      NCYCLE = NCYCLE+1
C-----CHECK CENTRAL PROCESSOR ELAPSED TIME
      CALL SECOND(TB)
      TC = 1.2*(TB-TA)
      TD = TERMIN-TB
      TA = TB
      IF(TC.GE.TD) PRINT 2001
C-----CHECK NUMBER OF TIME STEPS
      IF(INDEX.GT.NSTEPS) PRINT 2003
      IF(TC.GE.TD.OR.INDEX.GT.NSTEPS) GO TO 3
C-----CHECK FOR DIMENSION-LIMIT STOP OR MESH EXPENSION
      DVABS = ABS(V(1,N-1)-1.)
      IF (DVABS.GT.0.001) GO TO 3
      IF(N.GT.NFINAL) PRINT 2002
      IF(N.GT.NFINAL) GO TO 3
C-----DETERMINE PROPERTIES AT NEW TIME
      CALL FIDIF(INDEX,NCYCLE,NN)
      IF(DT.GT.0.) GO TO 4
      PRINT 2004
      GO TO 5
C-----DETERMINE NEXT TSTEP,TIME,AND REINITIAL PROPERTIES
    4 CALL TSTEP
C-----RECYCLE
      GO TO 2
C-----PUNCH RESTART AND TERMINATE
    3 IF(N.GT.1001) N = 1001
      IF(NPUNCH.LE.0) GO TO 5
      CALL RESTART(INDEX,LSTART,NCYCLE,NFINAL,NN)
    5 CALL EXIT
      END
```

```
      SUBROUTINE INITIAL(INDEX,NCYCLE,NFINAL,LSTART,NN)
      COMMON/ARRAYS/R(2,1001),U(2,1001),P(2,1001),V(2,1001),Q(2,1001),E(
     .2,1001),X(1001),PSII(1001),PSIEX(1001),PV(1001),TAU(1001),DQ(1001)
     .,A(1001),C(1001),AA(1001),BB(1001),CC(1001)
      COMMON/MIDVALU/D(1000),S(1000)
      COMMON/TIME/TERMIN,T,DT,DTL
      COMMON/PARAM/NSTEPS,N,J,G,CL,CO,BTA
      COMMON/EXC/C1,P1,E1,C2,P2,E2,C3,P3,E3,C4,P4,E4,CHI,PSIF,EXITMNO
 1000 FORMAT(3I5,E10.4)
 1001 FORMAT(2I5,4E10.4)
 1002 FORMAT(I5,5E15.9)
 1003 FORMAT(8E10.4)
 2000 FORMAT (1H ,*GEOMETRY *,I3/* 1ST TIME STEP =*,E12.6/* GAMMA  = *,E
     .12.6//)
 2001 FORMAT(1H1,*TIME =*,E12.6,3X,*DT =*,E12.6,5X,*INDEX =*,I5,8X,*VTIM
     .E =*,E12.6,7X,*CYCLE =*,I5/)
 2002 FORMAT(1H ,X,*NNN*,X,*CENTER DIST*,2X,*CENTER VEL*,3X,*CENTER PRES
     .S*,3X,*CELL SP VOL*,2X,*CELL VISC*,4X,*CELL ENERGY*,2X,*CM*)
 2003 FORMAT(1H ,I4,9(2X,E11.5))
 2004 FORMAT(1H ,*RESTART NUMBER *,I2)
 2005 FORMAT(1H ,*DESIGNATED MAX CPTIME =*,E10.4,* SECONDS*/* NUMBER OF
     .TIME STEPS =*,I5/)
 2006 FORMAT(1H ,*LINEAR ARTIFICIAL VISCOSITY COEFFICIENT =*,E12.6/* QUA
     .DRATIC ARTIFICIAL VISCOSITY COEFFICIENT =*,E12.6//)
 2007 FORMAT(1H ,6(E12.6,2X))
      IF(LSTART.NE.0) GO TO 4
      T = 0.
      DTL = 0.
C-----READ INPUT
      READ 1000,NSTEPS,NFINAL,NN,TERMIN
      IF(NN.LE.0) NN = 1
      READ 1001,N,J,CL,CO,G,EXITMNO
      READ 1003,CHI,V2F,C1,P1,E1,C2,P2,E2
      READ 1003,C3,P3,E3,C4,P4,E4
C-----CALCULATE PROGRAM CONSTANTS
      BTA = (G-1.)/(G+1.)
      PSIF = (1.+BTA)*(V2F-BTA)
    4 VTIME = T-.5*DTL
      NL = N-1
      IF(LSTART.NE.0) GO TO 6
C-----DEFINE INITIAL MESH POINTS AND CELL PARAMETERS
      DO 1 M = 1,1001
      DO 3 I = 1,2
      R(I,M) = (M-1)/60.0
      U(I,M) = 0.0
      P(I,M) = 1.0
      V(I,M) = 1.0
      Q(I,M) = 0.0
    3 E(I,M) = P(I,M)*V(I,M)/(G-1.)
      A(M) = 0.0
      C(M) = 0.0
      AA(M) = 0.0
      BB(M) = 0.0
      CC(M) = 0.0
      PSII(M) = 0.0
```

```
      PSIEX(M) = 0.0
      PV(M) = 0.0
      TAU(M) = 0.0
      DQ(M) = 0.0
      IF(M.EQ.1) GO TO 1
      X(M-1) = (R(1,M)**(J+1)-R(1,M-1)**(J+1))/V(1,M-1)/(J+1)
    1 CONTINUE
      X(M) = 0.
C-----DETERMINE INITIAL TIME STEP
      DT = 1.0
      TAU(1) = DT/C1/EXP(E1)
    6 IF(LSTART.EQ.0) GO TO 7
C-----PRINTING INSTRUCTIONS
      PRINT 2004,LSTART
    7 PRINT 2005,TERMIN,NSTEPS
      PRINT 2000,J,DT,G
      PRINT 2006,CL,CO
      PRINT 2007,EXITMNO,CHI,V2F
      PRINT 2007,C1,P1,E1,C2,P2,E2
      PRINT 2007,C3,P3,E3,C4,P4,E4
   11 PRINT 2001,T,DTL,INDEX,VTIME,NCYCLE
      PRINT 2002
      DO 5 M = 1,NL
      D(M) = (R(1,M)+R(1,M+1))/2.
      S(M) = (U(1,M)+U(1,M+1))/2.
      CM = (R(1,M+1)**(J+1)-R(1,M)**(J+1))/V(1,M)/(J+1)/X(M)
      PRINT 2003,M,D(M),S(M),P(1,M),V(1,M),Q(1,M),E(1,M),CM
    5 CONTINUE
      T = T+DT
      RETURN
      END
```

```
      SUBROUTINE RESTART(INDEX,LSTART,NCYCLE,NFINAL,NN)
      COMMON/ARRAYS/R(2,1001),U(2,1001),P(2,1001),V(2,1001),Q(2,1001),E(
     .2,1001),X(1001),PSII(1001),PSIEX(1001),PV(1001),TAU(1001),DQ(1001)
     .,A(1001),C(1001),AA(1001),BB(1001),CC(1001)
      COMMON/TIME/TERMIN,T,DT,DTL
      COMMON/PARAM/NSTEPS,N,J,G,CL,CD,BTA
      COMMON/EXO/C1,P1,E1,C2,P2,E2,C3,P3,E3,C4,P4,E4,CHI,PSIF,EXITMND
 1000 FORMAT(3I5,E10.4)
 1001 FORMAT(3I5)
 1002 FORMAT(2I5,3E12.6)
 1003 FORMAT(I3,7E11.5)
 1004 FORMAT(8E10.4)
 1005 FORMAT(4E12.6)
      IF(INDEX.EQ.0) GO TO 1
C-----PUNCH RESTART CARDS
      NPUNCH = 1
      NCYCLE = NCYCLE-1
      PUNCH 1001,LSTART,NCYCLE,NPUNCH
      T = T-DT
      PUNCH 1002,N,J,T,DT,DTL
      PUNCH 1005,CL,CD,G,EXITMND
      PUNCH 1004,CHI,PSIF,C1,P1,E1,C2,P2,E2
      PUNCH 1004,C3,P3,E3,C4,P4,E4,BTA
      DO 2 M = 1,N
      PUNCH 1004,A(M),C(M),AA(M),BB(M),CC(M),PV(M),PSII(M),PSIEX(M)
    2 PUNCH 1003,M,R(1,M),P(1,M),V(1,M),U(1,M),Q(1,M),X(M),TAU(M)
      GO TO 4
C-----READ RESTART CARDS
    1 READ 1000,NSTEPS,NFINAL,NN,TERMIN
      READ 1002,N,J,T,DT,DTL
      READ 1005,CL,CD,G,EXITMND
      READ 1004,CHI,PSIF,C1,P1,E1,C2,P2,E2
      READ 1004,C3,P3,E3,C4,P4,E4,BTA
      DO 3 M = 1,1001
      DQ(M) = 0.0
      IF(M.GT.N) GO TO 5
      READ 1004,A(M),C(M),AA(M),BB(M),CC(M),PV(M),PSII(M),PSIEX(M)
      READ 1003,K,R(1,M),P(1,M),V(1,M),U(1,M),Q(1,M),X(M),TAU(M)
      GO TO 6
    5 R(1,M) = R(1,N)+(M-N)*(R(1,N)-R(1,N-1))
      P(1,M) = 1.
      V(1,M) = 1.
      U(1,M) = 0.
      Q(1,M) = 0.
      A(M) = 0.0
      C(M) = 0.0
      AA(M) = 0.0
      BB(M) = 0.0
      CC(M) = 0.0
      PSII(M) = 0.0
      PSIEX(M) = 0.0
      TAU(M) = 0.0
      PV(M) = 0.0
      X(M-1) = (R(1,M)**(J+1)-R(1,M-1)**(J+1))/V(1,M-1)/(J+1)
    6 E(1,M) = P(1,M)*V(1,M)/(G-1.)
```

```
      R(2,M) = R(1,M)
      U(2,M) = U(1,M)
      P(2,M) = P(1,M)
      V(2,M) = V(1,M)
      Q(2,M) = Q(1,M)
      E(2,M) = E(1,M)
    3 CONTINUE
      X(M) = 0.
      IF(INDEX.EQ.0) CALL INITIAL(INDEX,NCYCLE,NFINAL,LSTART,NN)
      RETURN
      END
```

```
      SUBROUTINE FIDIF(INDEX,NCYCLE,NN)
      COMMON/ARRAYS/R(2,1001),U(2,1001),P(2,1001),V(2,1001),Q(2,1001),E(
     .2,1001),X(1001),PSII(1001),PSIEX(1001),PV(1001),TAU(1001),DQ(1001)
     .,A(1001),C(1001),AA(1001),BB(1001),CC(1001)
      COMMON/MIDVALU/D(1000),S(1000)
      COMMON/TIME/TERMIN,T,DT,DTL
      COMMON/PARAM/NSTEPS,N,J,G,CL,CD,BTA
      COMMON/EXG/C1,P1,E1,C2,P2,E2,C3,P3,E3,C4,P4,E4,CHI,PSIF,EXITMNO
 2001 FORMAT(1H ,*TIME =*,E12.6,3X,*DT =*,E12.6,5X,*INDEX =*,I5,3X,*VTIM
     .E =*,E12.6,7X,*CYCLE =*,I5,5X,*RSHOCK = *,E12.6/)
 2002 FORMAT(1H ,X,*NNN*,X,*CENTER DIST*,2X,*CENTER VEL*,3X,*CENTER PRES
     .S*,3X,*CELL SP VOL*,2X,*CELL VISC*,4X,*CELL ENERGY*,2X,*CM*,11X,*T
     .AUF*,9X,*PSI*)
 2003 FORMAT(1H ,I4,9(2X,E11.5))
 2004 FORMAT(1H0,*R1*,12X,*R2*,12X,*DVDR1*,9X,*DVDR2*/X,4(E12.6,2X))
 3000 FORMAT(1H1)
      VTIME = T-.5*DT
C-----MOMENTUM CONSERVATION
      CALL MOMENTA
C-----CONTINUITY CONSERVATION
      CALL CONTINU
C-----ARTIFICIAL VISCOSITY
      CALL ARTVISC
C-----ENERGY CONSERVATION
      CALL ENERGY
C-----MAXIMUM DENSITY GRADIENTS
      CALL DVDR(R1,R2,DVDR1,DVDR2)
C-----FIELD EXTENSION CRITERION
      NOLD = N
      CALL SHOCK(SSTA)
      NX = (NCYCLE/NN)*NN
      IF(NX.NE.NCYCLE) RETURN
C-----PRINT HEADERS
      PRINT 3000
      PRINT 2001,T,DT,INDEX,VTIME,NCYCLE,SSTA
      PRINT 2002
C-----CALCULATE CURRENT PROPERTIES
      NL = N-1
      DO 4 M = 1,NL
      D(M) = (R(2,M)+R(2,M+1))/2.
      S(M) = (U(2,M)+U(2,M+1))/2.
      CM = (R(2,M+1)**(J+1)-R(2,M)**(J+1))/V(2,M)/(J+1)/X(M)
      PSI = 0.0
      IF(TAU(M).LE.1.0) GO TO 1
      PSIC = (P(1,M)+BTA)*(V(1,M)-BTA)
      PSI = (PSIC-PSII(M))/(PSIF-PSII(M))
    1 CONTINUE
C-----PRINT CURRENT PROPERTIES
      PRINT 2003,M,D(M),S(M),P(2,M),V(2,M),Q(2,M),E(2,M),CM,TAU(M),PSI
    4 CONTINUE
      IF(NOLD.LE.2) RETURN
      PRINT 2004,R1,R2,DVDR1,DVDR2
      RETURN
      END
```

```
      SUBROUTINE MOMENTA
      COMMON/ARRAYS/R(2,1001),U(2,1001),P(2,1001),V(2,1001),Q(2,1001),E(
     .2,1001),X(1001),PSII(1001),PSIEX(1001),PV(1001),TAU(1001),DQ(1001)
     .,A(1001),C(1001),AA(1001),BB(1001),CC(1001)
      COMMON/TIME/TERMIN,T,DT,DTL
      COMMON/PARAM/NSTEPS,N,J,G,CL,CC,BTA
      DTN = .5*(DT+DTL)
      DO 1 M = 1,N
      IF(M.NE.1) GO TO 2
C-----LEFT BOUNDARY CONDITION
      U(2,1) = 0.0
C-----1ST SIGMA FORWARD
      SIGMAF = -P(1,1)-Q(1,1)
C-----1ST F1
      F1 = (R(1,2)-R(1,1))/V(1,1)
      GO TO 4
    2 IF(M.NE.N) GO TO 3
C-----RIGHT BOUNDARY CONDITION
      U(2,N) = 0.0
      GO TO 4
C-----VELOCITY AT GENERAL POINT
C-----INTERMEDIATE SIGMA VALUES
    3 SIGMAB = SIGMAF
      SIGMAF = -P(1,M)-Q(1,M)
C-----PHI PARAMETER
      F0 = F1
      F1 = (R(1,M+1)-R(1,M))/V(1,M)
      PHI = .5*(F1+F0)
C-----VELOCITY
      U(2,M) = U(1,M)+(DTN/PHI)*(SIGMAF-SIGMAB)
    4 CONTINUE
C-----TRAJECTORY
      R(2,M) = R(1,M)+U(2,M)*DT
    1 CONTINUE
      RETURN
      END
```

```
      SUBROUTINE CONTINU
      COMMON/ARRAYS/R(2,1001),U(2,1001),P(2,1001),V(2,1001),Q(2,1001),E(
     .2,1001),X(1001),PSII(1001),PSIEX(1001),PV(1001),TAU(1001),DQ(1001)
     .,A(1001),C(1001),AA(1001),BB(1001),CC(1001)
      COMMON/TIME/TERMIN,T,DT,DTL
      COMMON/PARAM/NSTEPS,N,J,G,CL,CO,BTA
      NL = N-1
      DO 1 M = 1,NL
C------CHI PARAMETER
      IF(J.NE.2) GO TO 3
      IF(M.NE.1) GO TO 8
      U13 = U(2,1)*U(2,1)*U(2,1)
    8 U03 = U13
      U13 = U(2,M+1)*U(2,M+1)*U(2,M+1)
      CHI = DT*DT*(U13-U03)/12.
      GO TO 4
    3 CHI = 0.
    4 IF(J.EQ.0) GO TO 6
      IF(M.NE.1) GO TO 9
      F1 = U(2,1)*((.5*(R(2,1)+R(1,1)))**J)
    9 F0 = F1
      F1 = U(2,M+1)*((.5*(R(2,M+1)+R(1,M+1)))**J)
      GO TO 7
    6 F1 = U(2,M+1)
      F0 = U(2,M)
    7 V(2,M) = V(1,M)+DT*(F1-F0+CHI)/X(M)
    1 CONTINUE
      RETURN
      END
```

```
      SUBROUTINE ARTVISC
      COMMON/ARRAYS/R(2,1001),U(2,1001),P(2,1001),V(2,1001),Q(2,1001),E(
     .2,1001),X(1001),PSII(1001),PSIEX(1001),PV(1001),TAU(1001),DQ(1001)
     .,A(1001),C(1001),AA(1001),BB(1001),CC(1001)
      COMMON/TIME/TERMIN,T,DT,DTL
      COMMON/PARAM/NSTEPS,N,J,G,CL,CO,BTA
      NL = N-1
      DO 1 M = 1,NL
C-----EXISTENCE CRITERIA
      IF(CL.LE.0..AND.CO.LE.0.) GO TO 2
      IF(U(2,M+1).GE.U(2,M)) GO TO 2
      IF(V(2,M).GE.V(1,M)) GO TO 2
C-----COMPLETELY CENTERED PARAMETERS
      AC = SQRT(.5*P(1,M)*(V(2,M)+V(1,M)))
      HETAC = .5*((1./V(2,M))+(1./V(1,M)))
C-----LINEAR TERM
      QL = CL*AC*HETAC*ABS(U(2,M+1)-U(2,M))
C-----QUADRATIC TERM
      QQ = CO*CO*HETAC*(U(2,M+1)-U(2,M))*(U(2,M+1)-U(2,M))
C-----TOTAL ARTIFICIAL VISCOSITY FOR 1/2 POSITION FORWARD
      Q(2,M) = QL+QQ
      GO TO 1
    2 Q(2,M) = 0.
    1 CONTINUE
      RETURN
      END
```

```
      SUBROUTINE ENERGY
      COMMON/ARRAYS/R(2,1001),U(2,1001),P(2,1001),V(2,1001),Q(2,1001),E(
     .2,1001),X(1001),PSII(1001),PSIEX(1001),PV(1001),TAU(1001),DQ(1001)
     .,A(1001),C(1001),AA(1001),BB(1001),CC(1001)
      COMMON/PARAM/NSTEPS,N,J,G,CL,CD,BTA
      NL = N-1
      DO 1 M = 1,NL
      QBAR = .5*(Q(2,M)+Q(1,M))
      ENUM = E(1,M)-(.5*P(1,M)+QBAR)*(V(2,M)-V(1,M))+DQ(M)
      EDEM = 1.+.5*(G-1.)*(1.-V(1,M)/V(2,M))
      E(2,M) = ENUM/EDEM
      P(2,M) = (G-1.)*E(2,M)/V(2,M)
    1 CONTINUE
      RETURN
      END
```

```
      SUBROUTINE TSTEP
      COMMON/ARRAYS/R(2,1001),U(2,1001),P(2,1001),V(2,1001),Q(2,1001),E(
     .2,1001),X(1001),PSII(1001),PSIEX(1001),PV(1001),T4U(1001),DQ(1001)
     .,A(1001),C(1001),AA(1001),BB(1001),CC(1001)
      COMMON/TIME/TERMIN,T,DT,DTL
      COMMON/PARAM/NSTEPS,N,J,G,CL,CO,BTA
      DTL = DT
      NL = N-1
C-----STABILITY CRITERIA
      DO 1 M = 1,NL
      AS2 = P(2,M)*V(2,M)*G
      VDOTN = 2.*(V(2,M)-V(1,M))/(V(2,M)+V(1,M))/DTL
      IF(VDOTN.GE.0.) GO TO 3
      BS2 = 64.*CO*CO*(R(2,M+1)-R(2,M))*(R(2,M+1)-R(2,M))*VDOTN*VDOTN
      GO TO 4
    3 BS2 = 0.
    4 DEM = 3.*SQRT(AS2+BS2)
      DT = 2.*(R(2,M+1)-R(2,M))/DEM
      IF(M.EQ.1) DTMIN = DT
      IF(DT.LT.DTMIN) DTMIN = DT
    1 CONTINUE
      DT = DTMIN
C-----LIMITING CONSTRAINT
      IF(DTL.GT.0..AND.DT.GT.1.4*DTL) DT = 1.4*DTL
      CALL EXCHEAT
      T = T+DT
C-----REINITIAL PROPERTIES
      DO 5 M = 1,N
      U(1,M) = U(2,M)
      R(1,M) = R(2,M)
      IF(M.EQ.N) GO TO 5
      V(1,M) = V(2,M)
      Q(1,M) = Q(2,M)
      P(1,M) = P(2,M)
      E(1,M) = E(2,M)
    5 CONTINUE
      RETURN
      END
```

```
      SUBROUTINE EXCHEAT
      COMMON/ARRAYS/R(2,1001),U(2,1001),P(2,1001),V(2,1001),Q(2,1001),E(
     .2,1001),X(1001),PSII(1001),PSIEX(1001),PV(1001),TAU(1001),DQ(1001)
     .,A(1001),C(1001),AA(1001),BB(1001),CC(1001)
      COMMON/TIME/TERMIN,T,DT,DTL
      COMMON/PARAM/NSTEPS,N,J,G,CL,CD,BTA
      COMMON/EXO/C1,P1,E1,C2,P2,E2,C3,P3,E3,C4,P4,E4,CHI,PSIF,EXITMNO
      NL = N-1
    1 I = 0
      DO 2 M = 1,NL
      IF(TAU(M).GT.1.0) GO TO 3
      PV(M) = P(2,M)*V(2,M)
      TIND = V(2,M)*C1*(PV(M)**P1)*EXP(E1/PV(M))
      TAU(M) = TAU(M)+DT/TIND
      IF(TAU(M).LE.1.0) GO TO 2
      QDOTMAX = C2*(PV(M)**P2)*EXP(E2/PV(M))
      PSIEX(M) = C3*(PV(M)**P3)*EXP(E3/PV(M))
      PSIHW = C4*(PV(M)**P4)*EXP(E4/PV(M))
      PSI1 = PSIEX(M)*(1.-SQRT(1./2./(1.-CHI)))
      PSI2 = PSI1+PSIHW
      XA = PSI2-PSIEX(M)
      XB = 1.-PSIEX(M)
      A(M) = (CHI-1.)*QDOTMAX/PSIEX(M)/PSIEX(M)
      C(M) = QDOTMAX
      BB(M) = (XB*XB-2.*XA*XA)/XA/XA/XB/XB
      AA(M) = QDOTMAX/(1.-1./(1.+BB(M)*XB*XB))
      CC(M) = QDOTMAX-AA(M)
      PSII(M) = (P(2,M)+BTA)*(V(2,M)-BTA)
    3 PSIC = (P(2,M)+BTA)*(V(2,M)-BTA)
      PSI = (PSIC-PSII(M))/(PSIF-PSII(M))
      IF(PSI.GE.1.0) GO TO 4
      Z = PSI-PSIEX(M)
      IF(Z.GE.0.0) GO TO 5
      QDOT = A(M)*Z*Z+C(M)
      DPSI = QDOT*PV(M)*2.*BTA
      DTHT = 0.2*PSIEX(M)*(PSIF-PSII(M))/DPSI
      GO TO 6
    5 QDOT = AA(M)/(1.+BB(M)*Z*Z)+CC(M)
      DPSI = QDOT*PV(M)*2.*BTA
      DTHT = 0.2*(1.-PSIEX(M))*(PSIF-PSII(M))/DPSI
      GO TO 6
    4 QDOT = 0.0
    6 DQ1 = (PSIF-PSIC)/2./BTA
      DQ2 = QDOT*DT*PV(M)
      DQ(M) = AMIN1(DQ1,DQ2)
      IF(DQ(M).LE.0.0) DQ(M) = 0.0
      IF(DQ(M).LE.0.0) GO TO 2
      I = I+1
      DTMI = AMIN1(DT,DTHT)
      IF(I.EQ.1) DTMIN = DTMI
      DTMIN = AMIN1(DTMI,DTMIN)
    2 CONTINUE
      IF(I.EQ.0) RETURN
      IF(DT.LE.DTMIN) RETURN
      DO 8 M = 1,NL
```

```
      PSIC = (P(2,M)+BTA)*(V(2,M)-BTA)
      IF(ABS(PSIC-PSII(M)).GT.0.0) GO TO 8
      TIND = V(1,M)*C1*(PV(M)**P1)*EXP(E1/PV(M))
      TAU(M) = TAU(M)-DT/TIND
    8 CONTINUE
      DT = DTMIN
      GO TO 1
      END
```

```
      SUBROUTINE SHOCK(SSTA)
      COMMON/ARRAYS/R(2,1001),U(2,1001),P(2,1001),V(2,1001),Q(2,1001),T(
     .2,1001),X(1001),PSII(1001),PSIEX(1001),PV(1001),TAU(1001),DQ(1001)
     .,A(1001),C(1001),AA(1001),BB(1001),CC(1001)
      COMMON/TIME/TERMIN,T,DT,DTL
      COMMON/PARAM/NSTEPS,N,J,G,CL,CO,BTA
      COMMON/EXO/C1,P1,E1,C2,P2,E2,C3,P3,E3,C4,P4,E4,CHI,PSIF,EXITMNO
      NOLD = N
      XNOLD = NOLD
      SSTA = T*SQRT(G)*EXITMNO
    1 FSTA = 1.5*R(2,N)-0.5*R(2,N-1)
      IF(SSTA.LT.FSTA) GO TO 2
      N = N+1
      IF(N.GT.1001) CALL EXIT
      GO TO 1
    2 IF(N.EQ.NOLD) RETURN
      TIND = C1*EXP(E1)
      NL = N-1
      XNL = NL
      DO 3 M = NOLD,NL
      XM = M
    3 TAU(M) = ((XNL-XM)/(XNL-XNOLD+1.))*DT/TIND
      RETURN
      END
```

```
      SUBROUTINE DVDR(R1,R2,DVDR1,DVDR2)
      COMMON/ARRAYS/R(2,1001),U(2,1001),P(2,1001),V(2,1001),Q(2,1001),E(
     .2,1001),X(1001),PSII(1001),PSIEX(1001),PV(1001),TAU(1001),DQ(1001)
     .,A(1001),C(1001),AA(1001),BB(1001),CC(1001)
      COMMON/PARAM/NSTEPS,N,J,G,CL,CG,BTA
      IF(N.LE.2) RETURN
      NL = N-1
      IPOS = 0
      INEG = 0
      DO 1 M = 2,NL
      XL = (R(2,M)+R(2,M-1))/2.
      XR = (R(2,M)+R(2,M+1))/2.
      Z = (V(2,M)-V(2,M-1))/(XR-XL)
      IF(Z.LT.0.0) GO TO 2
      IPOS = IPOS+1
      IF(IPOS.EQ.1) DVDR1 = Z
      IF(IPOS.EQ.1) R1 = R(2,M)
      IF(DVDR1.LT.Z) R1 = R(2,M)
      IF(DVDR1.LT.Z) DVDR1 = Z
      GO TO 1
    2 INEG = INEG+1
      IF(INEG.EQ.1) DVDR2 = Z
      IF(INEG.EQ.1) R2 = R(2,M)
      IF(DVDR2.GT.Z) R2 = R(2,M)
      IF(DVDR2.GT.Z) DVDR2 = Z
    1 CONTINUE
      IF(IPOS.EQ.0) R1 = 0.0
      IF(IPOS.EQ.0) DVDR1 = 0.0
      IF(INEG.EQ.0) R2 = 0.0
      IF(INEG.EQ.0) DVDR2 = 0.0
      RETURN
      END
```

APPENDIX E

APPROXIMATE SOLUTIONS

E.1. Pre-Ignition Period

When the thermal conductivity of the gas varies linearly with temperature, a = 1.0, the transformed energy Equation (5.1.13) becomes:

$$\frac{\partial U}{\partial t} = \alpha_{ig} \frac{\partial^2 U}{\partial \psi^2} \tag{E.1.1}$$

The boundary and initial conditions are given by:

$$U(0,t) = \frac{T_w}{T_{ig}} = \text{constant.} \tag{E.1.1.a}$$

$$U(\infty,t) = 1 \tag{E.1.1.b}$$

$$U(\psi,0) = 1 \tag{E.1.1.c}$$

The above equation, which is now linear, with the boundary and initial conditions is identical to a heat diffusion problem in a semi-infinite medium. The medium temperature is 1 initially and the wall temperature is changed to T_w/T_{ig}, [5]. The solution to this problem is:

$$\frac{U - T_w/T_{ig}}{1 - T_w/T_{ig}} = \text{erf}\left[\frac{\psi}{2\sqrt{\alpha_{ig} t}}\right] \tag{E.1.2}$$

or using the definition of U, Equation (5.1.12):

$$\frac{T - T_w}{T_{ig} - T_w} = \mathrm{erf}\left[\frac{\psi}{2\sqrt{\alpha_{ig}\, t}}\right] \tag{E.1.3}$$

The heat flux at the end wall can be evaluated using Equation (5.1.14) with a = 1.0.

$$q_w = -\, k_w \frac{T_{ig}^2}{T_w} \left.\frac{\partial U}{\partial \psi}\right|_{\psi = 0} \tag{E.1.4}$$

or substituting the partial derivative of U at $\psi = 0$;

$$q_w = k_w \frac{T_{ig}}{T_w} \frac{(T_w - T_{ig})}{\sqrt{\pi \alpha_{ig} t}} \tag{E.1.5}$$

E.2. Combustion Period

When the approximation a = 1.0 is made for the thermal conductivity, the transformed energy Equation (6.1.22) becomes:

$$\frac{\partial V}{\partial \tau} = \alpha_{ig} \frac{\partial^2 V}{\partial \psi^2} \tag{E.2.1}$$

The initial and boundary conditions are:

$$V(\psi, \tau_I) = F(\psi) \tag{E.2.1.a}$$

$$V(0, \tau) = \frac{T_w}{T_{ig}} \left[\frac{P}{P_{ig}}\right]^{\frac{1-\gamma}{\gamma}} \tag{E.2.1.b}$$

$$V(\delta,\tau) = \frac{T_\delta}{T_{ig}} \left[\frac{P}{P_{ig}}\right]^{\frac{1-\gamma}{\gamma}} \tag{E.2.1.c}$$

The above equation with the boundary conditions is identical to the one-dimensional heat transfer problem in a slab of thickness δ, which has an initial temperature distribution $F(\psi)$ and is subject to time varying temperatures at both ends [5]. The solution is given in a series form as:

$$V(\psi,\tau) = \frac{2}{\delta} \sum_{n=1}^{\infty} e^{-\alpha_{ig} n^2 \pi^2 \tau/\delta^2} \cdot \sin \frac{n\pi\psi}{\delta} \left\{ \int_0^\delta F(\psi') \cdot \sin \frac{n\pi\psi'}{\delta} d\psi' + \frac{n\alpha_{ig}\pi}{\delta} \int_0^\delta e^{\alpha_{ig} n^2 \pi^2 \xi/\delta^2} \cdot \left[V(0,\xi) - (-1)^n \cdot V(\delta,\xi)\right] d\xi \right\} \tag{E.2.2}$$

The heat flux at the end wall can be evaluated from Equation (6.1.23) with a = 1.0, as:

$$q_w = -k_w \frac{T_{ig}^2}{T_w} \left[\frac{P}{P_{ig}}\right]^{\frac{2\gamma-1}{\gamma}} \left.\frac{\partial V}{\partial \psi}\right|_{\psi=0} \tag{E.2.3}$$

or substituting the value of the partial derivative of the transformed temperature with respect to the transformed distance at $\psi = 0$,

$$q_w = -\frac{2\pi k_w T_{ig}^2}{\delta^2 T_w}\left[\frac{P}{P_{ig}}\right]^{\frac{2\gamma-1}{\gamma}} \sum_{n=1}^{\infty} n\, e^{-\alpha_{ig} n^2 \pi^2 \tau/\delta^2} \cdot$$

$$\cdot \left\{ \int_0^{\delta} F(\psi') \cdot \sin\frac{n\pi\psi'}{\delta}\, d\psi' + \frac{n\pi\alpha_{ig}}{\delta}\int_0^{\delta} e^{\alpha_{ig} n^2 \pi^2 \xi/\delta^2} \cdot \right.$$

$$\left. \cdot \left[V(0,\xi) - (-1)^n \cdot V(\delta,\xi)\right] \cdot d\xi \right\} \qquad \text{(E.2.4)}$$

APPENDIX F

INTEGRAL METHODS

F.1. Pre-Ignition Period

An approximate solution of the energy equation can be obtained by integrating the transformed energy Equation (5.1.13) from the wall $\psi = 0$ to the combustion boundary $\psi = \delta(t)$. A second order polynomial is used to approximate the transformed temperature, $U = \left(\frac{T}{T_{ig}}\right)^a$

$$U(\psi,t) = A(t) + B(t)\,\psi + C(t)\,\psi^2 \tag{F.1.1}$$

The boundary conditions to be satisfied are:

$$U(0,t) = \frac{T_w}{T_{ig}} = F \tag{F.1.1.a}$$

$$U(\delta,t) = 1 \tag{F.1.1.b}$$

$$\frac{\partial U}{\partial \psi}(\delta,t) = 0 \tag{F.1.1.c}$$

Using these conditions the coefficients in Equation (F.1.1) can be evaluated. The transformed temperature becomes:

$$U(\psi,t) = F - 2(F-1)\frac{\psi}{\delta} + (F-1)\left(\frac{\psi}{\delta}\right)^2 \tag{F.1.2}$$

For simplicity a = 1.0 is used in Equation (5.1.13).

$$\frac{\partial U}{\partial t} = \alpha_{ig}\,\frac{\partial^2 U}{\partial \psi^2} \tag{F.1.3}$$

The initial and boundary conditions are:

$$U(\psi,0) = 1 \tag{F.1.3.a}$$

$$U(0,t) = \frac{T_w}{T_{ig}} = F \tag{F.1.3.b}$$

$$U(\delta,t) = 1 \tag{F.1.3.c}$$

Integrating Equation (F.1.3) from $\psi = 0$ to $\psi = \delta$ gives

$$\int_0^\delta \frac{\partial U}{\partial t} d\psi = \alpha_{ig} \int_0^\delta \frac{\partial^2 U}{\partial \psi^2} d\psi \tag{F.1.4}$$

or

$$\frac{\partial}{\partial t}\int_0^\delta U\, d\psi - U(\delta)\frac{d\delta}{dt} = \alpha_{ig}\left[\left.\frac{\partial U}{\partial \psi}\right|_{\psi=\delta} - \left.\frac{\partial U}{\partial \psi}\right|_{\psi=0}\right] \tag{F.1.5}$$

Using Equations (F.1.1.b) and (F.1.1.c) yields:

$$\frac{\partial}{\partial t}\int_0^\delta U\, d\psi - \frac{d\delta}{dt} = -\alpha_{ig}\left.\frac{\partial U}{\partial \psi}\right|_{\psi=0} \tag{F.1.5}$$

Evaluating the integral, differentiating and substituting the value of the derivative of the transformed temperature at the wall we obtain:

$$\frac{d\delta^2}{dt} = 12\,\alpha_{ig} \tag{F.1.6}$$

or

$$\delta = \sqrt{12\,\alpha_{ig} t} \tag{F.1.7}$$

The heat flux given in Equation (5.1.14), for this case, becomes:

$$q_w = -k_w \frac{T_{ig}^2}{T_w} \left. \frac{\partial U}{\partial \psi} \right|_{\psi=0} \tag{F.1.8}$$

or

$$q_w = -k_w \frac{T_{ig}}{T_w} \frac{(T_{ig}-T_w)}{\sqrt{3\alpha_{ig} t}} \tag{F.1.9}$$

F.2. Combustion Period

In order to obtain an idea of the variation of the location of the combustion zone with time, the transformed energy equation is integrated from the wall, $\psi = 0$, to the combustion zone, $\psi = \psi_B(\tau)$. A second order polynomial is used to approximate the transformed temperature, ϕ, which is given by:

$$\phi(\psi,\tau) = \left[\frac{T}{T_{ig}}\right]^a \left[\frac{P}{P_{ig}}\right]^{\frac{a(1-\gamma)}{\gamma}} \tag{F.2.1}$$

The polynomial is given by:

$$\phi(\psi,\tau) = A(\tau) + B(\tau)\psi + C(\tau)\psi^2 \tag{F.2.2}$$

The following conditions are used to evaluate the coefficients:

$$\phi(0,\tau) = \left[\frac{T_w}{T_{ig}}\right]^a \left[\frac{P}{P_{ig}}\right]^{\frac{a(1-\gamma)}{\gamma}} = f(\tau) \tag{F.2.2.a}$$

$$\phi(\psi_B,\tau) = \left[\frac{T_\delta}{T_{ig}}\right]^a \left[\frac{P}{P_{ig}}\right]^{\frac{a(1-\gamma)}{\gamma}} = g(\tau) \qquad \text{(F.2.2.b)}$$

$$\frac{\partial\phi}{\partial\psi}(0,\tau) = -q_w \frac{a}{k_w} \frac{T_w^{\,a}}{T_{ig}^{(a+1)}} \left[\frac{P_{ig}}{P}\right]^{\frac{a(\gamma-1)}{\gamma}+1} = h(\tau) \qquad \text{(F.2.2.c)}$$

The above three conditions determine the three unknown coefficents. The transformed temperature then becomes:

$$\phi(\psi,\tau) = f(\tau) + h(\tau)\psi + \left[\frac{g(\tau)-f(\tau)}{\delta^2} - \frac{h(\tau)}{\delta}\right]\psi^2 \qquad \text{(F.2.3)}$$

Differentiation of Equation (F.2.2) with respect to ψ yields

$$\frac{\partial\phi}{\partial\psi} = h(\tau) + 2\left[\frac{g(\tau)-f(\tau)}{\delta^2} - \frac{h(\tau)}{\delta}\right]\psi \qquad \text{(F.2.4)}$$

Integrating Equation (6.1.22) with a = 1.0 yields:

$$\int_0^{\psi_B} \frac{\partial\phi}{\partial\tau}\, d\psi = \alpha_{ig} \int_0^{\psi_B} \frac{\partial^2\phi}{\partial\psi^2}\, d\psi \qquad \text{(F.2.5)}$$

or

$$\frac{\partial}{\partial\tau}\int_0^{\psi_B} \phi\, d\psi - \phi(\psi_B)\frac{d\psi_B}{d\tau} = \alpha_{ig}\left[\left.\frac{\partial\phi}{\partial\psi}\right|_{\psi_B} - \left.\frac{\partial\phi}{\partial\psi}\right|_0\right] \qquad \text{(F.2.6)}$$

Evaluating the integral and the derivatives at $\psi = 0$ and $\psi = \psi_B$ and substituting into Equation (F.2.5) yields:

$$\left[\frac{2}{3}\left(f(\tau) - g(\tau)\right) + \frac{1}{3}\psi_B h(\tau)\right]\frac{d\psi_B}{d\tau} = \alpha_{ig}\left[\frac{2\left(g(\tau) - f(\tau)\right)}{\psi_B} - 2h(\tau)\right] - \frac{2}{3}\psi_B\frac{df(\tau)}{d\tau} - \frac{1}{3}\psi_B\frac{dg(\tau)}{d\tau} - \frac{1}{6}\psi_B^2\frac{dh(\tau)}{d\tau} \quad \text{(F.2.7)}$$

or

$$\frac{d\psi_B}{d\tau} = \alpha_{ig}\frac{6\left(g(\tau) - f(\tau)\right) - 6\psi_B h(\tau)}{2\psi_B\left(g(\tau) - f(\tau)\right) + \psi_B^2 h(\tau)} - \frac{4\psi_B^2\frac{df(\tau)}{d\tau} + 2\psi_B^2\frac{dg(\tau)}{d\tau} + \psi_B^3\frac{dh(\tau)}{d\tau}}{4\psi_B\left(g(\tau) - f(\tau)\right) + 2\psi_B^2 h(\tau)} \quad \text{(F.2.8)}$$

The initial condition is:

$$\psi_B(0) = \psi_p \quad \text{(F.2.8.a)}$$

The above first order, non-linear, ordinary differential equation can be solved numerically. ψ_p is the thickness of the gas layer at the end of the pre-ignition period. The computer listing for the solution is given in Appendix J.

APPENDIX G

FORMULATION WITH DIFFUSION

Consider the energy Equation (6.1.2) and the species diffusion Equation (6.1.3)

$$\rho \frac{\partial h}{\partial t} + \rho u \frac{\partial h}{\partial x} = \frac{dp}{dt} + \frac{\partial}{\partial x}\left[k \frac{\partial T}{\partial x} - \sum_i \rho Y_i V_i h_i\right] \tag{G.1}$$

$$\rho \frac{\partial Y_i}{\partial t} + \rho u \frac{\partial Y_i}{\partial x} - \frac{\partial}{\partial x}\left[\rho D \frac{\partial Y_i}{\partial x}\right] = 0 \tag{G.2}$$

Using Fick's Law,

$$\rho Y_i V_i = -\rho D \frac{\partial Y_i}{\partial x} \tag{G.3}$$

the energy equation becomes:

$$\rho \frac{\partial h}{\partial t} + \rho u \frac{\partial h}{\partial x} = \frac{dp}{dt} + \frac{\partial}{\partial x}\left|k \frac{\partial T}{\partial x}\right| + \frac{\partial}{\partial x}\left[\sum_i \rho D h_i \frac{\partial Y_i}{\partial x}\right] \tag{G.4}$$

The ethalpy for the mixture is defined as:

$$h = \sum_i Y_i h_i \tag{G.5}$$

differentiating Equation (G.5) gives:

$$dh = \sum_i Y_i \, dh_i + \sum_i h_i \, dY_i$$
$$= \sum_i Y_i C_{p_i} \, dT + \sum_i h_i \, dY_i$$
$$= \bar{C}_p \, dT + \sum_i h_i \, dY_i \tag{G.6}$$

where

$$\bar{C}_p = \sum_i Y_i C_{p_i} \tag{G.7}$$

From Equation (G.6) the following derivatives are obtained:

$$\frac{\partial h}{\partial t} = \bar{C}_p \frac{\partial T}{\partial t} + \sum_i h_i \frac{\partial Y_i}{\partial t} \tag{G.8}$$

$$\frac{\partial h}{\partial x} = \bar{C}_p \frac{\partial T}{\partial x} + \sum_i h_i \frac{\partial Y_i}{\partial x} \tag{G.9}$$

Substituting into the energy equation yields

$$\rho \bar{C}_p \frac{\partial T}{\partial t} + \rho u \bar{C}_p \frac{\partial T}{\partial x} = \frac{dp}{dt} + \frac{\partial}{\partial x}\left[k \frac{\partial T}{\partial x}\right] + \sum_i \left[\frac{\partial}{\partial x}\left(h_i \rho D \cdot \frac{\partial Y_i}{\partial x}\right) - h_i \frac{\partial Y_i}{\partial t} \rho - \rho u h_i \frac{\partial Y_i}{\partial x}\right] \tag{G.10}$$

or

$$\rho \bar{C}_p \frac{\partial T}{\partial t} + \rho u \bar{C}_p \frac{\partial T}{\partial x} = \sum_i \left\{ \rho D \frac{\partial Y_i}{\partial x} \frac{\partial h_i}{\partial x} + h_i \left[\frac{\partial}{\partial x}\left(\rho D \frac{\partial Y_i}{\partial x}\right) - \rho \frac{\partial Y_i}{\partial t} - \rho u \frac{\partial Y_i}{\partial x}\right]\right\} + \frac{dp}{dt} + \frac{\partial}{\partial x}\left[k \frac{\partial T}{\partial x}\right] \tag{G.11}$$

In the above equation the coefficient of h_i is zero because of the species diffusion Equation (G.2). Using Equation (6.1.4) the energy equation becomes:

$$\rho \bar{C}_p \frac{\partial T}{\partial t} + \rho u \bar{C}_p \frac{\partial T}{\partial x} = \frac{dp}{dt} + \frac{\partial}{\partial x}\left[k \frac{\partial T}{\partial x}\right] + \sum_i \rho D C_{p_i} \frac{\partial T}{\partial x} \frac{\partial Y_i}{\partial x} \quad \text{(G.12)}$$

or

$$\rho \bar{C}_p \frac{\partial T}{\partial t} + \rho u \bar{C}_p \frac{\partial T}{\partial x} = \frac{dp}{dt} + \frac{\partial}{\partial x}\left[k \frac{\partial T}{\partial x}\right] + \rho D \frac{\partial T}{\partial x} \frac{\partial}{\partial x} \sum_i C_{p_i} Y_i \quad \text{(G.13)}$$

We had assumed that $\overline{Cp}$ was constant, therefore the last term is zero. The energy and species diffusion equations become:

$$\rho \bar{C}_p \frac{\partial T}{\partial t} + \rho u \bar{C}_p \frac{\partial T}{\partial x} = \frac{dp}{dt} + \frac{\partial}{\partial x}\left[k \frac{\partial T}{\partial x}\right] \quad \text{(G.14)}$$

$$\rho \frac{\partial Y_i}{\partial t} + \rho u \frac{\partial Y_i}{\partial x} = \frac{\partial}{\partial x}\left[\rho D \frac{\partial Y_i}{\partial x}\right] \quad \text{(G.15)}$$

The energy equation is the same as before. The species diffusion equation can be treated similar to the energy equation. Using the transformations (6.1.5) and (6.1.6) the species diffusion equation becomes:

$$\frac{\partial Y_i}{\partial t} = \frac{1}{\rho_{ig}} \frac{\partial}{\partial \psi}\left[\rho D \frac{\rho}{\rho_{ig}} \frac{\partial Y_i}{\partial \psi}\right] \quad \text{(G.16)}$$

Using Equation (6.1.11) yields:

$$\frac{\partial Y_i}{\partial t} = \alpha_i \frac{P}{P_{ig}} \frac{\partial}{\partial \psi}\left[\frac{k_i}{k_{ig}} Le_i \frac{T_{ig}}{T} \frac{\partial Y_i}{\partial \psi}\right]$$

where

$$\alpha_i = \frac{k_{ig}}{\rho_{ig} C_{p_i}} \tag{G.17}$$

$$Le_i = \frac{\rho D C_{p_i}}{k_i} \tag{G.18}$$

Using Equation (6.1.10) for each species with a = 1.0 and defining a new time variable according to:

$$d\tau = \frac{P}{P_{ig}} dt \tag{G.19}$$

yields:

$$\frac{\partial Y_i}{\partial \tau} = \alpha_i \, Le_i \frac{\partial^2 Y_i}{\partial \psi^2} \tag{G.20}$$

where Le_i has been assumed to be constant. The initial and boundary conditions are:

$$Y_i(\psi, 0) = Y_{io} \tag{G.20.a}$$

$$Y_i(0, \tau) = Y_{iw} \tag{G.20.b}$$

$$Y_i(\delta, \tau) = Y_{i\infty} \tag{G.20.c}$$

The gas layer thickness, δ, is a function of time and is determined as explained in Chapter 6. The transformed species diffusion equation is similar to the transformed energy equation with a = 1.0 which was discussed in Appendix E. The heat flux in the presence of diffusion

is given by:

$$q = -k \frac{\partial T}{\partial x} + \sum_i \rho Y_i V_i h_i \tag{G.21}$$

Using Fick's Law (G.3) yields:

$$q = -\left[k \frac{\partial T}{\partial x} + \rho D \sum_i h_i \frac{\partial Y_i}{\partial x} \right] \tag{G.22}$$

From Equation (G.9)

$$\frac{\partial T}{\partial x} = \frac{1}{\bar{C}_p} \left[\frac{\partial h}{\partial x} - \sum_i h_i \frac{\partial Y_i}{\partial x} \right] \tag{G.23}$$

Substituting into Equation (G.22) yields:

$$q = -\frac{k}{\bar{C}_p} \left[\frac{\partial h}{\partial x} + (Le - 1) \sum h_i \frac{\partial Y_i}{\partial x} \right] \tag{G.24}$$

where Le is the Lewis number defined by:

$$Le = \frac{\rho D \bar{C}_p}{k} \tag{G.25}$$

At the end wall there is no mass flux for any species, thus the concentration gradient is zero at the end wall. The last term in Equation (G.24) is zero. The wall heat flux is therefore given by:

$$q_w = -k \left. \frac{\partial T}{\partial x} \right|_w \tag{G.26}$$

APPENDIX H

COORDINATE TRANSFORMATION

H.1. ψ - x Transformation

The relation between ψ and x coordinates was defined in Equation (5.1.3) as:

$$\frac{\partial \psi}{\partial x} = \frac{\rho}{\rho_{ig}} \tag{H.1.1}$$

Using the ideal gas law, Equation (H.1.1) can be expressed in terms of temperatures and pressures.

$$\frac{\partial \psi}{\partial x} = \frac{P}{P_{ig}} \; \frac{T_{ig}}{T} \tag{H.1.2}$$

The ratio of temperatures can be evaluated in terms of the transformed temperature, V, which was used in Chapter 6. Equation (6.1.7) is:

$$V = \left[\frac{T}{T_{ig}}\right]^{a} \left[\frac{P}{P_{ig}}\right]^{\frac{a(1-\gamma)}{\gamma}} \tag{H.1.3}$$

which yields,

$$\frac{T}{T_{ig}} = V^{1/a} \left[\frac{P_{ig}}{P}\right]^{\frac{(1-\gamma)}{\gamma}} \tag{H.1.4}$$

Substituting Equation (H.1.4) into Equation (H.1.2) yields:

$$\frac{\partial \psi}{\partial x} = V^{-1/a}\left[\frac{p}{p_{ig}}\right]^{\frac{(1-\gamma)}{\gamma}+1} \tag{H.1.5}$$

or

$$dx = V^{1/a}\left[\frac{p}{p_{ig}}\right]^{-1/\gamma} d\psi \tag{H.1.6}$$

Integration of Equation (H.1.6) gives the untransformed space variable, x.

$$x = \int_0^{\psi} V^{1/a}\left[\frac{p}{p_{ig}}\right]^{-1/\gamma} d\psi \tag{H.1.7}$$

In Equation (H.1.7) only V is a function of ψ, therefore:

$$x = \left[\frac{p}{p_{ig}}\right]^{-1/\gamma} \int_0^{\psi} V^{1/a}\, d\psi \tag{H.1.8}$$

Two ψ - x curves are plotted for the combustion period at 20 μsec in Figure H.1. As seen from Equation (H.1.8), the ψ - x curves will be different for different times.

The penetration depth, δ, was defined for the pre-ignition period as the distance where the temperature reached the value 0.99 T_∞. For this period the pressure is a constant, $p = p_{ig}$ = constant, hence Equation (H.1.8) simplifies to:

$$\delta = \int_0^{\psi_B} V^{1/a}\, d\psi \tag{H.1.9}$$

This penetration depth was calculated and plotted in Chapter 5 (Figures 5.7 and 5.8).

For the combustion period, the penetration depth, δ_B, was defined as the distance where the temperature reached 0.99 T_δ. Using Equation (H.1.8) δ_B can be calculated as:

$$\delta_B = \left[\frac{P}{P_{ig}}\right]^{-1/\gamma} \int_0^{\psi_B} V^{1/a}\, d\psi \qquad \text{(H.1.10)}$$

δ_B was calculated and plotted in Chapter 6 (Figures 6.12 and 6.13).

H.2. t - τ Transformation

The relation between t and τ was given in Equation (6.1.21) as:

$$d\tau = \left[\frac{P}{P_{ig}}\right]^{\frac{a\gamma - a + 1}{\gamma}} dt \qquad \text{(H.2.1)}$$

The pressure is a known function of time, therefore to evaluate τ we must integrate Equation (H.2.1).

$$\tau = \int_0^t \left[\frac{P}{P_{ig}}\right]^{\frac{a\gamma - a + 1}{\gamma}} dt \qquad \text{(H.2.2)}$$

To evaluate t from τ the reverse should be done.

$$t = \int_0^\tau \left[\frac{P}{P_{ig}}\right]^{\frac{a - a\gamma - 1}{\gamma}} d\tau \qquad \text{(H.2.3)}$$

t and τ are shown in Table H.1 for runs 214 and 219.

Table H.1

	Run 219	Run 214
τ (μsec)	t (μsec)	t (μsec)
0	0	0
10	10	10
20	19.9999	19.9999
21	20.9995	20.9995
22	21.9987	21.9988
23	22.9975	22.9977
24	23.9956	23.9960
25	24.9930	24.9936
26	25.9892	25.9895
27	26.9829	26.9830
28	27.9725	27.9734
29	28.9570	28.9598
30	29.9356	29.9410
31	30.9078	30.9162
32	31.8729	31.8844
33	32.8309	32.8448
34	33.7818	33.7975
35	34.7262	34.7432
36	35.6656	35.6828
37	36.6004	36.6168
38	37.5309	37.5458
39	38.4569	38.4702
40	39.3783	39.3901
41	40.2950	40.3060
42	41.2068	41.2172
43	42.1128	42.1225
44	43.0117	43.0206
45	43.9029	43.9096
		44.7885
		45.6567

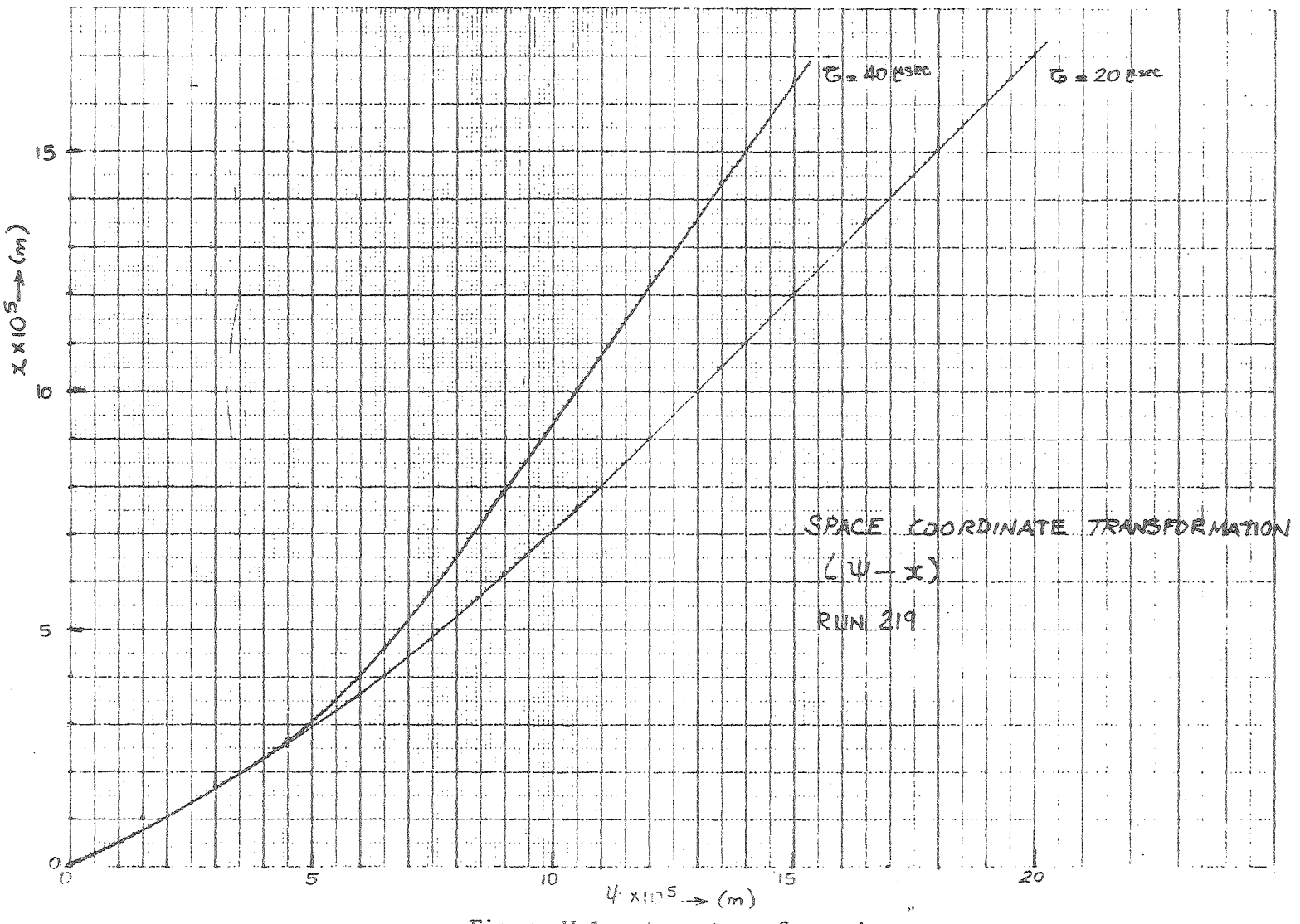

Figure H.1. ψ - x transformation.

APPENDIX I

HALF-SLAB IMPROVEMENT

In order to obtain the derivative of the temperature with respect to distance more accurately the heat storage in the space elements can be considered. In Figure I.1.A a space element adjacent to the wall is shown. A heat balance on the element yields:

$$q_1 = q_w + \rho C_p \frac{\partial T}{\partial t} \frac{\Delta \psi}{2} \tag{I.1}$$

or

$$q_w = q_1 - \rho C_p \frac{\partial T}{\partial t} \frac{\Delta \psi}{2} \tag{I.2}$$

The heat flux coming into the element is given by Equation (6.1.24) as:

$$q_1 = - \frac{k_w}{a} \frac{(T_{ig})^{(a+1)}}{T_w^{\,a}} \left[\frac{P}{P_{ig}}\right]^{\frac{a(\gamma-1)}{\gamma}+1} \left.\frac{\partial V}{\partial \psi}\right|_{\psi=0} \tag{I.3}$$

The heat storage term, second term, in Equation (I.2) can be expressed in terms of temperature and pressure as follows:

$$\rho C_p \frac{\partial T}{\partial t} = \frac{P C_p}{R T} \frac{\partial T}{\partial t} \tag{I.4}$$

The temperature can be evaluated from Equation (6.1.17)

$$V = \left[\frac{T}{T_{ig}}\right]^{a} \left[\frac{P}{P_{ig}}\right]^{\frac{a(1-\gamma)}{\gamma}} \tag{I.5}$$

or

$$T = T_{ig}\, V^{1/a} \left[\frac{P}{P_{ig}}\right]^{\frac{\gamma-1}{\gamma}} \tag{I.6}$$

The derivative of the temperature with respect to time can also be evaluated from the transformed temperature and the time variable as follows:

$$\frac{\partial T}{\partial t} = \frac{\partial T}{\partial V}\,\frac{\partial V}{\partial \tau}\,\frac{\partial \tau}{\partial t} \tag{I.7}$$

Substitution of the partial derivatives yield:

$$\frac{\partial T}{\partial t} = \frac{T_{ig}^{a}}{a}\, T^{(1-a)} \left[\frac{P}{P_{ig}}\right]^{\frac{a(\gamma-1)}{\gamma}} \left[\frac{P}{P_{ig}}\right]^{\frac{a\gamma+1-a}{\gamma}} \frac{\partial V}{\partial \tau} \tag{I.8}$$

or

$$\frac{\partial T}{\partial t} = \frac{T_{ig}^{a}}{a}\, T^{(1-a)} \left[\frac{P}{P_{ig}}\right]^{\frac{2a\gamma-2a+1}{\gamma}} \frac{\partial V}{\partial \tau} \tag{I.9}$$

Substituting Equations (I.6) and (I.9) into Equation (I.4) we obtain:

$$\rho C_p \frac{\partial T}{\partial t} = \frac{P C_p}{a R V} \left[\frac{P}{P_{ig}}\right]^{\frac{a(\gamma-1)+1}{\gamma}} \frac{\partial V}{\partial \tau} \tag{I.10}$$

Then the heat flux at the end wall can be calculated from Equation (I.2).

$$q_w = -\frac{k_w}{a}\,\frac{T_{ig}^{(a+1)}}{T_w^{a}} \left[\frac{P}{P_{ig}}\right]^{\frac{a(\gamma-1)+\gamma}{\gamma}} \left.\frac{\partial V}{\partial \psi}\right|_{\psi=0} - \frac{\Delta\psi}{2}\,\frac{P C_p}{a R}\,\cdot$$

$$\cdot \left[\frac{P}{P_{ig}}\right]^{\frac{a(\gamma-1)+1}{\gamma}} \frac{1}{V}\,\frac{\partial V}{\partial \tau} \tag{I.11}$$

The time derivative of the transformed temperature was evaluated using the average of the temperatures at the wall and the first grid point. In finite difference form the heat flux at the wall is given by:

$$q_w = -\frac{k_w}{a}\frac{T_{ig}^{(a+1)}}{T_w^{a}}\left[\frac{P}{P_{ig}}\right]^{\frac{a(\gamma-1)+\gamma}{\gamma}}\frac{V_1-V_w}{\Delta\psi} - \frac{\Delta\psi}{2}\frac{\rho C_p}{aR\Delta\sigma}\cdot$$

$$\cdot\left[\frac{P}{P_{ig}}\right]^{\frac{a(\gamma-1)+1}{\gamma}}\left\{\frac{V_w'+V_1'}{V_w+V_1}-1\right\} \qquad \text{(I.12)}$$

The primes in the equation denote the next time step.

A space element at the edge of the gas boundary layer is shown in Figure I.1.B. A heat balance on the element yields:

$$q_\delta = q_m + \rho C_p \frac{\partial T}{\partial t}\frac{\Delta\psi}{2} \qquad \text{(I.13)}$$

The storage term can be evaluated in the same way as was done for the element at the end wall. The heat flux is given by:

$$q_\delta = -\frac{k_\delta}{a}\frac{T_{ig}^{(a+1)}}{T_\delta^{a}}\left[\frac{P}{P_{ig}}\right]^{\frac{a(\gamma-1)+\gamma}{\gamma}}\left.\frac{\partial V}{\partial\psi}\right|_{\psi=\delta} - \frac{\rho C_p\Delta\psi}{2aR}\cdot$$

$$\cdot\left[\frac{P}{P_{ig}}\right]^{\frac{a(\gamma-1)+1}{\gamma}}\frac{1}{V}\frac{\partial V}{\partial\sigma} \qquad \text{(I.14)}$$

or in finite difference form:

$$q_\delta = -\frac{k_\delta}{a}\,\frac{T_{ig}^{(a+1)}}{T_\delta^{\,a}}\left[\frac{P}{P_{ig}}\right]^{\frac{a(\gamma-1)+\gamma}{\gamma}}\frac{V_\delta - V_m}{\Delta\psi} - \frac{PC_p\Delta\psi}{2aR\,\Delta\tau}\cdot$$

$$\cdot\left[\frac{P}{P_{ig}}\right]^{\frac{a(\gamma-1)+1}{\gamma}}\left\{\frac{V_\delta' + V_m'}{V_\delta + V_m} - 1\right\} \qquad \text{(I.15)}$$

As before the primes denote the temperatures at the next time step.

The results obtained by this method were very close to the previous results. The difference was less than 2%, which is well within the range of our accuracy.

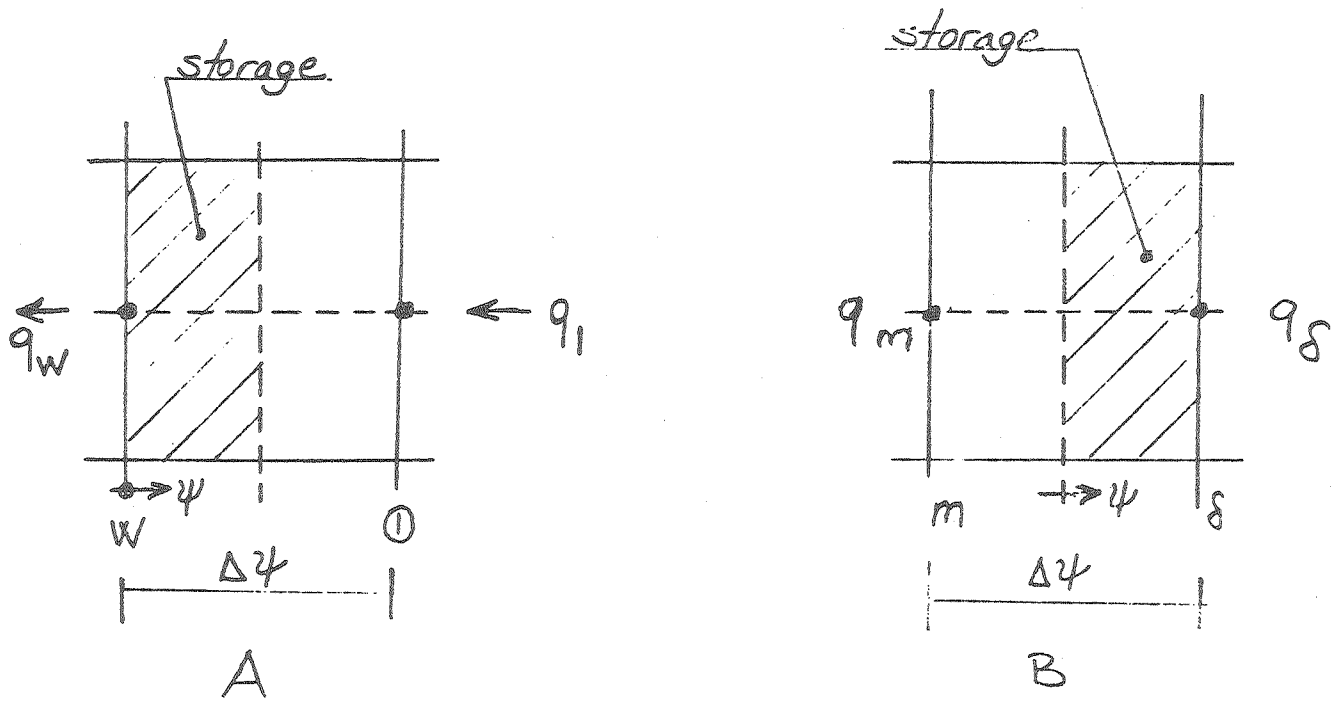

Figure I.1. Half slab grids.

APPENDIX J

COMPUTER LISTINGS FOR "GSHEAT" AND "DELTA" PROGRAMS

```
      PROGRAM GSHEAT (INPUT,OUTPUT)
      DIMENSION TEMPP(30)
      DIMENSION PHI(60,30),TEMP(60,30),PINF(60),T(60),PSI(30),TINF(60)
      DIMENSION F(60),G(60),HEATF1(60),HEATF2(60),HEATF3(60),H1(60)
      DIMENSION H2(60),H3(60),CCF(60),PHIIN(60),HINF1(60),HINF2(60)
      DIMENSION HINF3(60),DELTA(60),DEL(60,30)
      DIMENSION V(30,30),TTEMP(30,30),HTF1(30),HTF2(30),HTF3(30)
      DIMENSION HH1(30),HH2(30),HH3(30),DDEL(30,30),DDELTA(30)
      REAL KW
      READ 100, N,M,PING,TING,STABF,TW,GAMMA,DTAU,A
  100 FORMAT (2I5,7F10.5)
      READ 105, KW,ALFAI
  105 FORMAT (2E11.5)
      READ 106, LM
  106 FORMAT (I5)
C     TEMPERATURES ARE IN KELVIN
C     PRESSURES ARE IN ATMOSPHERES
C     THERMAL CONDUCTIVITY IS IN WATTS/M .K
C     TIME IS IN MICROSECONDS
C     SPACE IS IN METERS
C     ALFAI IS IN M2/MICROSEC
C     A IS THE POWER FOR THERMAL CONDUCTIVITY
      READ 110,(PINF(K),K=1,N)
  110 FORMAT (10F8.5)
      READ 120, (TINF(K), K=1,N)
  120 FORMAT(10F8.2)
      GAM = (GAMMA-1.)/GAMMA
      AA = A*(1.-GAMMA)/GAMMA
      AAA = 1./A
      AAAA = A+1.
      B = KW*(TING**AAAA)/(TW**A)/A
      DPSI = SQRT(ALFAI*DTAU/STABF)
      AB = (A-1.)/A
C     PREIGNITION PROGRAM
      FF = (TW/TING)**A
      READ 90, NP,MP
   90 FORMAT (2I5)
C     SPECIFY INITIAL AND BOUNDARY CONDITIONS
      DO500 J=1,MP
      V(J,1) = 1.
  500 CONTINUE
      DO505 K=2,NP
      V(1,K) = FF
      V(MP,K) = 1.
  505 CONTINUE
C     START CALCULATION
      MPP = MP-1
      DO520 K=1,NP
      DO510 J=2,MPP
      V(J,K+1) = (1.-2.*STABF*(V(J,K)**AB))*V(J,K)+(V(J,K)**AB)*STABF*(V
     1(J+1,K)+V(J-1,K))
  510 CONTINUE
  520 CONTINUE
C     CALCULATE HEAT FLUXES AT THE WALL
      S = TING-TW
      DO540 K=2,NP
      DO530 J=1,MP
      TTEMP(J,1) = TING*(V(J,1)**AAA)
      TTEMP(J,K) = TING*(V(J,K)**AAA)
  530 CONTINUE
      HTF1(K) = 0.-B*(V(2,K)-V(1,K))/DPSI
```

```
      HTF2(K) = 0.-B*(4.*V(2,K)-V(3,K)-3.*V(1,K))/2./DPSI
      HTF3(K) = 0.-B*(2.*V(4,K)-9.*V(3,K)+18.*V(2,K)-11.*V(1,K))/6./DPSI
C     CALCULATE HEAT TRANSFER COEFFICIENTS
      HH1(K) = HTF1(K)/S
      HH2(K) = HTF2(K)/S
      HH3(K) = HTF3(K)/S
      DDEL(1,K) = 0.
      MMP = K
      DO535 J=1,MMP
      DDEL(J+1,K) = DDEL(J,K)+(V(J,K)+V(J+1,K))*DPSI/2.
  535 CONTINUE
      DDELTA(K) = DDEL(MMP,K)
  540 CONTINUE
C     PRINT THE RESULTS
      PRINT 600
  600 FORMAT (/,5X,*RESULTS FOR THE PREIGNITION PERIOD*)
      PRINT 610
  610 FORMAT (//,5X,*INPUT DATA*)
      PRINT 620, NP,MP,STABF,DTAU,DPSI,LM
  620 FORMAT (/,5X,*NP= *,I5,5X,*MP= *,I5,5X,*STABF= *,E11.5,5X,*DTAU= *
     1,E11.5,5X,*DPSI= *,E11.5,5X,*LM= *,I5)
      PRINT 630, TING,TW,FF
  630 FORMAT (/,5X,*TING= *,F8.2,5X,*TW= *,F8.2,5X,*FF= *,E11.5)
      PRINT 640, GAMMA,KW,ALFAI,A
  640 FORMAT (/,5X,*GAMMA= *,F8.5,5X,*KW= *,E11.5,5X,*ALFAI= *,E11.5,5X,
     1*A= *,F8.5)
      DO7CC K=1,NP
      DO655 J=1,NP
      TEMPP(J) = TTEMP(J,K)
  655 CONTINUE
      PRINT 650, K,HTF1(K),HTF2(K),HTF3(K)
  650 FORMAT (/,5X,*TAU= *,I5,/,5X,*HTF1= *,E11.5,5X,*HTF2= *,E11.5,5X,*
     1HTF3= *,E11.5)
      PRINT 660, HH1(K),HH2(K),HH3(K)
  660 FORMAT (/,5X,*HH1= *,E11.5,5X,*HH2= *,E11.5,5X,*HH3= *,E11.5)
      PRINT 670
  670 FORMAT (/,5X,*TEMPERATURE DISTRIBUTION IN THE GAS LAYER*)
      PRINT 680, (TEMPP(J), J=1,MP)
  680 FORMAT (8(5X,F10.5))
  70C CONTINUE
      PRINT 430
      PRINT 460, (HTF1(K),K=1,NP)
      PRINT 440
      PRINT 460, (HTF2(K),K=1,NP)
      PRINT 450
      PRINT 460, (HTF3(K),K=1,NP)
      PRINT 470
      PRINT 480, (DDELTA(K),K=1,NP)
      J = 0
      K = 0
C     COMBUSTICN PERICD PROGRAM
      PRINT 710
  710 FORMAT (///,5X,*RESULTS OF ANALYSIS FOR THE COMBLSTION PERIOD*)
      DO 3 K=1,N
      F(K) = ((TW/TING)**A)*((PINF(K)/PING)**AA)
      G(K) = ((TINF(K)/TING)**A)*((PINF(K)/PING)**AA)
      COF(K) = (PINF(K)/PING)**(1.-AA)
    3 CONTINUE
C     PRINT THE INPUT DATA
      PRINT 300
  300 FORMAT (5X,*INPUT DATA*)
      PRINT 310, N,M,STABF,DTAU,DPSI
```

```
  310 FORMAT (/,5X,*N= *,I5,*M= *,I5,5X,*STABF= *,E11.5,5X,*DTAU= *,E11.
     15,5X,*DPSI= *,E11.5)
      PRINT 320, PING,TING,TW
  320 FORMAT (/,5X,*PING= *,F8.5,5X,*TING= *F8.2,5X,*TW= *,F8.2)
      PRINT 330, GAMMA,KW,ALFAI,A
  330 FORMAT (/,5X,*GAMMA= *,F8.5,5X,*KW= *,E11.5,5X,*ALFAI= *,E11.5,5X,
     1*A= *,F8.5)
      PRINT 340
  340 FORMAT (/,5X,*DELTA CONDITION FOR TEMPERATURE*,10X,*WALL CONDITION
     1FOR TEMPERATURE*)
      DO5 K=1,N
      PRINT 350, G(K),F(K)
  350 FORMAT (5X,E11.5,34X,E11.5)
    5 CONTINUE
C     SPECIFY INITIAL AND BOUNDARY CONDITIONS
      DO130 J=1,M
      PHIIN(J) = V(J,NP)
  130 CONTINUE
      DO6 J=1,M
      PHI(J,1) = PHIIN(J)
    6 CONTINUE
      DO7 K=2,N
      PHI(1,K) = F(K)
    7 CONTINUE
      LLN = 2*(M-LM)+2
      NN = LLN-2
      DO9 K=2,NN,2
      MM = M-(K/2)
      DO8 J=MM,M
      PHI(J,K) = G(K)
    8 CONTINUE
    9 CONTINUE
      NNN = LLN-1
      DO15 K=3,NNN,2
      MM = M-((K-1)/2)
      DO14 J=MM,M
      PHI(J,K) = G(K)
   14 CONTINUE
   15 CONTINUE
      DO20 K=LLN,N
      MM = LM
      DO19 J=MM,M
      PHI(J,K) = G(K)
   19 CONTINUE
   20 CONTINUE
      DO30 K=1,N
      TEMP(1,K) = TW
   30 CONTINUE
C     START CALCULATION
      DO50 K=1,NNN
      L = (-1)**(K+1)
      IF(L.EQ.1) GO TO 45
      GO TO 46
   45 MM = M-(K+1)/2
   46 DO49 J=2,MM
      PHI(J,K+1) = (1.-2.*STABF*(PHI(J,K)**AB))*PHI(J,K)+(PHI(J,K)**AB)*
     1(PHI(J+1,K)+PHI(J-1,K))*STABF
   49 CONTINUE
   50 CONTINUE
      MMM = LM-1
      DO60 K=LLN,N
      DO59 J=2,MMM
```

```
      PHI(J,K+1) = (1.-2.*STABF*(PHI(J,K)**AB))*PHI(J,K)+(PHI(J,K)**AB)*
     1(PHI(J+1,K)+PHI(J-1,K))*STABF
   59 CONTINUE
   60 CONTINUE
      GAMM = 0.-1./GAMMA
      DO70 K=2,N
      DO65 J=2,M
      TEMP(J,1) = TING*((PINF(1)/PING)**GAM)*(PHI(J,1)**AAA)
      TEMP(J,K) = TING*((PINF(K)/PING)**GAM)*(PHI(J,K)**AAA)
   65 CONTINUE
C     CALCULATE HEAT FLUX AT THE WALL
      HEATF1(K) = 0.-COF(K)*B*(PHI(2,K)-PHI(1,K))/DPSI
      HEATF2(K) = 0.-COF(K)*B*(4.*PHI(2,K)-PHI(3,K)-3.*PHI(1,K))/2./DPSI
      HEATF3(K) = 0.-COF(K)*B*(2.*PHI(4,K)-9.*PHI(3,K)+18.*PHI(2,K)-11.*
     1PHI(1,K))/6./DPSI
C     CALCULATE HEAT TRANSFER COEFFICIENTS
      H1(K) = HEATF1(K)/(TINF(K)-TW)
      H2(K) = HEATF2(K)/(TINF(K)-TW)
      H3(K) = HEATF3(K)/(TINF(K)-TW)
C     CALCULATE HEAT FLUX AT DELTA
      IF (K.GT.NNN) GO TO 68
      L = (-1)**K
      IF(L.EQ.1) GO TO 67
      GO TO 68
   67 MM = M-K/2
   68 HINF1(K) = 0.-COF(K)*B*(PHI(MM-1,K)-PHI(MM,K))/DPSI
      HINF2(K) = 0.-COF(K)*B*(PHI(MM-1,K)*4.-PHI(MM-2,K)-3.*PHI(MM,K))/2
     1./DPSI
      HINF3(K) = 0.-COF(K)*B*(2.*PHI(MM-3,K)-9.*PHI(MM-2,K)+18.*PHI(MM-1
     1,K)-11.*PHI(MM,K))/6./DPSI
      DEL(1,K) = 0.
      DO69 J=1,MM
      DEL(J+1,K) = DEL(J,K)+(PHI(J,K)+PHI(J+1,K))*DPSI/2.
   69 CONTINUE
      DELTA(K) = ((PINF(K)/PING)**GAMM)*DEL(MM,K)
   70 CONTINUE
C     PRINT THE RESULTS
      DO80 K=1,N
      PRINT 360, K,TINF(K),HEATF1(K),HEATF2(K),HEATF3(K)
  360 FORMAT (/,5X,*TAU= *,I5,/,5X,*TINF= *,F10.5,5X,*HEATF1= *,E11.5,5X
     1,*HEATF2= *,E11.5,5X,*HEATF3= *,E11.5)
      PRINT 370, H1(K),H2(K),H3(K)
  370 FORMAT (/,5X,*H1= *,E11.5,5X,*H2= *,E11.5,5X,*H3= *,E11.5)
      PRINT 380, HINF1(K),HINF2(K),HINF3(K)
  380 FORMAT (/,5X,*HINF1= *,E11.5,5X,*HINF2= *,E11.5,5X,*HINF3= *,E11.5
     1)
      PRINT 390
  390 FORMAT (/,5X,*TEMPERATURE DISTRIBUTION IN THE GAS LAYER*)
      PRINT 400, (TEMP(J,K), J=1,M)
  400 FORMAT (8(5X,F10.5))
   80 CONTINUE
      PRINT 410
  410 FORMAT (/,5X,*TINF*)
      PRINT 420,(TINF(K),K=1,N)
  420 FORMAT (8(5X,F10.5))
      PRINT 430
  430 FORMAT (/,5X,*HEAT FLUX,FIRST ORDER*)
      PRINT 460, (HEATF1(K),K=1,N)
      PRINT 440
  440 FORMAT (/,5X,*HEAT FLUX ,SECOND ORDER*)
      PRINT 460, (HEATF2(K),K=1,N)
      PRINT 450
```

```
450 FORMAT (/,5X,*HEAT FLUX,THIRD ORDER*)
    PRINT 460,(HEATF3(K),K=1,N)
46C FORMAT (8(5X,E11.5))
    PRINT 470
470 FORMAT (/,5X,*GAS LAYER THICKNESS*)
    PRINT 480, (DELTA(K),K=1,N)
480 FORMAT (8(5X,E11.5))
    STOP
    END
```

```
      PROGRAM DELT (INPUT,OUTPUT)
      DIMENSION PHI(60,30),TEMP(60,30),PINF(60),TINF(60),HFW(60)
      DIMENSION DELTA(60),F(60),G(60),H(60),FF(60),GG(60),HH(60)
      DIMENSION S(60),T(60),Y(60),Z(60)
      REAL KW
      READ 100, N,PING,TING,TW,A,GAMMA,D,B
  100 FORMAT (I5,6F10.5,E11.5)
      READ 110, M,STABF,KW,ALFAI
  110 FORMAT (I5,F10.5,2E11.5)
      READ 120, (PINF(K), K=1,N)
  120 FORMAT (10F8.5)
      READ 130, (TINF(K), K=1,N)
  130 FORMAT (10F8.2)
C     TEMPERATURES ARE IN KELVIN
C     PRESSURES ARE IN ATMOSPHERES
C     THERMAL CONDUCTIVITY IS IN WATTS/M OK
C     ALFAI IS IN M2/MICROSEC
C     SPACE IS IN METERS
C     TIME IS IN MICROSECONDS
C     A IS THE POWER FOR THERMAL CONDUCTIVITY
C     B IS THE INITIAL VALUE OF THE ZONE THICKNESS
      GAM = A*(1.-GAMMA)/GAMMA
      COF = A*((TW/TING)**A)/KW/TING
      GAMM = 1.-GAM
      READ 140, (HFW(K), K=1,N)
  140 FORMAT (8E10.4)
      AA = 1./A
      DO 200 K=1,N
      F(K) = ((TW/TING)**A)*((PINF(K)/PING)**GAM)
      G(K) = ((TINF(K)/TING)**A)*((PINF(K)/PING)**GAM)
      H(K) = HFW(K)*COF*((PING/PINF(K))**GAMM)
      S(K) = G(K)-F(K)
  200 CONTINUE
      DELTA(1) = B
C     START CALCULATION
      NN = N-1
      DO 300 K=1,NN
      T(K) = 2.*DELTA(K)*S(K)+H(K)*((DELTA(K))**2)
      Y(K) = (6.*S(K)-6.*DELTA(K)*H(K))/T(K)
      FF(K) = (F(K+1)-F(K))/D
      GG(K) = (G(K+1)-G(K))/D
      HH(K) = (H(K+1)-H(K))/D
      Z(K) = (4.*(DELTA(K)**2)*FF(K)+2.*(DELTA(K)**2)*GG(K)+(DELTA(K)**3
     1)*HH(K))/2./T(K)
      DELTA(K+1) = DELTA(K)+D*ALFAI*Y(K)-D*Z(K)
  300 CONTINUE
C     CALCULATE THE TEMPERATURE DISTRIBUTION
      DPSI = SQRT(ALFAI*D/STABF)
      DO 400 K=1,N
      DO 350 J=1,M
      DDPSI = (J-1)*DPSI
      PHI(J,K) = F(K)+H(K)*DDPSI+(S(K)/(DELTA(K)**2)-H(K)/DELTA(K))*((
     1DDPSI**2))
      TEMP(J,K) = (PHI(J,K)*(((PINF(K)/PING)**GAM)**AA))*TING
  350 CONTINUE
  400 CONTINUE
C     PRINT THE RESULTS
      DO 600 K=1,N
      PRINT 510, K,TINF(K),DELTA(K)
  510 FORMAT (/,5X,*TAU= *,I5,/,5X,*TINF= *,F10.5,5X,*DELTA= *,E11.5)
      PRINT 520
```

```
520 FORMAT (/,5X,*TEMPERATURE DISTRIBUTICN IN THE GAS LAYER*)
    PRINT 530, (TEMP(J,K), J=1,M)
530 FORMAT (8(5X,F10.5))
600 CONTINUE
    PRINT 610
610 FCRMAT (/,5X,*GAS LAYER THICKNESS*)
    PRINT 620, (DELTA(K), K=1,N)
620 FORMAT (8(5X,F11.5))
    STOP
    END
```

REFERENCES

1. C. J. Scott, "Transient Experimental Technique for Surface Heat Flux Rates," in Measurement Techniques in Heat Transfer, second edition, E. R. G. Eckert and R. J. Goldstein, Editors, McGraw-Hill Book Company, 1976.
2. R. J. Vidal, "Transient Surface Temperature Measurements," Symposium: "Measurements in Unsteady Flow," ASME Hydraulic Div. Conf., New York, May 1962.
3. H. W. Liepmann and A. Roshko, Elements of Gasdynamics, John Wiley & Sons, Inc., 1957.
4. A. K. Oppenheim, L. M. Cohen, J. M. Short, R. K. Cheng, K. Hom, "Dynamics of the Exothermic Process in Combustion," 15th Symposium (International) on Combustion, Tokyo, 1974.
5. H. S. Carslaw and J. C. Jaeger, Conduction of Heat in Solids, Oxford University Press, second edition, 1959.
6. D. G. Grossman, Corning Glass Works, personal communication; also, Pamphlet MGS 274-2.
7. D. J. Collins, R. Greif and A. E. Bryson, Jr., "Measurements of the Thermal Conductivity of Helium in the Temperature Range 1600 to 6700 Degrees Kelvin," Int. J. Heat and Mass Transfer 8, 1209, 1965.
8. B. Carnahan, H. A. Luther, J. O. Wilkes, Applied Numerical Methods, John Wiley & Sons Inc., 1969.

9. I. Glassman, Combustion, Academic Press, 1977.

10. D. J. Collins, "Measurement of the Thermal Conductivity of Noble Gases in the Temperature Range 1500 to 5000 Degrees Kelvin," Journal of Heat Transfer, 88, 52, 1966.

11. N. V. Tsederberg, Thermal Conductivity of Gases and Liquids, The M.I.T. Press, 1965.

12. L. M. Cohen (1975)," Gasdynamic Analysis of Exothermic Processes in Combustion," Ph.D. Thesis, Department of Mechanical Engineering, University of California, Berkeley, CA.

13. A. G. Gaydon, I. R. Hurk, The Shock Tube in High Temperature Chemical Physics, Reinhold Publishing Corporation, New York, 1963.

14. R. von Mises, completed by H. Geiringer, G. S. S. Ludford, Mathematical Theory of Compressible Fluid Flow, Academic Press Inc., New York, 1958.

15. W. M. Rohsenow and J. P. Hartnett (editors), Handbook of Heat Transfer, Mc Graw Hill Book Company, 1973.

16. G. J. Van Wylen and R. E. Sonntag, Fundamentals of Classical Thermodynamics, second edition, SI version, John Wiley and Sons, Inc., 1976.

17. L. M. Cohen, J. M. Short and A. K. Oppenheim, "A Computational Technique for the Evaluation of Dynamic Effects of Exothermic Reactions," Combustion and Flame, 24, pp. 319-334, 1975.

18. M. Nikanjam (1977), "An Experimental and Theoretical Study of Unsteady Heat Transfer During Piston Compression," Ph.D. Thesis, Department of Mechanical Engineering, University of California, Berkeley.

19. J. W. Meyer and A. K. Oppenheim, "On the Shock-Induced Ignition of Explosive Gases," 13th Symposium (International) on Combustion, Salt Lake City, 1970.

20. L. M. Cohen and A. K. Oppenheim, "Effects of Size and Dilution on Dynamic Properties of Exothermic Centers," Combustion and Flame, 25, pp. 207-211, 1975.

21. A. K. Oppenheim, L. M. Cohen, J. M. Short, R. K. Cheng and K. Hom, "Shock Tube Studies of Exothermic Processes in Combustion," 10th International Shock Tube Symposium, Kyoto, Japan, 1975.

22. A. K. Oppenheim, K. Teichman, K. Hom, and H. E. Stewart, "Jet Ignition of an Ultra-Lean Mixture", Society of Automotive Engineers Technical Paper Series, Paper No. 780637, Passenger Car Meeting, Troy, MI., June 5-9, 1978.

23. N. Isshiki and N. Nishiwski, "Basic Study on Inside Convective Heat Transfer of Internal Combustion Engines," Fifth International Heat Transfer Conference, Tokyo, 1974.

This report was done with support from the Department of Energy. Any conclusions or opinions expressed in this report represent solely those of the author(s) and not necessarily those of The Regents of the University of California, the Lawrence Berkeley Laboratory or the Department of Energy.

TECHNICAL INFORMATION DEPARTMENT
LAWRENCE BERKELEY LABORATORY
UNIVERSITY OF CALIFORNIA
BERKELEY, CALIFORNIA 94720